PHASE BEHAVIOR AND RHEOLOGY OF LATEX, THICKENER, SURFACTANT MIXTURES AND LIQUID CRYSTAL BASED COMPOSITIONS FOR PRINTING HIGH-EFFICIENCY FLEXIBLE ELECTRONICS

A Project Report

presented to

the Faculty of California Polytechnic State University,

San Luis Obispo

In Partial Fulfillment

of the Requirements for the Degree

Master of Science in Polymers and Coatings

by

Franceska Anna Santos

December 2013

COMMITTEE MEMBERSHIP

TITLE:	Phase Behavior and Rheology of Latex, Thickener, Surfactant Mixtures and Liquid Crystal Based Compositions for Printing High-Efficiency Flexible Electronics
AUTHOR:	Franceska Anna Santos
DATE SUBMITTED:	December 2013

COMMITTEE CHAIR:	Raymond Fernando, Ph.D. Professor, Department of Chemistry and Biochemistry
COMMITTEE MEMBER:	Shanju Zhang, Ph.D. Assistant Professor, Department of Chemistry and Biochemistry
COMMITTEE MEMBER:	Dane Jones, Ph.D. Professor, Department of Chemistry and Biochemistry

ABSTRACT

Phase Behavior and Rheology of Latex, Associative Thickener, and Surfactant Mixtures and Liquid Crystal Based Compositions for Printing High-Efficiency Flexible Electronics

Franceska Santos

This project consists of two parts. One area of focus in the first part is understanding the interactions between a non-ionic, block copolymer type dispersant and hydrophobically-modified, ethoxylated urethane (HEUR) associative thickeners in water. The dispersant was mixed at various concentrations (0-2% by weight) with HEUR thickeners at 1% by weight concentration in the aqueous medium. This study is an integral part of our attempts to determine mechanisms of viscosity drop when colorant dispersions are added to latex tint base formulations thickened with associative thickeners. One of the HEUR thickeners is a product that has been available for over three decades (HEUR RM-825), whereas the other, HEUR RM-995 is a product recently introduced to minimize the tint base viscosity drop. The old HEUR showed a definitive viscosity maximum as a function of the dispersant concentration. However, the new generation product did not indicate a viscosity maximum within the dispersant concentration range studied; instead it showed a small, but linear increase in viscosity as dispersant level was increased.

The next area of focus was on understanding the phase behavior, rheology, and interactions between polymer latex particles and a hydrophobically-modified, ethoxylated urethane (HEUR) associative thickener in water. The influence of the addition of surfactant in some of the systems was also studied. Several types of dispersions were made using two types of polymer latex, two associative thickeners, and two surfactants. Mixtures containing a small particle size acrylic latex and HEUR RM-825 exhibited the most interesting and

complex phase behavior and rheology. In experiments wherein the latex particle volume fraction was kept constant, the addition of HEUR caused stable, followed by phase separated (syneresis) and stable mixtures as HEUR concentration was increased. The observed phase behavior is consistent with previous work reported by other investigators. However, detailed rheological data on systems such as these have not been reported, and this report presents the rheological data and correlate rheology with the phase behavior. The stable latex-HEUR mixtures at low HEUR levels show shear-thinning viscosity with well-defined low-shear Newtonian plateaus. As HEUR level is increased wherein syneresis is observed, erratic rheological profiles with shear-thickening are observed. When HEUR level is increased to a region where no syneresis is observed, low shear Newtonian plateaus re-appeared albeit at higher viscosities. The effects of added non-ionic and anionic surfactants on the dispersion are also studied.

The main focus of the second part of this project is hybrid organic-inorganic photovoltaics. They have been the focus of recent studies due to their promising use in low-cost, flexible electronics, which can be processed from solution by printing and coating techniques. Understanding the rheology of these nanocomposites is essential in controlling shear flows during printing and application processes. Through rheology, we can determine different properties of poly(3-hexylthiophene) and dodecanethiol (DDT) modified zinc oxide (ZnO-DDT). Semiconductor nanowires such as ZnO have rigid or rod-like macromolecule geometry. Therefore, they have a tendency to have a lytropic liquid crystal (LLC) phase. LLC orders occur spontaneously in solutions with rod-shaped or anistropic objects from isotropic phase to nematic phase above a critical volume fraction which was studied using ZnO-DDT. The shear-induced alignment of the liquid crystal molecules was analyzed,

serving as a guide for LLC printing. Furthermore by using this nanocomposite we are able to induced gelation using the ZnO-DDT nanowires in what is considered as a “good solvent,” dichlorobenzene. The kinetics of this gelation process was determined to be of first-order reaction kinetics. Furthermore, a mechanism of this gelation process is also presented.

ACKNOWLEDGMENTS

I would like to give special thanks to Dr. Ray Fernando, Dr. Dane Jones, and Dr. Shanju Zhang for guiding me throughout my research and helping me become a better scientist. Also, I would like to thank the Cal Poly Bill Moore Fellowship Fund and National Science Foundation (NSF) for the financial support for these projects. Lastly, I want to thank my family for their never ending love and support and my friends at Cal Poly, who kept me sane throughout my years at Cal Poly.

TABLE OF CONTENTS

Page

LIST OF TABLES

LIST OF FIGURES

PART A

1 Introduction

1.1 Rheology

Polymers are unique in the aspect of molecular weight. In general, high molecular weight of polymers is prepared via the linkage of organic moieties into linear and chain-like structures. Other polymer structures can be complex due to the continuous network-like structure that can extend indefinitely in three dimensions.[1] The high molecular weight can be correlated with the viscosity of the polymers. Generally, the higher the molecular weight, the higher the viscosity. Systems with complex structure and interactions can be studied using rheology.

Rheology is the study of deformation and flow of materials and how factors including stress, strain, and time can affect that.[2] Rheology is also important in the study of the viscous flow of polymers. In a coating formulation, the understanding of rheology is crucial. This allows the coating formulators to achieve the right coating properties according to their desired applications. The flow of materials as defined by rheological studies is highly dependent on the viscosity of the materials.[3] One of the most important factors to control in paint formulation is the viscosity. Viscosity is the measurement of a fluid's resistance to a gradual deformation by shear stress or tensile stress.[1] The higher the viscosity, the more difficult it is for the liquid to flow. Viscosity is defined by factors such as shear stress and shear rate as shown in Figure 1.

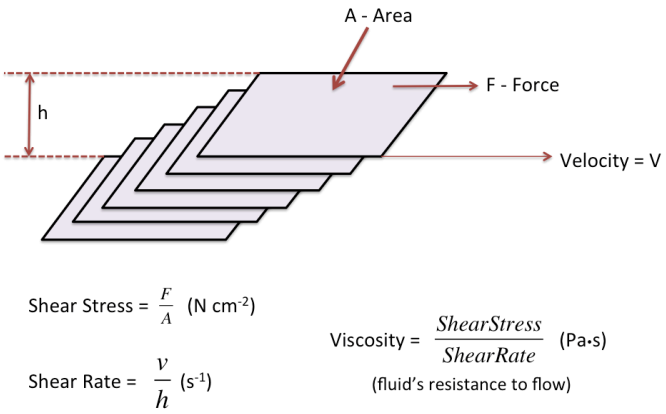

Figure 1. Definitions of shear stress, shear rate, and viscosity.

In a steady-shear flow experiment, the viscosity of a material is calculated by the ratio of shear stress to shear rate. Shear stress is defined by the force (F) over the area (A) the force acted on. In Figure 1, the sample is ideally confined in a small gap with the bottom as a stationary plate and the top plate a movable plate, when a force F is applied to the plate with an area A, the sample will continually be deformed at a constant rate V. Shear rate is the rate of deformation in terms of the velocity gradient.[2] The top plate that is moving at velocity V decreases approaching the stationary plate creating a velocity gradient where the gradient is constant over a section of the liquid is equivalent to V/h.[2] There are various rheological techniques to assess a system.

1.1.1 Steady-State Shear Rheology

To study the flow behavior of structured fluids can be accomplished through a steady-state shear rheology. This is where the change in viscosity is observed as the shear rate is increased. There are different types of viscosity behavior that are seen in paints and coatings depending on the composition, as shown in Figure 2. If the viscosity of a fluid is constant at different shear rates, the fluid is said to exhibit an ideal or Newtonian behavior. Newtonian flow is generally found only with low molecular weight liquids such as water and common solvents.[3]

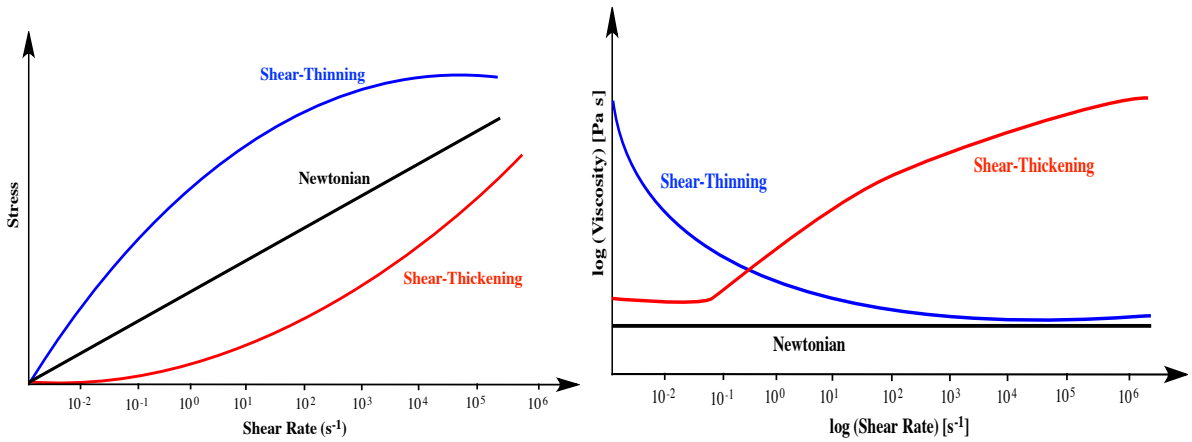

Figure 2. Various viscosity behaviors observed in paint systems: Newtonian, Shear-Thinning, and Shear-Thickening.

If the viscosity decreases with increasing shear rate, the flow behavior is said to be shear-thinning or pseudoplastic. One of the many mechanism why this occurs is when stress is applied, molecules line up parallel to the direction of the flow, thus reducing the energy required to displace them further.[2] Most coatings and polymer solutions exhibit shear-thinning behavior. Another class of liquids exhibits increasing viscosity as the shear rate increases, this behavior is called shear-thickening. Examples of a shear-thickening substance are pigments and resin dispersions where the dispersed phase is concentrated so that particles are randomly close packed. If enough stress is applied for flow, microscopic voids are created, increasing the volume occupied the molecules and increasing the energy needed to induce flow, thus the viscosity increases.[1]

Paint and coatings are applied to substrates with different shear rates, as seen in Figure 3.

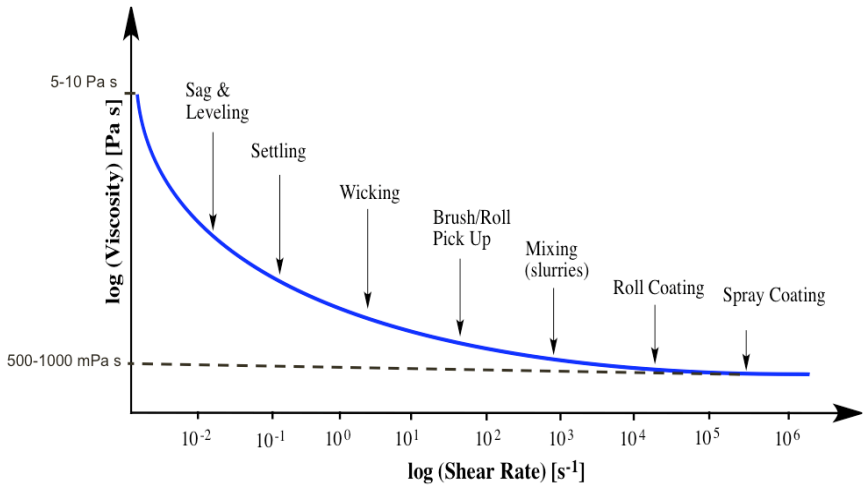

Figure 3. Shear rates of various coatings applications to a substrate.

During a dispersing process, low viscosities are necessary but the storage of coatings should take place at high viscosity so that the pigments are prevented from settling out. For spray application, under a very high shear rate, the paint should have a low enough viscosity but as soon as the paint is applied to the substrate, the coating should assume a high viscosity to prevent sagging.[4] Viscosity and shear rates are two important factors that should be taken into account when formulating and applying coatings.

In this project, the system that is observed is comprised of latex, associative thickener, and surfactants. Due to the increase in viscosity upon the addition of associative thickener in the system, rheology can be used to study and monitor the hydrophobic interactions in the dispersion. Numerous studies have been focused on the effects of hydrophobic interactions in the rheology of the system.[5-9] Using a steady state shear test, where the change in viscosity is observed as the shear rate is increased, the hydrophobic interactions in the latex, associative thickener, and surfactant mixtures can be studied.

1.2 Paints and Coatings

Paints and coatings are everywhere; they made their earliest appearance about 30,000 years ago.[9] One of the earliest examples of the use of paints was by cave dwellers, who used crude paints as a graphic representation of their day-to-day lives. However, the paint and coatings industry did not contribute any significance in the economy until the Industrial Revolution.[10] In 2006, it was reported that the total sales for the industry was approximately $20.9 billion in the US.[10] The formulation of paints and coatings is continually changing and improving especially with the increasing environmental restrictions.

Majority of architectural coatings can be described as a dispersion, which after application to a substrate is dried into a solid film. Paint and coatings not only serve an aesthetic purpose but for protection as well. Most coatings are composed of four basic ingredients: binder, pigments, additives, and solvents or volatile components as shown in Figure 4. Some coatings may not have all four of these depending on the application of the finished coatings. It is important for formulators to be familiar with these ingredients and how they interact with one another. With the understanding of how these ingredients interact with each other also gives formulators a better understanding of the mechanism of different types of interactions in a coating system.

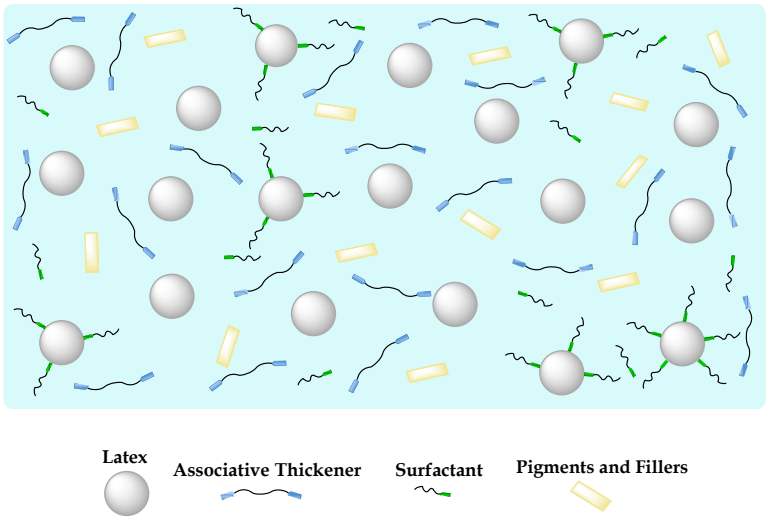

Figure 4. Ingredients in a typical coatings formulation.

1.3 Binder

Arguably, the most important ingredient in a coating system is the binder. The binder serves as the film-forming component in the coating.[1] The binder acts as "glue" holding all the components of the coating together and is responsible for the adhesion of the coating to a substrate. There are different kinds of binders used for various applications: alkyd resins, polyester, epoxy, and latex, just to name a few. Binders are categorized according to the mechanisms of the drying or curing of the film. The properties of the binder largely determine the properties of the paint film such as gloss, flexibility, and adhesion. Typically, in a solventborne coating, the binder is usually an alkyd, which is a natural drying oil that is modified to be tough and long lasting. Instead in a waterborne coating, the binder is a latex composed of vinyl and/or acrylic copolymers. Due to the increasingly strict environmental restrictions, the use of solventborne coatings is decreasing whereas the use of waterborne coatings is becoming more prominent. Because of this, in architectural coatings, a latex is used as a binder.

1.3.1 Latex

Latexes can be defined as a stable dispersion of polymer particles in an aqueous medium. Latexes can be natural or synthetic. Latex is found naturally occurring in some plants. However, the latex that is used in coatings is synthesized using emulsion polymerization. The history of the use of latex in coatings dates back in the 1960s when environmental restrictions became prominent. Before latex paints were invented, oil-based paints were commonly used.. Latex dispersion are a product of emulsion polymerization and undergo film formation by coalescence. The molecular weights of polymers polymerized via emulsion polymerization are typically high. However, the molecular weight of the polymers does not affect the viscosity of the latex. Instead, the viscosity of the latex is dependent on the medium in which the particles are dispersed in, the continuous phase, particle size, and size distribution, among others.[1]

1.4 Pigments

The pigment added in coating formulation is key to getting the right optical properties for the intended use of the coatings. Pigments are described as insoluble fine particle size materials used in coatings. They are used in coatings for several reasons: to provide color, to hide the substrate, to modify the application properties of a coating, to modify the performance properties of films, and to reduce the cost.[1] One the most important properties that affects the performance of pigments in coatings is the particle size. Particle size affects the color strength, transparency or opacity, exterior durability, and solvent resistance. Pigments are commonly grouped into two categories: inorganic and organic.

Inorganic pigments consist of fine particles, which are dispersed in paints with the aid of special additives, improving its compatibility with various resin systems.[11] Inorganic pigments can contribute to the corrosion resistance, physical properties, and aesthetics of the coating. Two of the most common inorganic pigments are titanium dioxide (TiO_2) and iron oxide. TiO_2 is most commonly used white pigment, particularly in architectural coatings. Due to its high refractive index, it provides the coating a great hiding power.[1] Under inorganic pigments, there are the extender pigments. Unlike white pigments, extenders provide a minimal color and corrosion resistance to the coating. The main effect of extenders in the coating is in density, hardness, permeability, and flow. Three of the most commonly used extenders are calcium carbonate, various types of silicates (kaolin and talc), and barium sulfate.[10]

Organic pigments are used widely in coatings. Majority of these pigments are chemically synthesized. They are a type of organic molecules based on carbon chains and carbon rings and some are partially soluble in certain resins and solvents. Organic pigments are mainly used in applications needing high tinting strength and brilliant shades whereas inorganic pigments are mainly used where high opacity is needed.

1.5 Volatile Components

The volatile components in coatings play a variety of important roles in resin manufacture, coating production and application, and film formation. Volatile components are the liquids that provide coatings an appropriate viscosity for application, they evaporate during and after application. Until about 1945, almost all volatile components in paints were low molecular weight organic solvents.[1] However, because of environmental restrictions and

the need to lower the volatile organic compound (VOC) emissions from paints, the use of organic solvents are reduced. They are instead replaced by making the coatings highly concentrated with solids thereby using less solvent or by the use of water instead of organic solvents (waterborne). Although volatile organic solvents are still used in coatings (even in waterborne coatings) the levels are significantly less. Most coating requires the volatile component to dissolve the binder and to modify the viscosity so that the coating can be applied to the substrate by conventional methods. After application, the volatile component evaporates and aid flow and leveling of the coating, as well as the wetting of the substrate.

The rate of the evaporation of the volatile components in coatings is crucial. The rate of evaporation can have a major influence on the properties of the coatings and common defects can be traced from the inappropriate use of volatile components. If it evaporates too quickly, the coating does not have a chance to flow into a smooth, continuous film. While too slow evaporation can cause undesirable sagging.

1.6 Additives

Additives are materials that are added in the formulation in small quantities to modify some properties of the coatings. These include rheology modifiers, surfactants, coalescing agents, defoamers, UV-light absorbers, dispersing agents, biocide, and plasticizers. The scope of this project is focusing on the rheology modifiers, surfactants, and dispersing agents.

1.6.1 Rheology Modifiers

Rheology modifiers are also known as thickeners. Latex paints and waterborne formulations require thickeners to adjust and control the viscosity. Rheology modifiers are additives that are added to a coating formulation in order to control the viscosity of the system. Controlling the viscosity of the system is integral to the application of the coatings due to the shear rates of various coating process. Furthermore, rheology modifiers control sag, leveling, penetration, and application properties as well as many other coating characteristics. Rheology modifiers can be divided into two types non-associative thickeners and associative thickeners.

1.6.1.1 Non-associative Thickener

Non-associative thickeners are typically high-molecular weight water-soluble polymers, consisting of a hydrophilic backbone but lacking hydrophobic groups. The most widely used non-associative thickeners are cellulosic thickeners as shown in Figure 5.

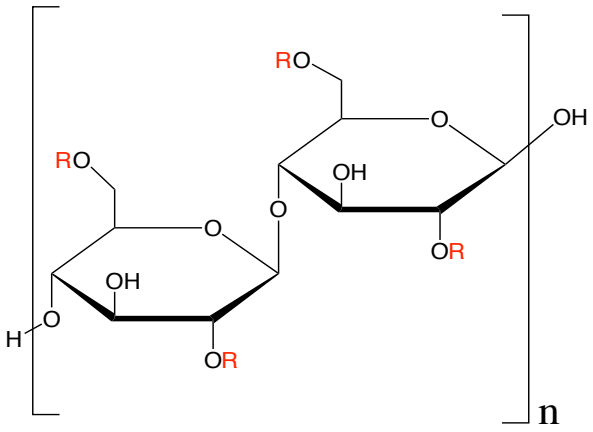

R = $-CH_2CH_2OH$ = Hydroxyethyl

R = $-CH_2COO^-Na^+$ = Carboxymethyl

R = $-C_2H_5$, $-CH_2CH_2OH$ = Ethyl, Hydroxytethyl

R = $-CH_3$, $-CH_2CH_2OH$ = Methyl, Hydroxyethyl

Figure 5. General strucure of cellulosic thickeners.

The water-soluble hydroxyethylcellulose (HEC) is the most commonly used within cellulosic thickeners. HEC is derived from cellulose and is used in cosmetics and other household products as well. Non-associative thickeners have different thickening mechanisms: contributions to hydrodynamic volume, chain entanglements, and depletion flocculation. Hydrodynamic volume is the volume of a polymer coil when it is in solution. When cellulosic thickeners are dissolved in water, due to the high molecular weight of the polymers, they occupy a large hydrodynamic volume in solution and immobilize large volumes of water within the coils of their backbones. This will increase the viscosity of the continuous water phase.

Another thickening mechanism of cellulosic thickeners is through chain entanglement. Chain entanglement is a type of intermolecular interaction that occurs due to the physical interlocking of polymers, which are long and flexible in nature.[12] This entanglement between polymers causes an increase in viscosity. Depletion flocculation is recognized as the primary mode of thickening in non-associative thickeners.[13] In a dispersed phase system, depletion flocculation begins when latex particles randomly approach each other, when the distance between the particles are close enough, thickener molecules are excluded from the interparticle region. As the latex particles touch, they form flocs causing an increase in viscosity. Although the non-associative thickeners are low cost universal thickeners and based on natural resources, there are plenty of disadvantages in using them as the rheology modifier in a paint system: poor leveling, reduction of gloss (due to depletion flocculation), roller spatter, water sensitivity, bio-degradation, and syneresis. Because of

these disadvantages, associative thickeners were developed to address the problems regarding non-associative thickeners.[14]

1.6.1.2 Associative Thickeners

Associative thickeners were first introduced to the Coating Industry in the late 1970s.[6] Associative thickeners are moderately low molecular weight hydrophilic polymer with two or more hydrophobic segments in the form of nonpolar hydrocarbon groups spaced along the backbone. There are several different types of associative thickeners in the market: hydrophobically-modified ethoxylated urethanes (HEUR), hydrophobically-modified alkali-swellable emulsions (HASE), hydrophobically-modified HEC, hydrophobically-modified polyether (HMPE), and hydrophobically-modified aminoplast ether (HEAT). In associative thickeners, the thickening effect is caused by interactions of the hydrophobic end groups of the thickener with other components in the formulation. Upon the addition of associative thickeners to water, the water-soluble backbone polymer is dissolved and the hydrophobic groups form intramolecular interaction and intermolecular interactions with other hydrophobic components in the system. These interactions form micelle-like structures and reversible dynamic network, increasing the high and mid-shear viscosity of the system.[15] Associative thickeners can produce the ideal rheology for the application of paints and coatings. They are often used to adjust the application properties such as spattering or brushing resistance. Furthermore, formulations with associative thickeners often exhibit high gloss and good leveling. However, associative thickeners are highly sensitive to the addition of most coating formulation components, such as latex particle characteristics, surfactant, dispersants, and cosolvents. This is a major drawback with the use of associative thickeners;

as a result, a significant amount of formulation development is needed in order to produce superior results using associative thickeners.

Despite the degree of reformulation needed when incorporating associative thickeners in the formulation, the use of associative thickener is preferred over non-associative thickeners. An area of study where this can be proven is through rheology. Non-associative thickeners and HEUR type associative thickeners have two different rheological profiles, which are significant for their application, as shown in Figure 6.

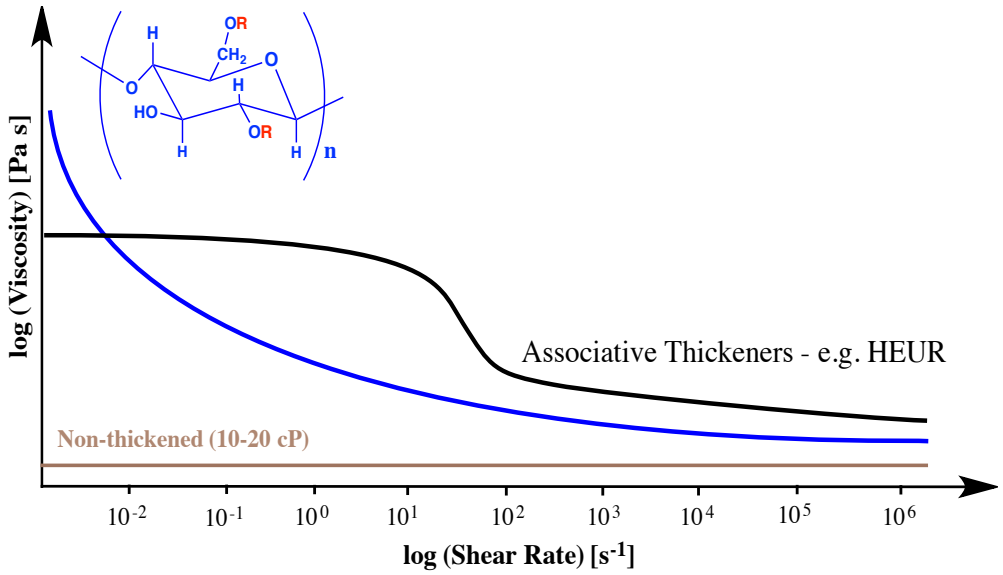

Figure 6. Rheological profiles comparing non-associative thickeners and associative thickeners.

The rheological profile of paint thickened with cellulosic thickeners starts at a high viscosity at low shear rates and shear thins as the shear rate is increased. At high shear rates, the viscosity of the paints thickened with cellulosic thickeners is low. The addition of associative thickener in place of cellulosic thickeners compensates for the too high and too low viscosity profiles of cellulosic thickeners. Relative to non-associative thickener, the rheological profile of associative thickeners show Newtonian plateaus and it exhibits less shear-thinning. Due to this, the viscosity at high shear rates is high enough to apply a thicker wet film, thereby promotes leveling, flow, and better application of the paint.

Figure 7 shows an example of a system showing three different rheological phenomena that are observed in systems such as the ones observed in this project.

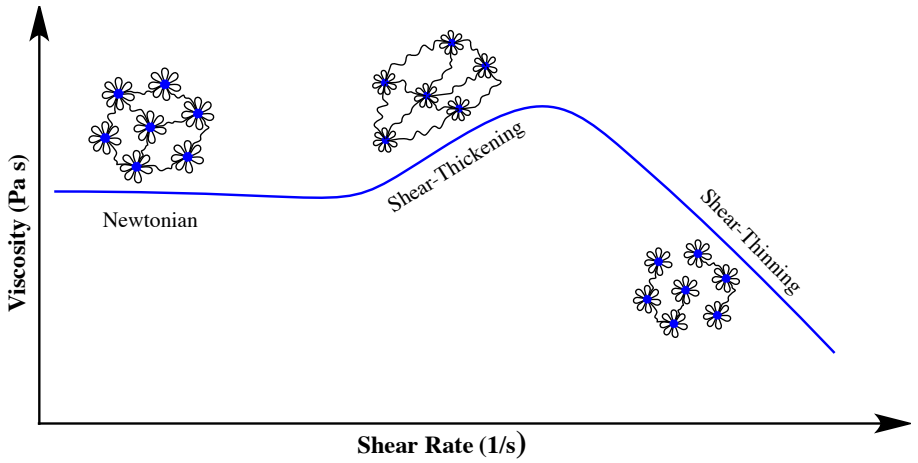

Figure 7. Three different rheological phenomena in an aqueous dispersion of associative thickener.

This is an aqueous dispersion of an associative thickener. The hydrophobic segments of associative thickeners associate intramolecularly and intermolucarly forming aggregates. Due to this, the hydrophilic segments of associative thickeners form a loop, allowing the hydrophobic segments to interact with each other, forming Rosetta-like micelles. This interaction creates a unique rheological profile as seen in Figure 7. Associative thickener in water can have different rheological phenomena: Newtonian, shear-thickening, and shear-thinning. A Newtonian rheological profile indicates that the viscosity is independent of the shear rate; this phenomenon is common in dispersions with low viscosity and usually occurs at low shear rates. Shear-thickening typically occurs at mid-shear rates; many mechanisms have been proposed for this phenomenon. In the system studied, this occurs due to the shear-induced decrease of resistance, thereby the viscosity increased. In addition, at mid-shear, the shear induced extension and elongation of the hydrophilic segments in the network, increasing the viscosity. Shear-thinning typically occurs at a higher shear rate. Shear-thinning

occurs when the said bridges and networks are broken down due to the high shear rate applied to the sample. In typical paint formulations thickened with associative thickener, the rheological profiles show a Newtonian plateau at low shear rates followed by shear-thinning at higher shear rates.

1.6.2 Surfactants and Dispersants

Another important additive in formulation of paints and coatings are surfactants and dispersants. A surfactant is a compound that alters the surface tension of a liquid or a solid. Surfactants are amphiphilic molecules having both a hydrophobic and hydrophilic segments. Surfactants are used in coating formulations to stabilize the system. In waterborne systems, stabilization occurs through lowering the surface tension of water (72 mN/m), making the system thermodynamically stable, allowing wetting of pigment particles.[9] Furthermore, surfactants are added in formulations in order to add stability to the latex polymer particles and to prevent aggregation. Surfactants fall into one of three categories: anionic surfactants, cationic surfactants, and nonionic surfactants.

Anionic surfactants ionize in solution to produce a negatively charged group on the hydrophilic end such as a carboxylate, sulfonate, or sulfate group. An important and one of the most widely used anionic surfactant is sodium dodecylsulfate (SDS), belonging to the class of sodium alkylsulfates.[11] In water, SDS dissociates as shown in Figure 8.

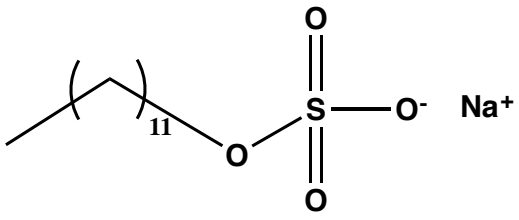

Figure 8. Products of the dissociation of sodium dodecylsulfate (SDS) in water.

Cationic surfactants are used less in paint formulations. Cationic surfactants ionize in solution to produce a positively charged end group. They are often based on amine salts and quaternary ammonium compounds. An example of a cationic surfactant is dodecyl trimethylammonium bromide, which dissociates in water to molecules shown in Figure 9.

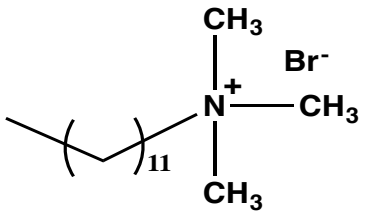

Figure 9. Products of the dissociation of sodium dodecyltrimethylammonium bromide in water.

Unlike anionic and cationic surfactants, nonionic surfactants do not dissociate in solution. The hydrophobic ends of nonionic surfactants usually consist of long hydrocarbon chain while the hydrophilic end consists of relatively polar organic molecules such as hydroxyl and ether groups. An example of a nonionic surfactant is poly(ethylene oxide) *iso*-octylphenyl ether, as shown in Figure 10. The Triton X series, supplied by DOW Chemical Company, is a poly(ethylene oxide) *iso*-octylphenyl ether varying in CMC and the length of the hydrocarbon.

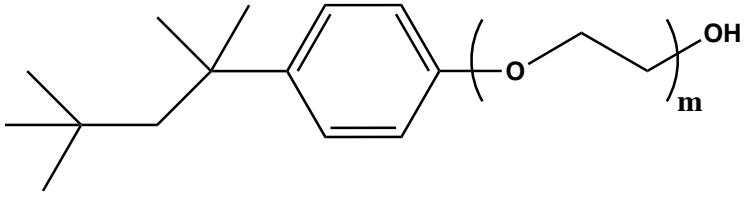

Figure 10. General structure of a nonionic surfactant, poly(ethylene oxide) *iso*-octylphenyl ether.

Similar to surfactants, some dispersants are also amphiphilic but are more conveniently classified based on their specific end-use, rather than on their chemical properties.[3] Dispersants are either a non-surface active polymer or a surface-active ingredient added to a suspension to improve the separation of particles, thus preventing flocculation. In paints and coatings, when pigment particles are added, they are unstable and have a tendency to flocculate affecting the optical properties of the film. The addition of dispersants keeps the pigment particles stable, preventing flocculation. The most effective type of dispersants are dispersants with polar functional groups and a less polar tail that is soluble in the medium.[1] Controlled free radical polymerization is used to synthesize certain types of dispersants. Some examples of dispersants are polycaprolactonepolyol-polyethyleneimine block copolymers and polycaprolactone capped with toluene diisocyanate postreacted with triethylenetetramine.[1]

1.7 Particle Dispersion

It has been shown that the addition of additives such as rheology modifiers and surfactants causes difficulty in the control of dispersion due to the complex interactions of these additives with the particles in the paint.[8,15-17] Due to their hydrophobic functionality, associative thickeners interact with the latex particles, pigments, fillers, surfactants and solvents in the paint system. A schematic representations of these hydrophobic interactions are shown in Figure 11.

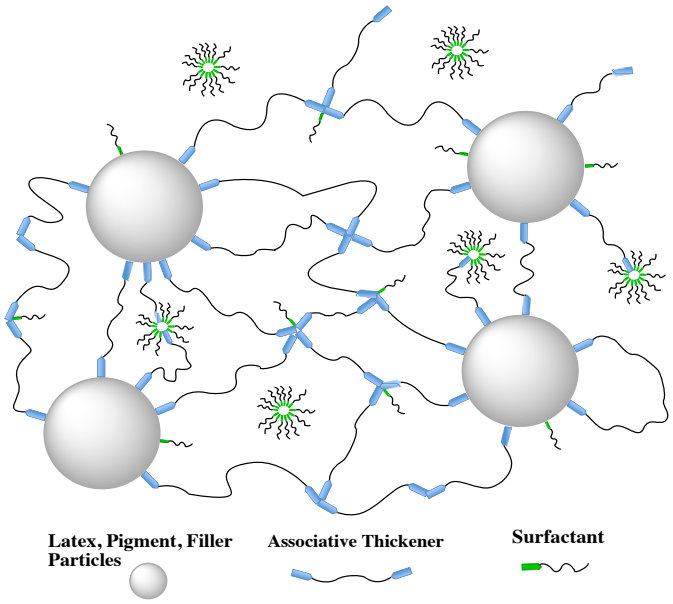

Figure 11. Interaction between latex particles, associative thickener, and surfactant molecules. Associative thickeners are endcapped with hydrophobes and surfactants have a hydrophobic head.

These interactions can often lead to different dispersion behaviors of the system. One can be a good particle dispersion, which in turn results in desirable rheological and optical properties. Additionally, hydrophobic interactions can cause particle flocculation relative to the amount of the other additives added to the paint. Particle flocculation such as bridging and depletion flocculation causes degradation on the properties of the latex paint. This study is mainly focused on the interaction of the latex particles with the associative thickener; the effects of the addition of nonionic and anionic surfactants were also studied.

In order to focus on the interactions between the latex, associative thickener, and surfactants in a latex paint system, a simple system with latex, associative thickener, and surfactants were studied instead of fully formulated systems. The hydrophobic tails of the associative thickeners and latex particles form bridges, allowing associative thickeners to be absorbed, thus increasing the viscosity of the system. The amount of associative thickener absorbed is influenced by the surface properties of the latex particles. Through a complex

mix of inter- and intra-molecular interaction, associative thickeners thicken the aqueous dispersion.[18] Associative thickener molecules are absorbed into the latex particles and interact with the surfactant molecules in the dispersion.

1.7.1 Bridging Flocculation

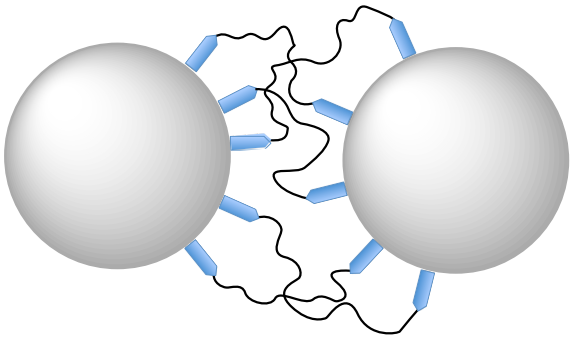

Bridging Flocculation

Figure 12. Bridging flocculation.

As shown in Figure 12, bridging flocculation is a dispersion behavior where a thickener molecule is adsorbed on two different particles resulting to the formation of bridges.[8] Bridging flocculation is a physical process, occurring at low associative thickener concentration and where polymers are well-adsorbed. There is more particle surface available than there are adsorbing species. Bridging flocculated system causes a complex rheology and a phase separated system. Bridging flocculation relies on the addition of high-molecular weight polymer, where a single polymer can adsorb on two or more particles, physically holding them together.[19] Bridging flocculation occurs rapidly and is effective at a very low concentration, giving rise to aggregates clearly showing the morphology of the flocs. In dispersions, bridging flocculation can be alleviated by the addition of more associative thickener and surfactants or both to the system.

1.7.2 Good Dispersion

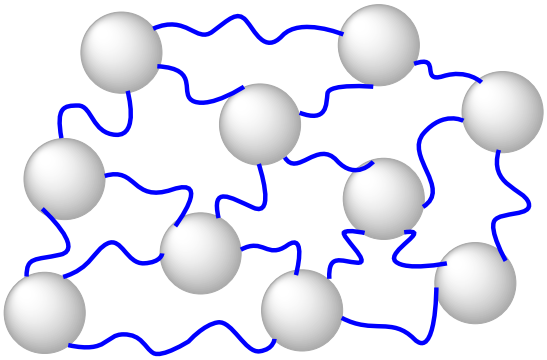

Figure 13. Good dispersion.

A good dispersion is shown in Figure 13; this is the ideal phase behavior in a paint system. In a good dispersion, there is no flocculation resulting in an optimum rheology property as well as good optical properties. In a good dispersion, there is enough adsorbing species that it does not cause bridging or depletion flocculation. Good dispersion lacks Brownian motion because it is thickened.[8] From a bridging flocculated system, the addition of surfactants can lead a latex dispersion into a good dispersion system.

1.7.3 Depletion Flocculation

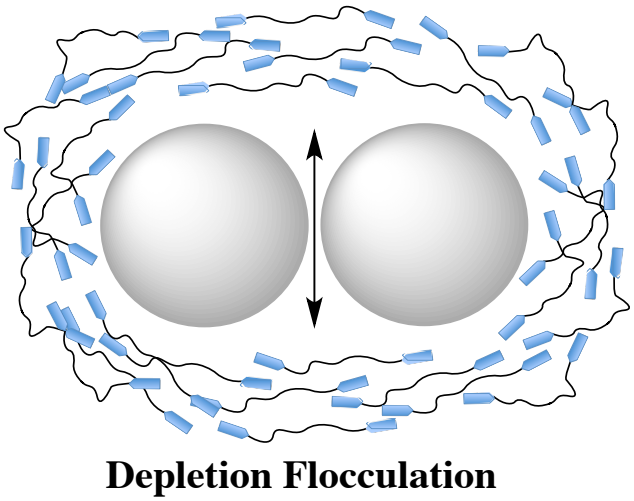

Figure 14. Depletion flocculation.

Figure 14 is a schematic representing particles exhibiting depletion flocculation. Depletion flocculation occurs at a higher associative thickener concentration, where polymers are poorly absorbed. Nonadsorbed thickener molecules are excluded from the space between particles, causing particles to flocculate. When particles approach another particle, polymer coils are not able to fit between them and due to osmotic pressure, the remaining solvent between the particles is removed bringing the two particles closer together. Depletion flocculation is highly dependent on the particle volume solids, particle size, thickener molecular size, and concentration. Depletion flocculated system results to a complex rheology and phase separation in the mixtures. The dispersion state of a system is determined by not only the osmotic attraction energy but the whole interparticle potential energy (V_{tot}) of the system.[8] The total interparticle potential energy can be expressed as:

$$V_{tot} = V_{vdw} + V_{elec} + V_{depl} \qquad (1)$$

where V_{vdw} is the Van der Waals attractive energy, V_{elec} is the electrical repulsive energy, and V_{depl} is the attractive depletion energy, comprising of the particle radius, polymer radius, and osmotic pressure.

For further clarification, potential energy curves for a well-dispersed system and a depletion flocculated system are shown in Figure 15.

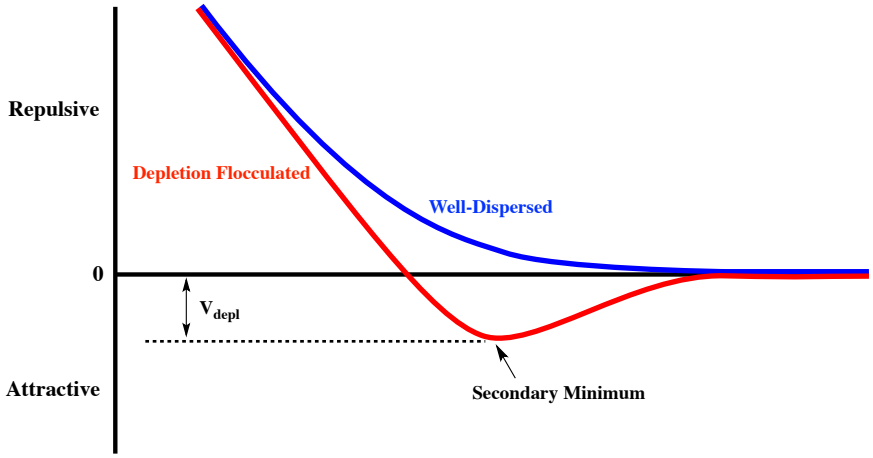

Figure 15. Total potential energy curves for particles that are well-dispresed and particles that are depletion flocculated

The effect of depletion flocculation is that the particles are grouped close to each other in a shallow secondary energy minimum. The depth of the secondary minimum well is equal to the attractive depletion energy. Mechanical energy such as shear can remove particles from this secondary minimum, but the flocculated structure will quickly reform as soon as the mechanical shear is removed.[8] Due to the higher levels of thickeners incorporated in formulations, depletion flocculation is more commonly encountered in coatings than bridging flocculation. The poor particle dispersion in a depletion flocculated system leads to lower gloss, lower hiding, and poorer film integrity and adhesion.

1.8 Objective

The objective of this project is to study the complex interactions between latex, associative thickener, and surfactant in a simple system. Detailed measurements related to the phase behavior and rheological properties of various latex/associative thickener and latex/associative thickener/surfactant systems were made. A clear correlation was made between the phase behavior and rheology of various latex/associative thickener and later/associative thickener/surfactant mixtures.

2 Methods and Materials

In this study, the complex interactions between ingredients in a paint formulation are examined. Simple systems were developed to probe these interactions. Mixtures of associative thickener/dispersants, latex/associative thickener and latex/associative thickener/surfactants were made. Dispersions were made to test different latexes, associative thickeners, surfactants and dispersants.

2.1 Thickener/Dispersant Study

The most commonly used nonionic associative thickener is hydrophobically-modified ethoxylated urethane (HEUR). HEUR has a polyethylene oxide (PEO) backbone, chain-extended by diisocyanates, and endcapped by hydrophobic alkyl chains as shown in Figure 16.

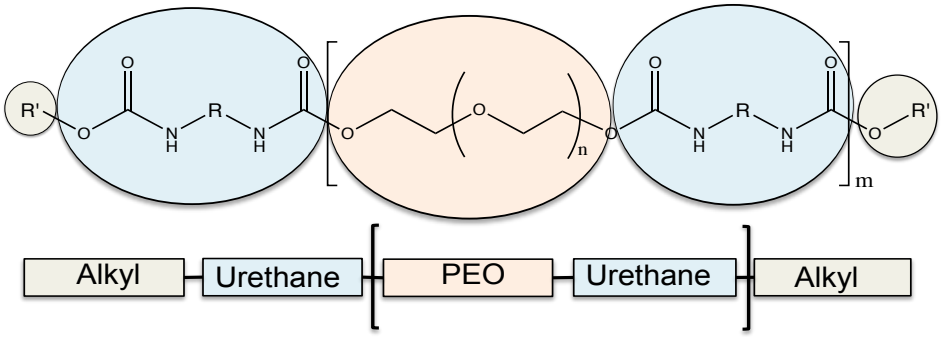

Figure 16. General structure of a hydrophobically-modified urethane thickener (HEUR).[8]

In studies where the interaction between the associative thickener and dispersants were examined, four different commercially available HEUR thickeners were used: HEUR RM-825, HEUR RM-995 and HEUR SCT-275, sold under the trade name Acrysol, were supplied by DOW Chemical Company and Rheovis PU-1191 was supplied by BASF. The non-associative thickener, HEC that was used was Natrosol 250GR supplied by Ashland Inc., used as a control. The dispersants that were used in this part of the study were Disperbyk 192, 190, 187, and 185, which were all supplied by BYK. Thickeners were diluted with

deionized (DI) water making aqueous solutions at constant one weight percent while various dispersant weight percent concentrations were used: 0.25. 0.50, 0.75, 1, 1.5 and 2%. Dilution of thickeners and dispersants at a specified weight percent concentration were made and was allowed to mix and equilibrate overnight. These solutions were then blended and were allowed to mix and equilibrate overnight before any testing was performed.

2.2 Latex/Thickener and Latex/Thickener/Surfactant Study

The latex, Rhoplex VSR-1050, was supplied by Dow Chemical Company (formerly Rohm and Haas) and Hybdridur 570 was supplied by Air Products. Rhoplex VSR-1050 is a 100% acrylic emulsion at 49.5-50.5% solids by weight. Hybridur 570 is an anionically stabilized acrylic urethane hybrid polymers at 40-42% solids by weight The HEUR thickener HEUR RM-825 and HEUR RM-995 are supplied by Dow Chemical Company (formerly Rohm and Haas) at 25% solids by weight in a 75/25 solvent mixture of water and butyl carbitol for HEUR RM-825 and at 23.5% solids by weight in water for HEUR RM-995. Two types of surfactants were used: nonionic and anionic surfactants. The nonionic surfactant Triton X-405 is supplied by Dow Chemical Company at 70% weight active ingredients with a HLB value of 17.6 and a CMC of 2,442 mg/L. The anionic surfactant Ninate 411 is supplied by Stepan at 88% weight active ingredients with a CMC of 1,214 mg/L. A series of dispersions in water were prepared. These dispersions contained latex, HEUR thickener, and nonionic and anionic surfactants:

- Latex – 25% (vol) (Rhoplex VSR-1050 and Hybridur 570)
- HEUR Thickener – 0%-2.0% (wt) (HEUR RM-825 and HEUR RM-995)
- Surfactants – 0%-2.0% (wt) (Triton X-405 and Ninate 411)

2.3 Characterization

Syeneris tests were performed on the dispersion with latex/associative thickener and latex/associative thickener/surfactants after letting the dispersion equilibrate for 24 hrs to study the phase behavior, as shown in Figure 17.

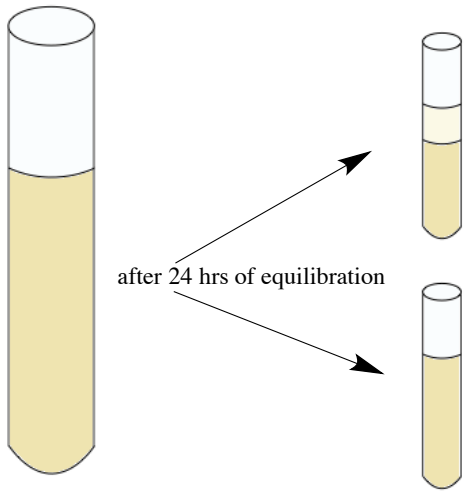

Figure 17. A syneresis test was performed to study the phase behavior of the dispersions.

After 24 hrs of equilibration, there can be two outcomes from the syneresis test, one can be a test with no phase separation, indicating good dispersion. Another is a phase-separated system indicating a bridging flocculated or a depletion flocculated system.

The molecular weight of the raw materials used in the dispersion made with thickeners and dispersants were characterized through gel permeation chromatography (GPC). This was done using Agilent 1200 series with tetrahyrofuran (THF) as the solvent. Furthermore, the pH of the dispersions containing thickeners and dispersants were obtained using Fisher Scientific Accumet AR50.

To study the rheological profiles of all the dispersions, a steady-shear test was conducted using TA Instruments HR-2 Rheometer equipped with a 40 mm, 2° cone, and 55

μm gap. Viscosities were measured in steady-state flow mode in the shear rate range of 0.01-1000 s^{-1}.

3 Results and Discussion

3.1 Thickener and Dispersant Blends

GPC is used to characterize the thickeners and surfactants that were used in this project. All of the materials that were used were commercial products and information, including their structure and molecular weight, are proprietary. Table 1 and 2 listed thickeners and surfactants, respectively, with their following molecular weight, molecular distribution and type of polymer it can be, the molecular weight distribution obtained via GPC is shown in Appendix A. In table 1, it is shown that the molecular weights of the thickeners ranges from 16,000-29,000 g/mol based on polystyrene calibration. Thickeners are associative polymers, usually a block copolymer, with hydrophobic and hydrophilic polymers.[20]

Table 1. GPC Results of Thickeners.

Thickener	Type	M_n (g/mol)	M_w (g/mol)	MWD	Comments
HEUR RM-825	HEUR	16,714	21,614	1	monomodal, can be a block copolymer
HEUR RM-995	HEUR	17,989	20,938	2	Bimodal, showing a distinct copolymer
HEUR SCT-275	HEUR	25,107	28,454	2	Bimodal, showing a distinct copolymer
Rheovis PU-1191	HEUR	16,905	22,788	3	trimodal, fractions can represent block copolymer (A,B, A-B-A)
Natrosol 250GR	HEC	--	--	--	

The GPC result and analysis in Table 2, shows that the dispersants used in this research were copolymers, determined based on the shape of the molecular weight distribution. Disperbyk 190 has the highest molecular weight, followed by Disperbyk 192, Disperbyk 187, and Disperbyk 185 has the lowest molecular weight. The molecular weight of the raw materials can qualitatively show us the starting viscosity of the materials that were used. The molecular weight distribution (MWD) can give us an insight of the possible structure of the polymer in

the thickeners and dispersants. For instance, Disperbyk 190 is shown to have three fractions on its MWD, this can signify a copolymer that A, B, or A-B-A.

Table 2. GPC Analysis of Dispersants.

Dispersant	Type	M_n (g/mol)	M_w (g/mol)	MWD	Comments
Disperbyk 192	nonionic	1080.1	1491.8	1	monomodal, can be a block copolymer
Disperbyk 190	nonionic	10,585	19,399	3	trimodal, block copolymer, fractions can ne A, B, or A-B-A
Disperbyk 187	cationic	2036.8	7000.4	4	4 peaks (fractions), complex structure
Disperbyk 185	nonionic	360.93	1032.1	2	bimodal, with small peaks within a fraction that can represent various MW PEG

Table 3 describes the visual description of the thickener/dispersant blends. Most of the blends were clear homogenous liquid but thickeners such as HEUR RM-995 and Natrosol 250GR resulted in cloudy solution blends. This was due to the solubility of the molecules in the solution. HEUR RM-995 and Natrosol 250GR were both dispersed in water, the cloudiness can be due to the suspended insoluble solid.

Table 3. Visual Description of Thickener/Dispersant Blends.

Thickener	Dispersant	Description
HEUR RM-825	Disperbyk 192	clear, homogenous liquid
	Disperbyk 190	clear, homogenous liquid
	Disperbyk 187	clear, homogenous liquid
	Disperbyk 185	cloudy, homogenous liquid
HEUR RM-995	Disperbyk 192	clear, homogenous liquid
	Disperbyk 190	started from cloudy to clear as the dispersant concentration increased
	Disperbyk 187	cloudier as dispersant concentration increased
	Disperbyk 185	cloudy across all dispersant concentration
HEUR SCT-	Disperbyk 192	clear, homogenous liquid

275	Disperbyk 190	clear, homogenous liquid
	Disperbyk 187	clear, homogenous liquid
	Disperbyk 185	cloudy, homogenous liquid
Rheovis PU-1191	Disperbyk 192	clear, homogenous liquid
	Disperbyk 190	clear, homogenous liquid
	Disperbyk 187	clear, homogenous liquid
	Disperbyk 185	cloudy, homogenous liquid
Natrosol 250GR	Disperbyk 192	very cloudy solution
	Disperbyk 190	clear, homogenous liquid
	Disperbyk 187	clear, homogenous liquid
	Disperbyk 185	cloudy, homogenous liquid

3.1.1 Rheology of Thickener and Dispersant Blends

The addition of surfactants or dispersants in a paint formulation with associative thickeners can both negatively and positively impact the paint system. Associative thickeners consist of hydrophobic and hydrophilic regions similar to surfactants and some dispersants, where they can self-associate forming micelles resulting to unique rheological properties. The addition of surfactants and dispersants to associative thickeners even enhances that unique rheological property making their interaction a subject of great interest. The addition of surfactants and dispersants to associative thickeners can substantially alter the physical properties of the starting polymer in thickener.[22] Upon addition of surfactant or dispersants there is an increase in viscosity in the system until a critical concentration is reached, past this concentration a viscosity drop in the system is observed. This phenomenon can be seen with the addition of colorant to a paint base. Colorants are stabilized by surfactants and upon the addition of the colorant to a base paint, as viscosity drop is observed. The mechanism of this can be described in Figure 18.

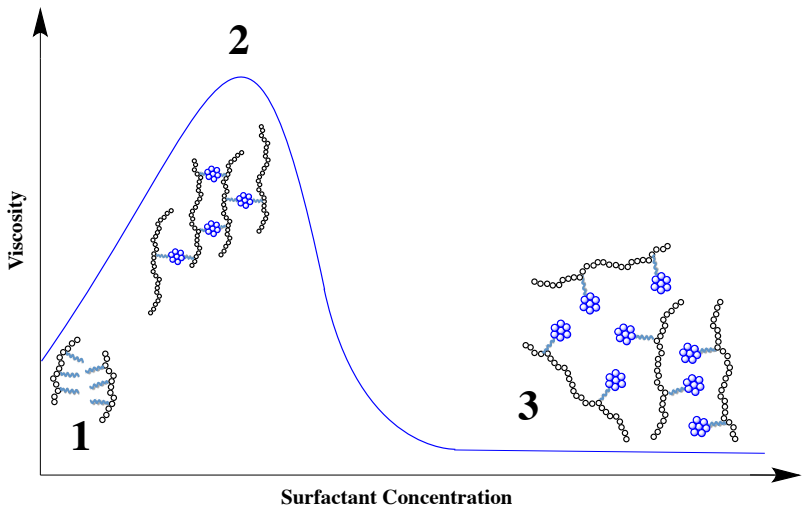

Figure 18. A schematic illustration of the influence of surfactant concentration on the viscosity of dispersions of associative thickeners.

Upon the addition of surfactant, there is an increase in viscosity due to hydrophobic interactions between the hydrophobic moieties from the associative thickener and the surfactant as seen in region 1. In region 2, the hydrophobic moieties from both the thickener and surfactant are interacting with each other forming a network, resulting an increase in the viscosity of the solution. In this network, a number of bridging chains appear and crosslink the hydrophobic micelles together into clusters. The highest viscosity was observed at a critical concentration of surfactant and a region where a viscosity drop was then observed (region 3). This is due to the competitive adsorption of surfactants.[21-24] The increase in surfactant concentration resulted in an increase of surfactant molecules in the system therefore there was a competition for adsorption sites between the thickener and surfactant molecules. As a result, the bridges and network that were previously formed are broken down, thus lowering the viscosity of the system.

The viscosity profile for a low viscosity fluid is typically Newtonian. The associative thickener and dispersant mixtures have low viscosities therefore their rheological profile are

Newtonian. The associative thickeners used can be categorized into two different groups “old generation HEUR” and “new generation HEUR”. HEUR RM-995 is considered as a “new generation HEUR” because it was recently developed and reformulated relative to HEUR RM-825, which has been available for the past three decades. HEUR RM-995 was recently introduced to minimize the tint base viscosity drop. Figure 19 and 21 show graphs of HEUR RM-825 and HEUR RM-995, respectively, with four different dispersants. Figure 20 and Figure 22 show graphs describing the change in viscosity as the concentration of dispersant is increased upon addition to HEUR RM-825 and HEUR RM-995, respectively.

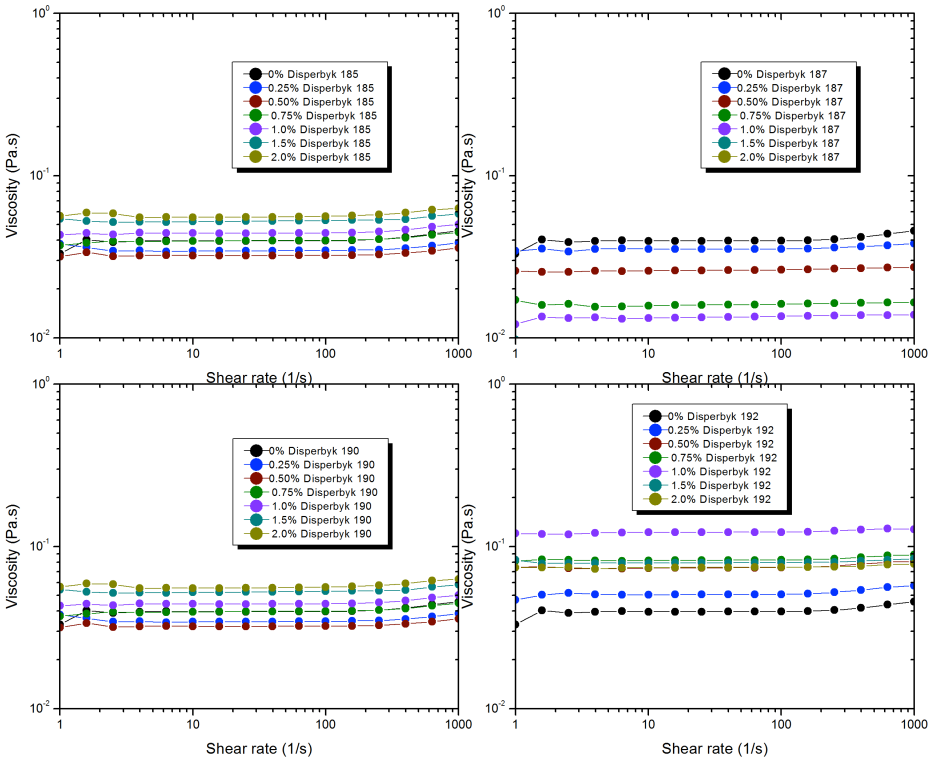

Figure 19. Rheological profiles of HEUR RM-825 with four different dispersants: Disperbyk 185 (top left), Disperbyk 187 (top right), Disperbyk 190 (bottom left), and Disperbyk 192 (bottom right).

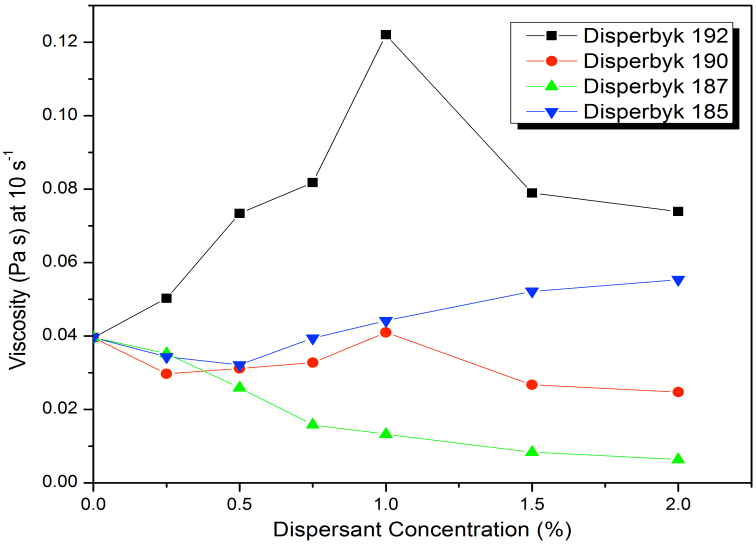

Figure 20. Graph of viscosity at 10 s^{-1} versus dispersant concentration to monitor the viscosity change upon the addition of dispersants for mixtures with HEUR RM-825 with four dispersants.

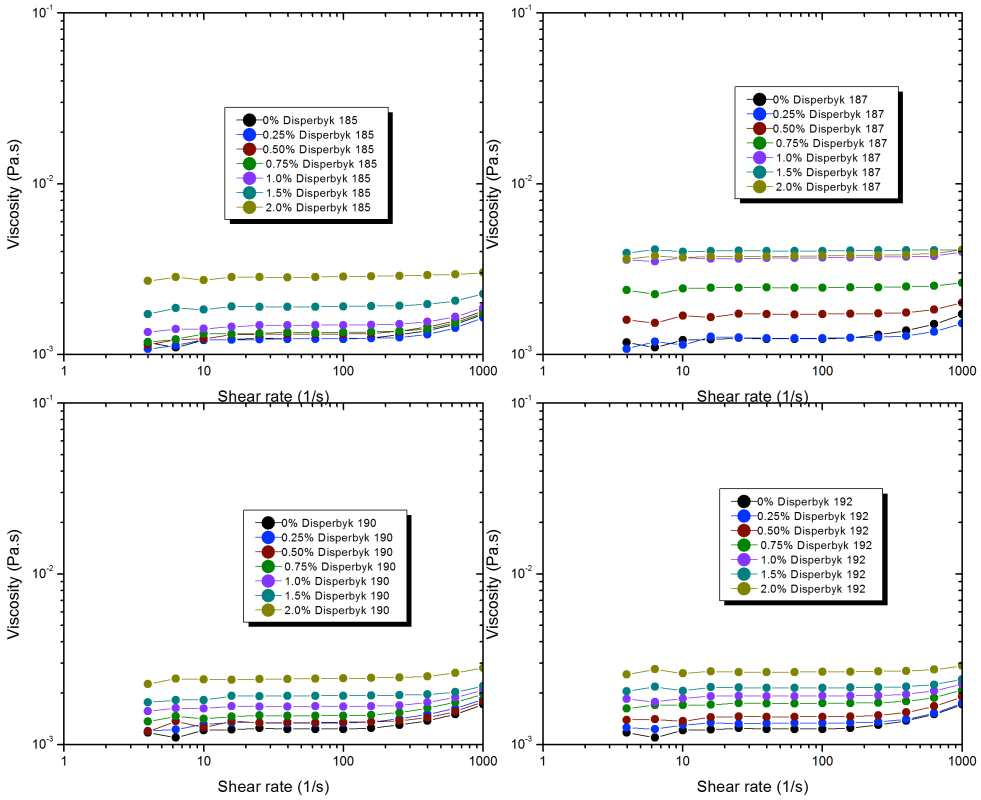

Figure 21. Rheological profiles of HEUR RM-995 with four different dispersants: Disperbyk 185 (top left), Disperbyk 187 (top right), Disperbyk 190 (bottom left), and Disperbyk 192 (bottom right).

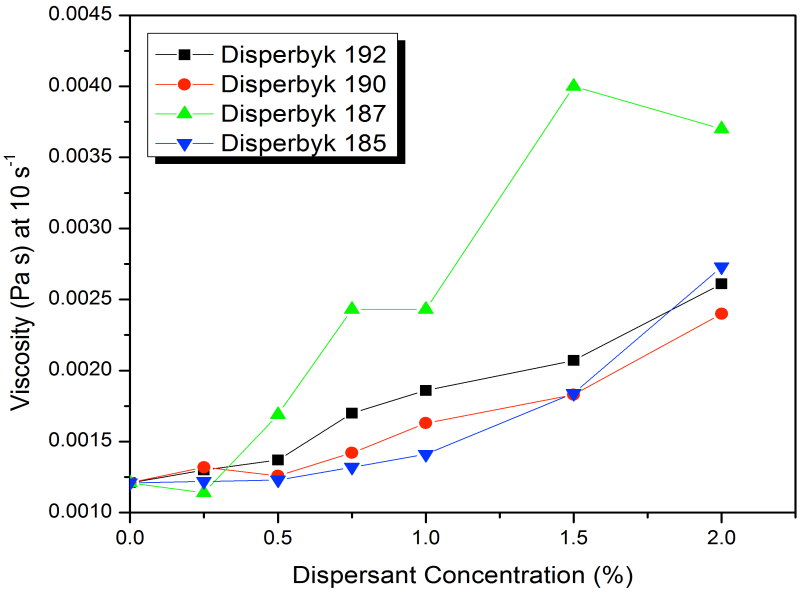

Figure 22. Graph of viscosity at 10 s^{-1} versus dispersant concentration to monitor the viscosity change upon the addition of dispersants for mixtures with HEUR RM-995 with four dispersants.

HEUR RM-825, showed a definitive viscosity maximum as a function of the dispersant concentration. However, HEUR RM-995 did not indicate a viscosity maximum; instead it showed a small, but linear increase in viscosity as dispersant level was increased.

3.2 Latex/Associative Thickener and Latex/Associative Thickener/Surfactant Dispersions

3.2.1 Rheology

The main focus of the next part of the project is to study the effects of thickener concentration on the viscosity of a 25% (vol) dispersion of latex. Results are shown in Figure 23.

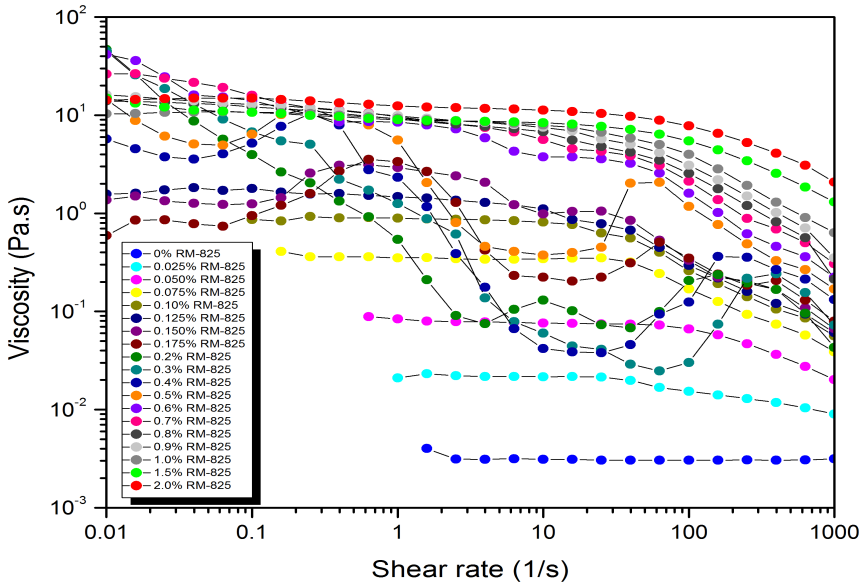

Figure 23. Viscosity dependence on shear rate of latex and HEUR thickener aqueous mixtures.

The stable latex-HEUR mixtures at low HEUR levels (0%-0.125%) show shear-thinning viscosity with well-defined low-shear rate Newtonian plateaus. As HEUR level is increased wherein syneresis is observed (0.15%-0.7%), as shown in Figure 5, erratic rheological profiles with shear-thickening is observed. When HEUR level is increased to a region where no syneresis is observed (08%-2.0%), low-shear rate Newtonian plateaus re-apperaed albeit at higher viscosities. One possible mechanism of the shear-thickening observed is due to the shear induced association of the associative thickener, surfactant, and latex. Data from Figure 23 representing samples that showed a complex rheological profile were replotted in Figure 24.

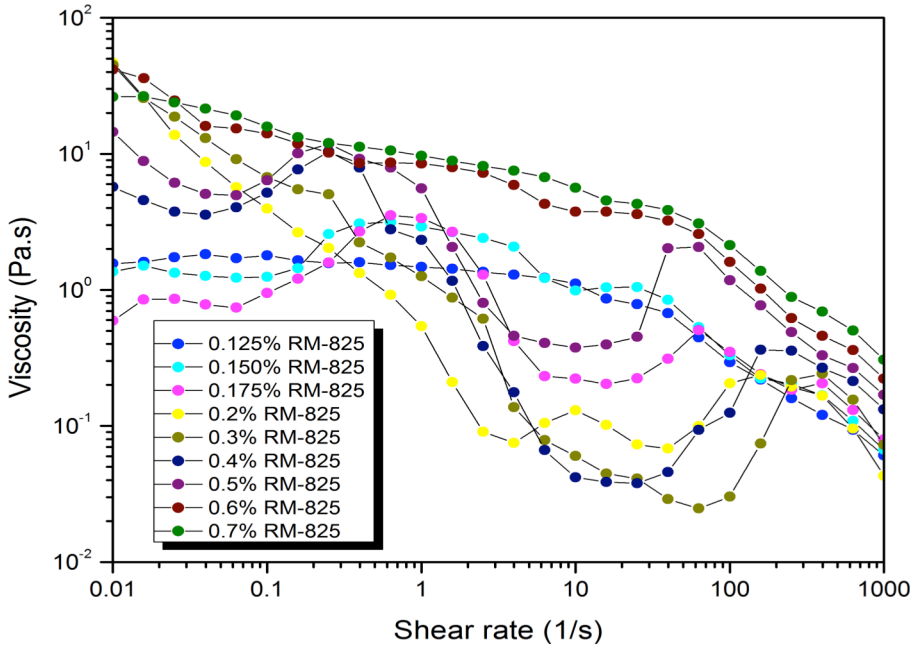

Figure 24. Viscosity dependence on shear rate of latex and HEUR thickener at 0.125%-0.7% addition of thickener in the dispersions.

Between 0.15% and 0.3% HEUR level, the 2nd viscosity maximum shifted to a higher shear rate. However, between 0.4% and 0.7% HEUR level, an opposite trend was observed, where the 2nd viscosity maximum shifted to a lower shear rate until low-shear rate Newtonian plateaus reappeared at higher HEUR levels. Between the addition of 0.8% and 2.0%, a saturation point was reached where the viscosity of the system did not change significantly. The trend observed is due to stronger associations until the addition of 0.4% HEUR thickener where the shear-thickening moved to lower shear rates as the HEUR level was increased. The erratic rheological profiles observed can also be due to reversible, nonequilibrium associations of the hydrophobic moieties in the system.

Upon the addition of surfactants (nonionic and anionic) the complex or erratic rheological profiles disappeared, being replace by low-shear rate Newtonian plateaus, as shown in Figure 25. This is an evidence of the added stability provided by surfactants.

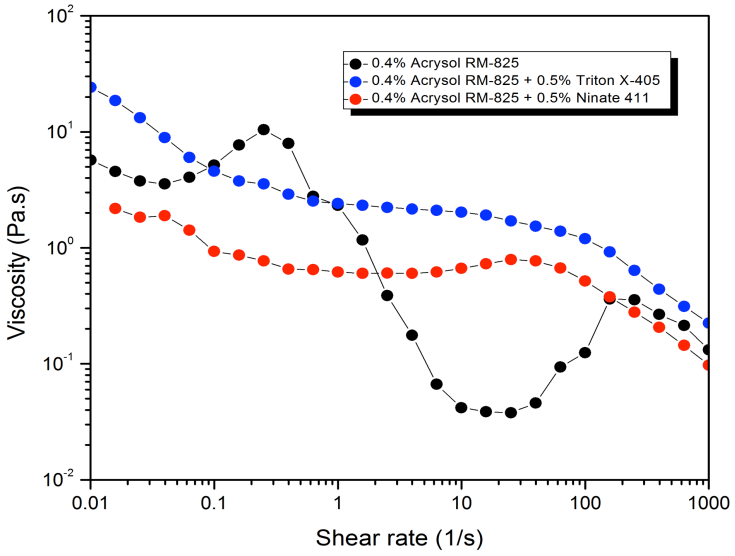

Figure 25. Viscosity dependence on shear rate of latex, HEUR thickener, and surfactant dispersions.

3.2.2 Phase Behavior

Phase behavior results form syneresis test are shown in Figure 26 while detailed descriptions of phase separated dispersions are shown in Table 4.

Table 4. Description of Phase Separated Dispersions.

Sample	Top Layer (cm)	Total Height (cm)	Phase Separation (%)	Comments
0.150%	3.0	8.9	33.7	Top layer milky, hard to distinguish from bottom layer without extra lighting
0.175%	3.0	8.9	33.7	Top layer milky but relatively easier to see
0.200%	2.9	8.9	32.6	Top layer less milky, height was progressively decreasing
0.300%	2.6	8.9	29.2	Top layer still milky, height less than the 0.2%
0.400%	2.2	8.9	24.7	Top layer cloudy, more transparent than 0.3% but decreased in height
0.500%	1.9	8.9	21.3	Top layer cloudy but more transparent, height decreased
0.600%	1.4	8.9	15.7	Top layer cloudy and more transparent, height of separation decreased
0.700%	0.8	8.9	9.0	Top layer cloudy and transparent, significantly less separation relative to other samples

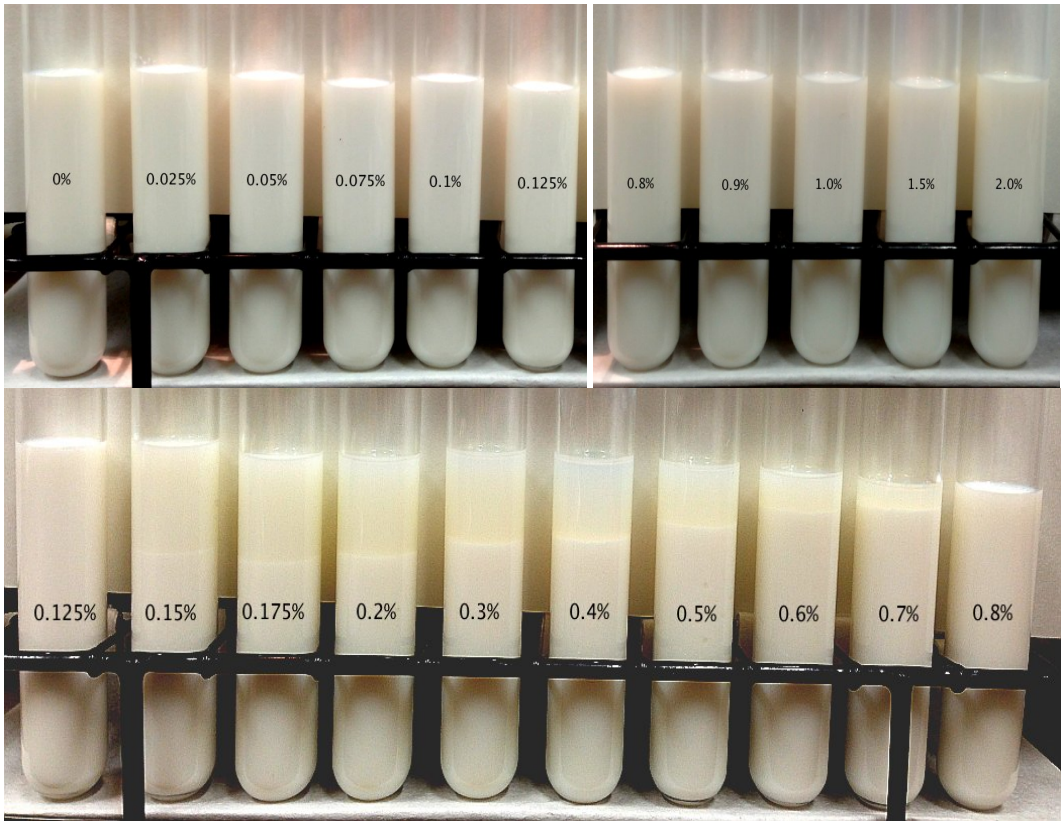

Figure 26. Photographs of syneresis test.

In the syneresis test, phase separation was observed between the HEUR thickener addition of 0.15% and 0.7%. This correlates with the rheology. The dispersion with HEUR thickener level that showed phase separation showed a complex rheology characterized by shear-thickening bumps with at least two viscosity maxima. At HEUR thickener level where the rheological profiles were Newtonian at lower shear rate and shear-thinning at higher shear rates, no phase separation was observed. This shows a clear correlation between the rheology and phase behavior of these systems.

Upon the addition of surfactants, the complex rheology disappeared and the dispersions with phase separations no longer showed any phase separation. This indicates a well-dispersed system without bridging or depletion flocculation.

4 Conclusions

In studies where the rheological profiles were analyzed with thickeners and dispersants, it is evident that the addition of dispersants to thickeners caused an increase in viscosity until a critical concentration is reached, which is then followed by a drop in viscosity. This phenomenon is based on the hydrophobic interactions between the thickener and dispersant molecules. This phenomenon however was not observed with the addition of the "new generation HEUR" HEUR RM-995.

In the second part of this study where latex, associative thickener, and surfactants were examined, the rheological and phase behaviors of the systems were highly dependent on the HEUR level and the surfactants used. A clear correlation between rheological behavior and phase behavior has been demonstrated for the system studied. Such a correlation has not been reported. In order to achieve superior paint properties, the latex, associative thickeners, and surfactants must be carefully selected.

5 Future Work

For the next steps of this project, a study of fully formulated systems will be conducted. In this study, we can see if we can observe the same trend and if inorganic particles such as pigments and fillers have an effect in the system. In addition, a detailed optical microscopy study will be done to observe polymer bridges. Lastly, dynamic oscillatory testing will be conducted to study the viscoelastic property of different dispersions, along with creep and recovery testing to study the dispersions behaviors.

References

(1) Wicks Jr. Z.; Jones, F.; Pappas, S.; Wicks, D. *"Organic Coatings: Science and Technology, Third Edition."* Wiley-Interscience. © 2007 by John Wiley & Sons, Inc.

(2) Schoff, C.K. Rheology. Federation Series on Coatings Technology. 1991, 1-41

(3) Tego, E. Technical Background Rheological Additives. 2012, 1–10.

(4) Saucy,D. Avoiding Viscosity Loss on Tinting. Paint & Coatings Industry 2008, 24, 2–5.

(5) Kostansek, E. Using dispersion/flocculation phase diagrams to visualize interactions of associative polymers, latexes, and surfactants. J. Coatings Tech. 2003, 75, 1–8.

(6) Otsubo, Y. Rheology control of suspensions by soluble polymers. Langmuir 1995, 11, 1893–1898.

(7) Otsubo, Y. Effect of surfactant adsorption on the polymer bridging and rheological properties of suspensions. Langmuir 1994, 10, 1018–1022.

(8) Kostansek, E. Controlling particle dispersion in latex paints containing associative thickeners. J Coat Technol Res 2007, 4, 375–388.

(9) Horigome, M.; Otsubo, Y. Long-Time Relaxation of Suspensions Flocculated by Associating Polymers. Langmuir 2002, 18, 1968–1973.

(10) American Coatings Association: "*Historical Context*." https://www.paint.org/about-our-industry/historical-context.html (accessed November 2, 2013)

(11) Weldon, D.G. "*Failure Analysis of Paints and Coatings*." Wiley-Interscience. © 2001 by John Wiley & Sons, Inc.

(12) Graessley, W. "*The Entanglement Concept in Polymer Rheology*." Berlin: Springer-Verlag, 1974.

(13) Koleske, J. V. *Paint and Coating Testing Manual: Fourteenth Edition of the Gardner-Sward Handbook*. Philadelphia, PA: ASTM, 1995.

(14) Fernando, R.H. Lecture Slides: Rheology Modifiers. Cal Poly San Luis Obispo Polymers and Coatings. Spring 2012

(15) Dziwok, K. Associative Thickeners for Viscosity Retention Upon Thickening. *Paint and Coatings Industry.* [Online]. http://www.pcimag.com/articles/associative-thickeners-for- viscosity-retention-upon-tinting

(16) Wang, L.; Tiu, C.; Liu, T.-J. Effects of nonionic surfactant and associative thickener on the rheology of polyacrylamide in aqueous glycerol solutions. Colloid and Polymer Science 1996, 274, 138–144.

(17) Butt, H.; Karlheinz G.; Michael K. "*Physics and Chemistry of Interfaces" WILEY-VCH GmbH & Co . KGaA*. 2003.

(18) Manion, S. J.; Johnson, L. L.; Fernando, R. H. Shear-thickening in aqueous surfactant-associative thickener mixtures. *J Coat Technol Res* 2011, *8*, 299–309.

(19) Fellows, C. M.; Doherty, W. O. Insights into bridging flocculation. 2005, *231*, 1–10.

(20) Gaillard, N.; Claverie, J.; Guyot, A. Synthesis and characterization of block-c copolymer surfactants with specific interactions with associative thickeners. Progress in Organic Coatings 2006, 57, 98–109.

(21) Wang, L.; Tiu, C.; Liu, T.-J. Effects of nonionic surfactant and associative thickener on the rheology of polyacrylamide in aqueous glycerol solutions. Colloid and Polymer Science 1996, 274, 138–144.

(22) Mahli, D. M.; Steffenhagen, M. J.; Xing, L.-L.; Glass, J. E. Surfactant behavior and its influence on the viscosity of associative thickeners solutions, thickened latex dispersions, and waterborne latex coatings. J. Coatings Tech. 2003, 75, 39–51.

(23) Piculell, L.; Thuresson, K.; Lindman, B. Mixed solutions of surfactant and hydrophobically modified polymer. Polymers for Advanced Technologies 2001, 12, 44–69.

(24) Svanholm, T.; Molenaar, F.; Toussaint, A. Associative thickeners: their adsorption behaviour onto latexes and the rheology of their solutions. Progress in Organic Coatings 1997, 30, 159–165.

Appendices

Appendix A: pH of Thickener and Dispersant Mixtures

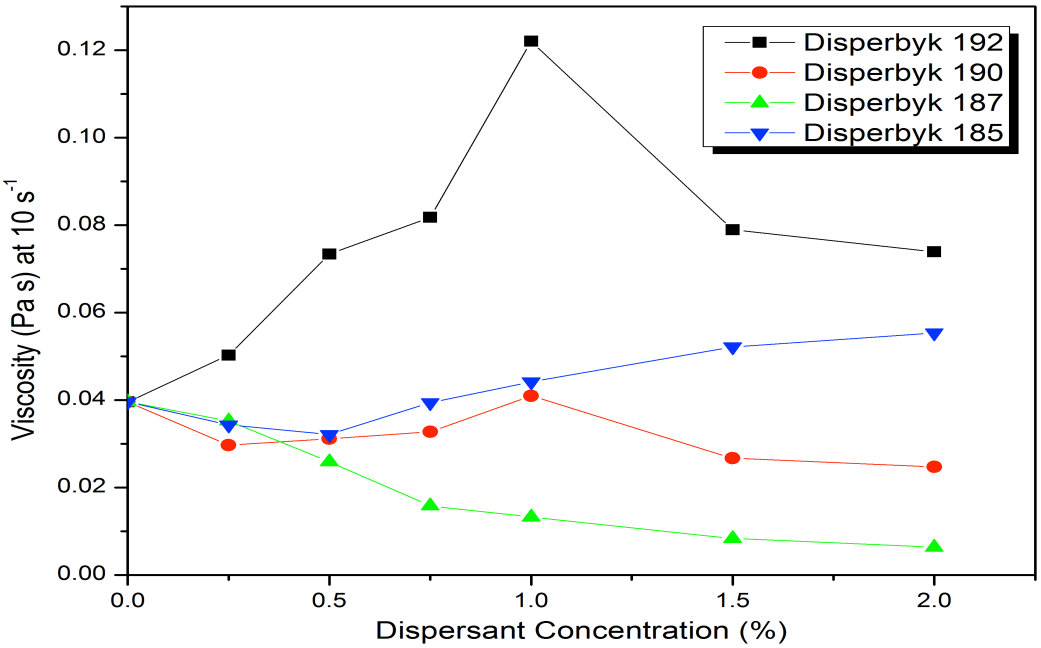

HEUR RM-825 + Dispersants

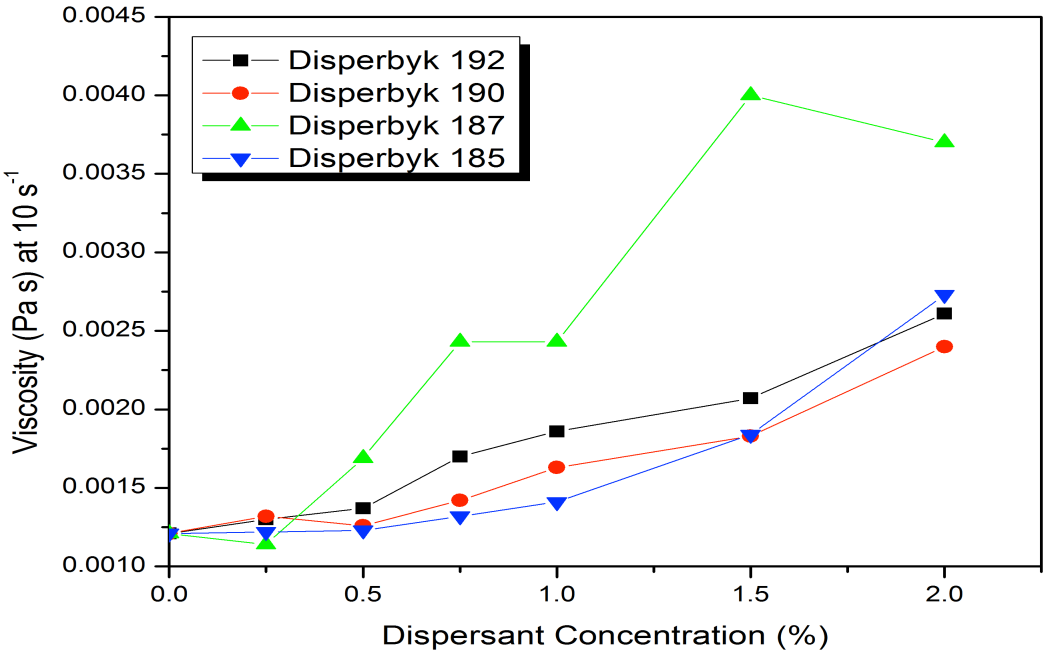

HEUR RM-995 + Dispersants

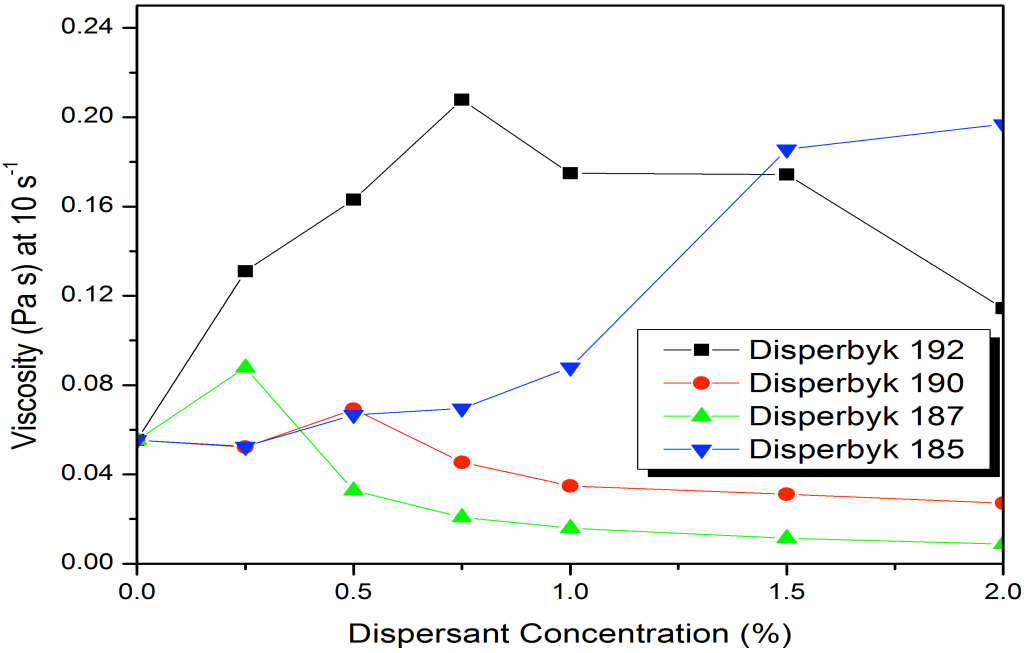

HEUR SCT-275 + Disperbyk

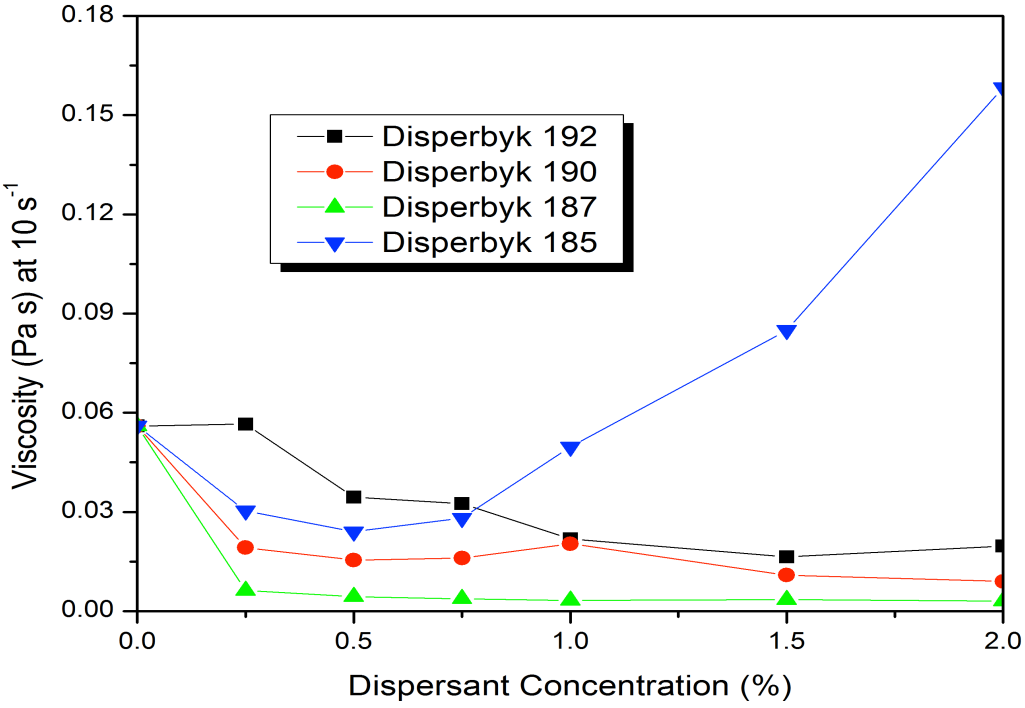

Rheovis PU-1191 + Disperbyk

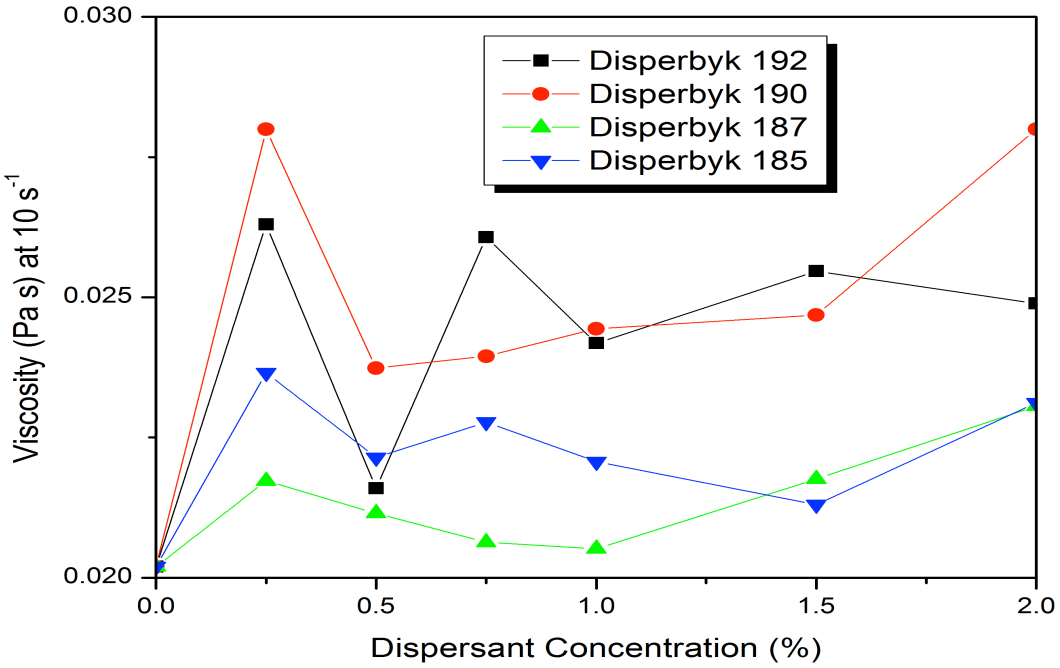

Natrosol 250GR + Disperbyk

Appendix B: Rheological Profiles of Thickener/Dispersant Blends

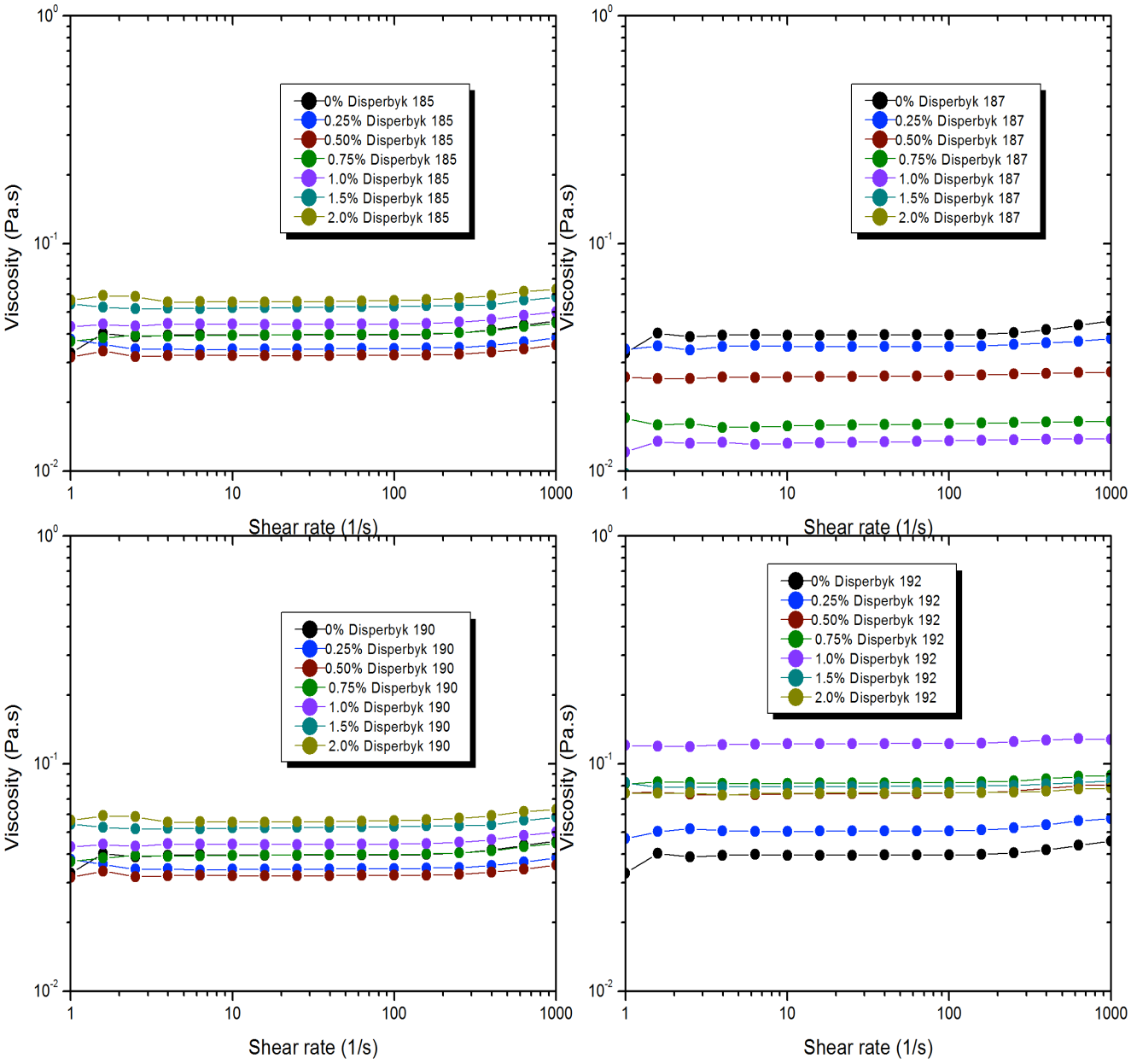

HEUR RM-825 + Dispersants at different loading

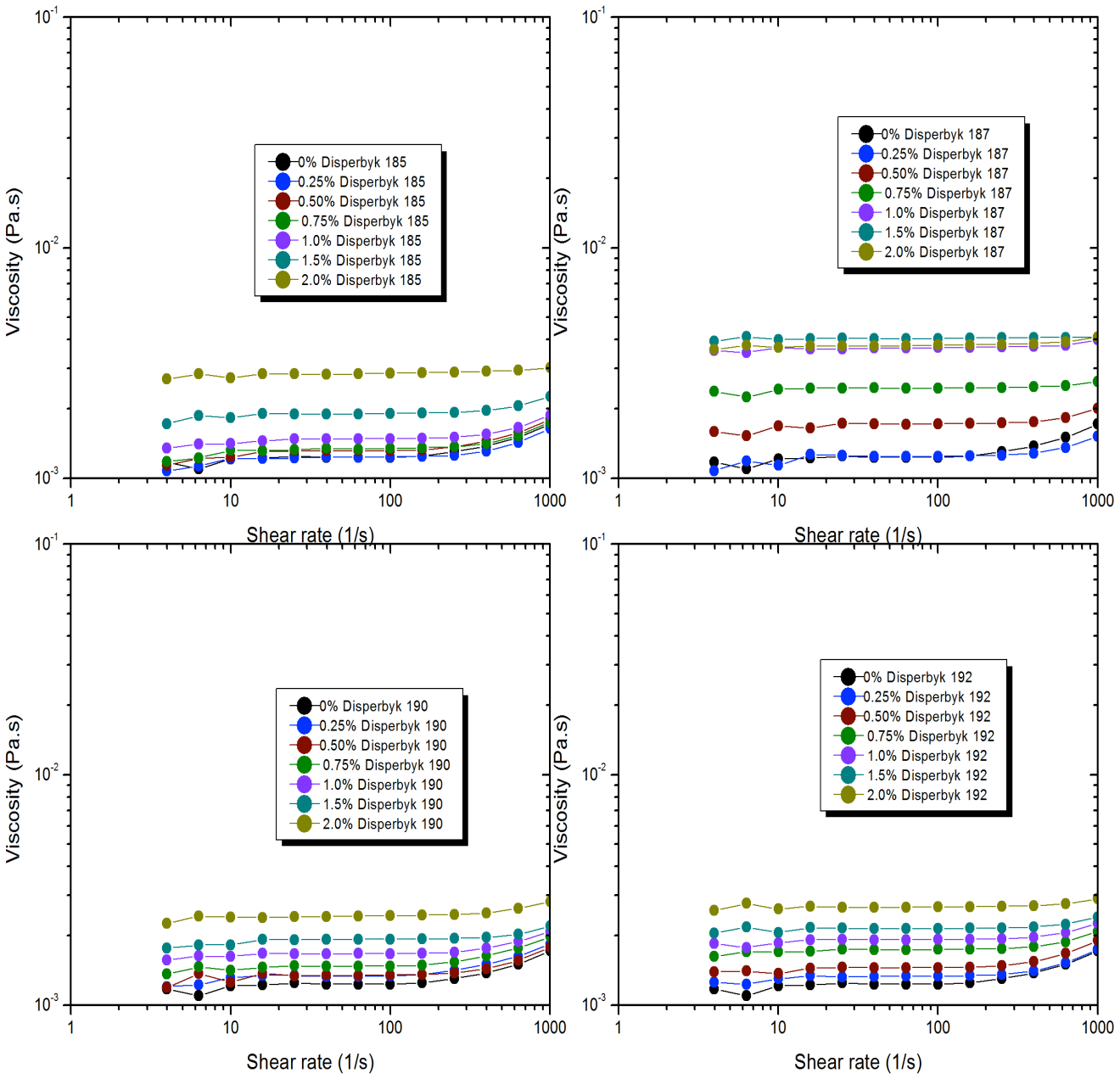

HEUR RM-995 + Dispersants at different loading

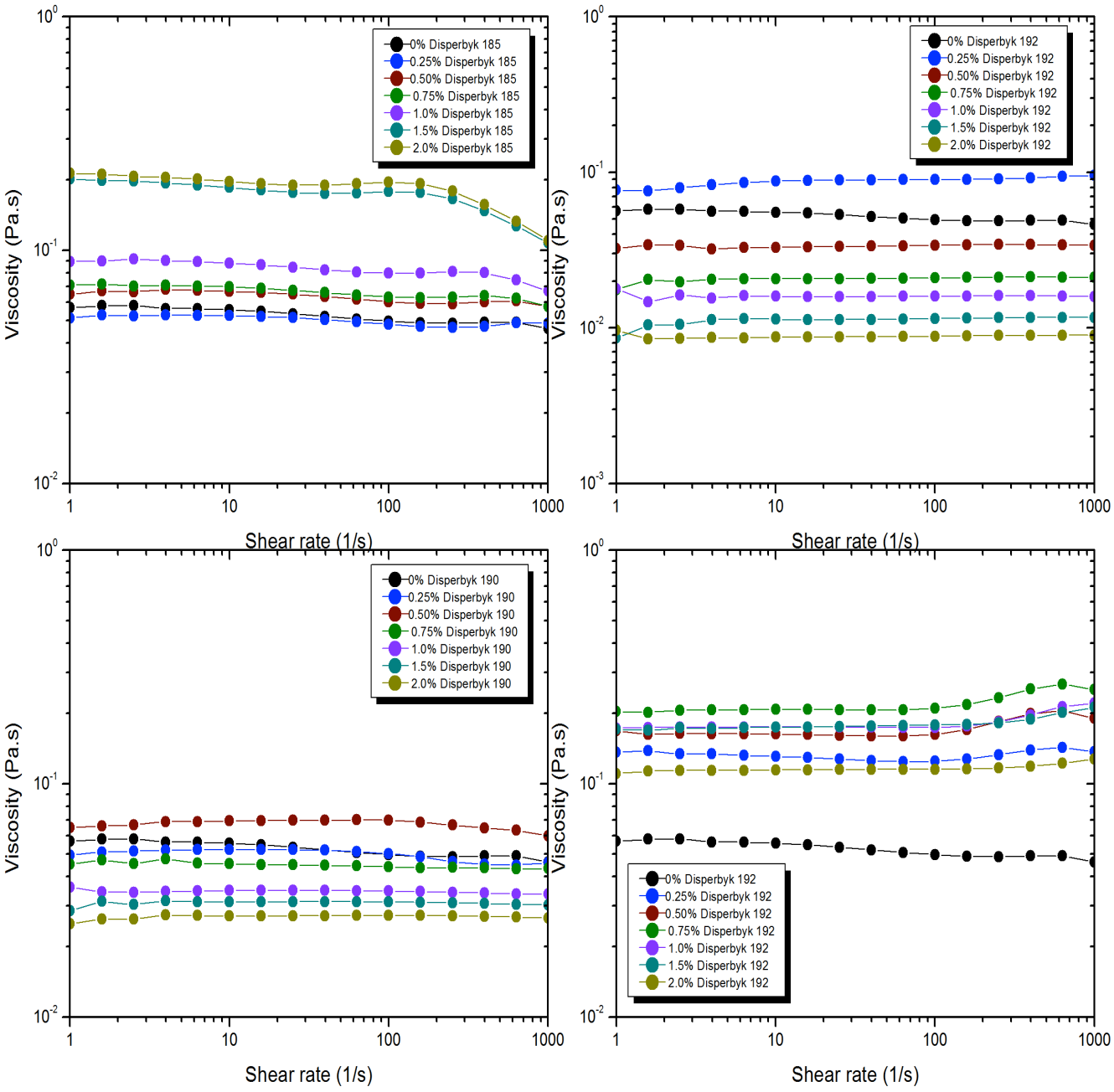

HEUR SCT-275 + Dispersants at different loading

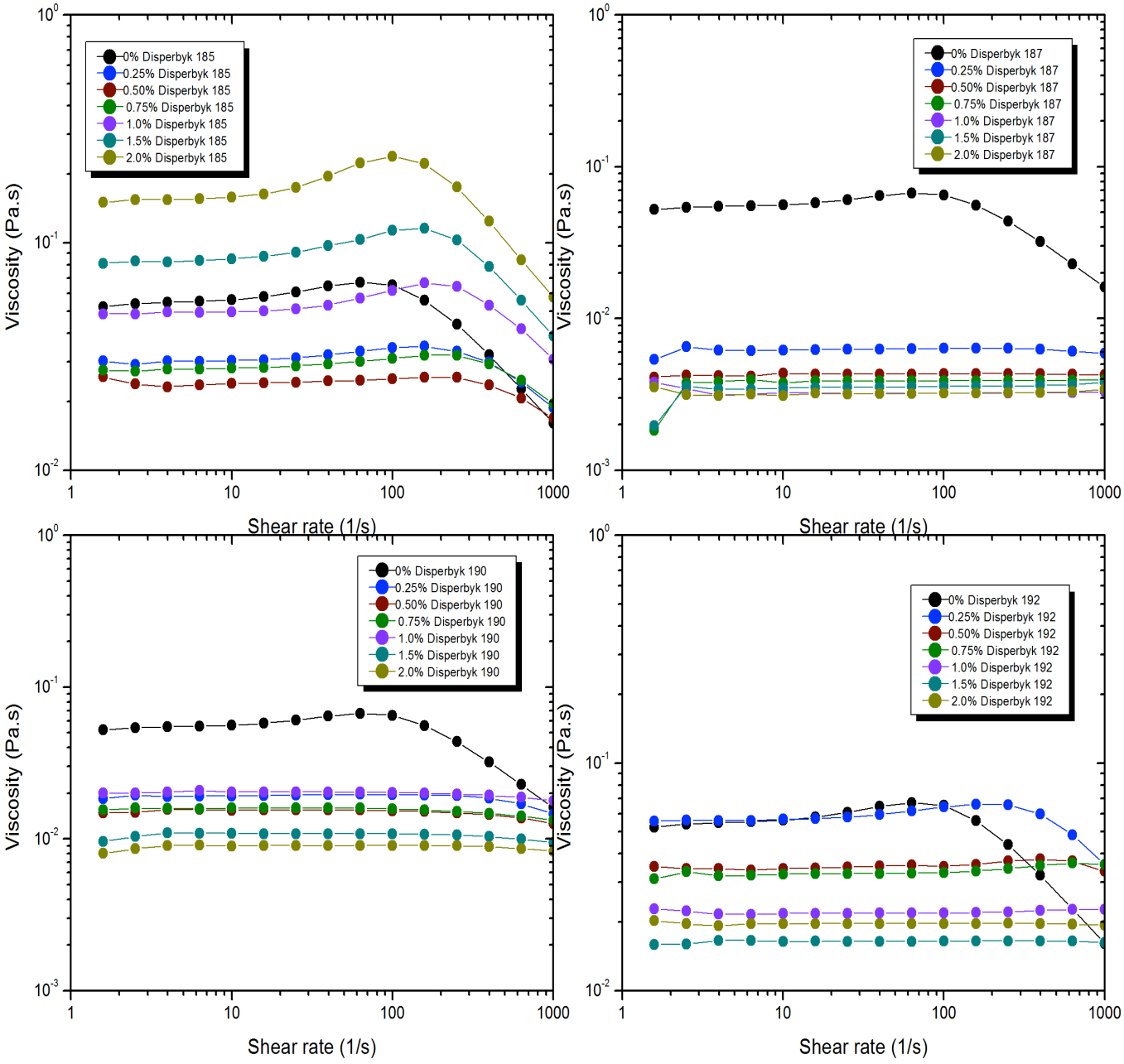

Rheovis PU-1191 + Dispersants at different loading

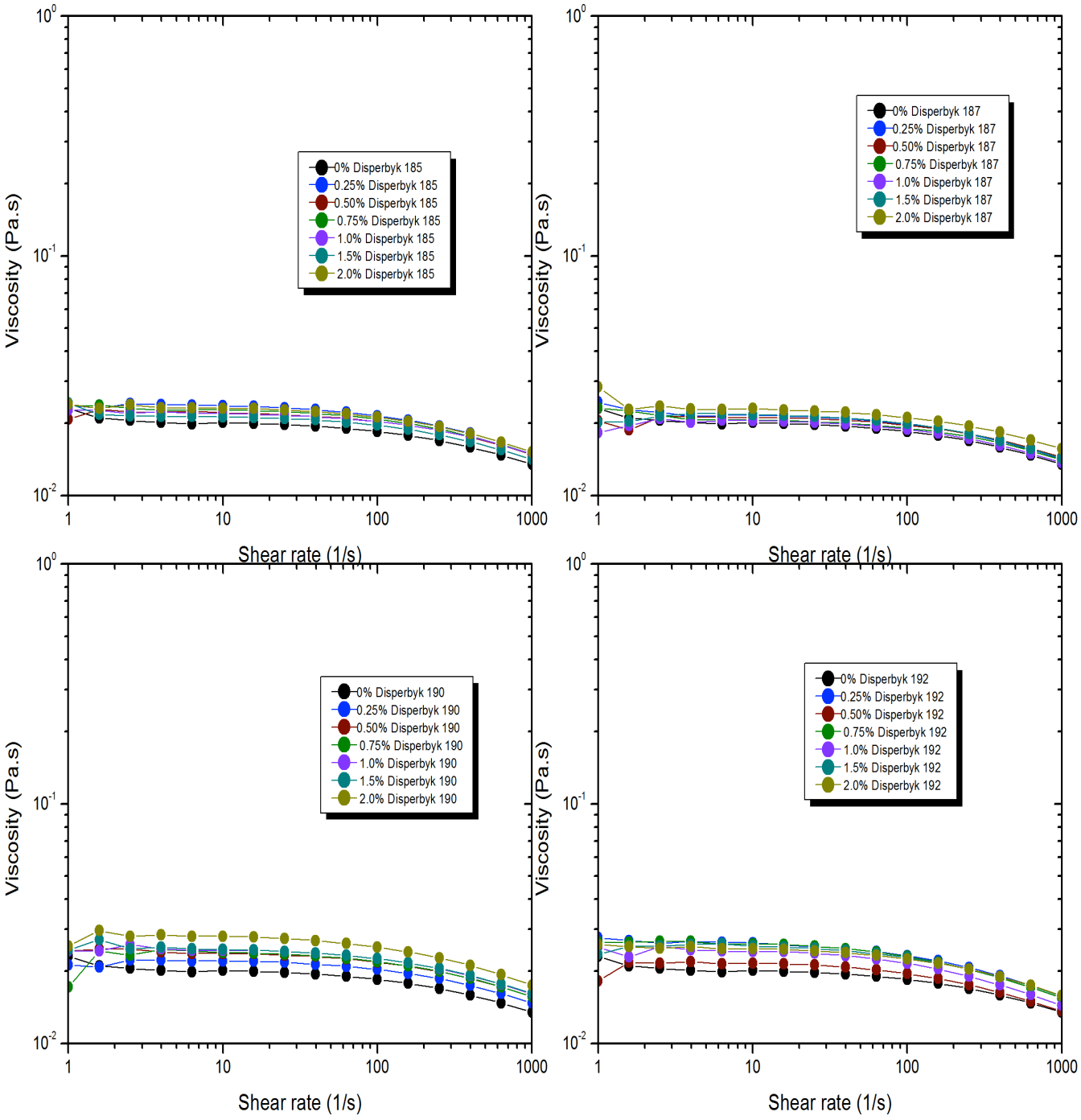

Natrosol 250GR + Dispersants at different loading

Appendix C: Rheological Profiles of Latex/Thickener/Surfactant Study

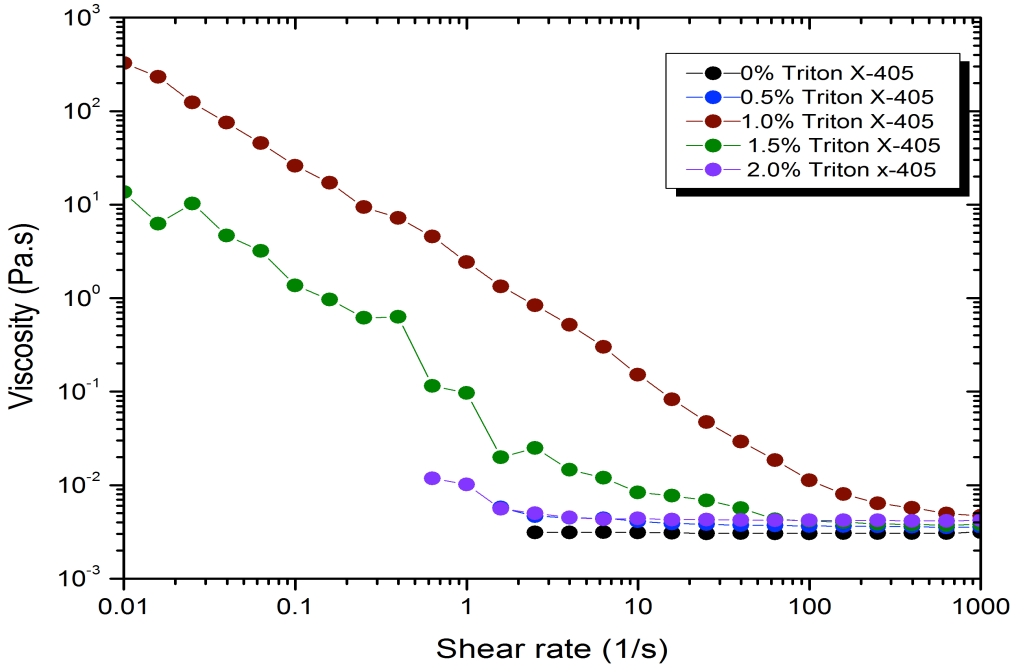

Rhoplex VSR-1050 + 0% HEUR RM-825 + Triton X-405

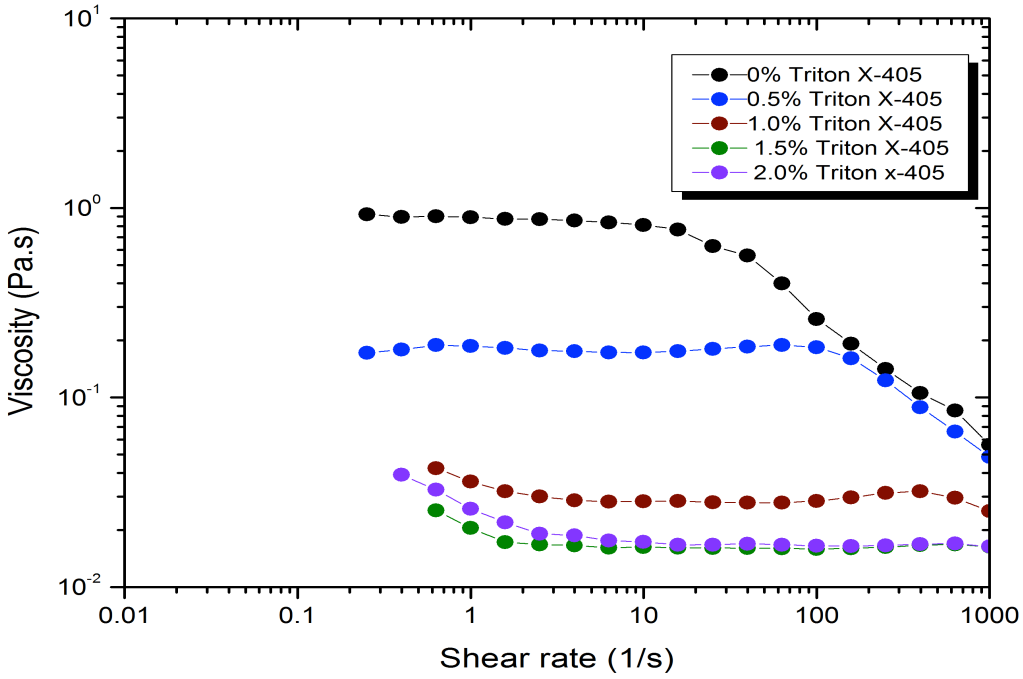

Rhoplex VSR-1050 + 0.1% HEUR RM-825 + Triton X-405

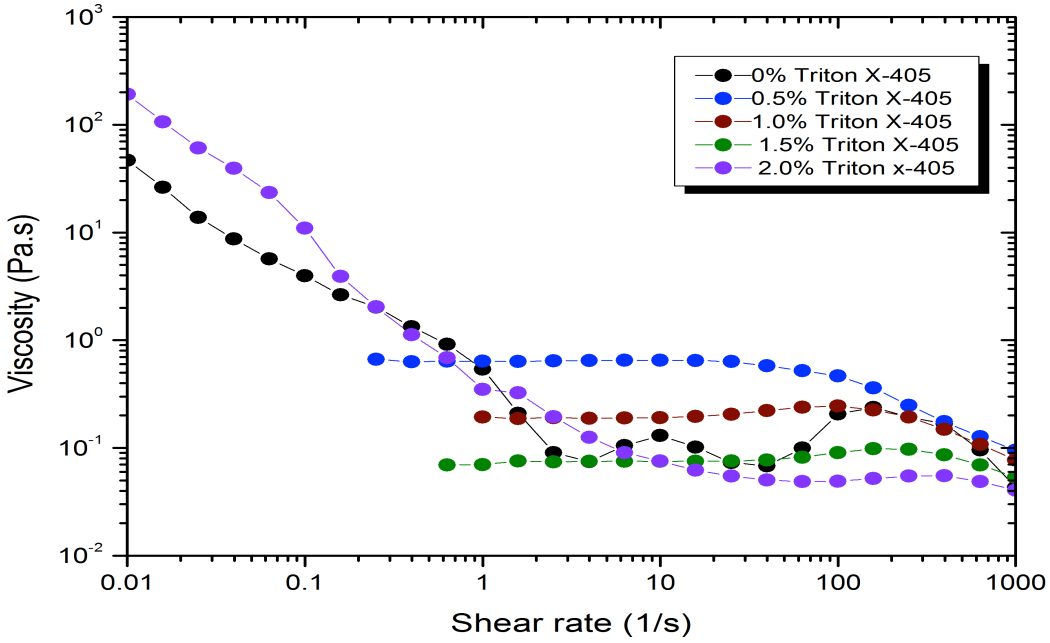

Rhoplex VSR-1050 + 0.2% HEUR RM-825 + Triton X-405

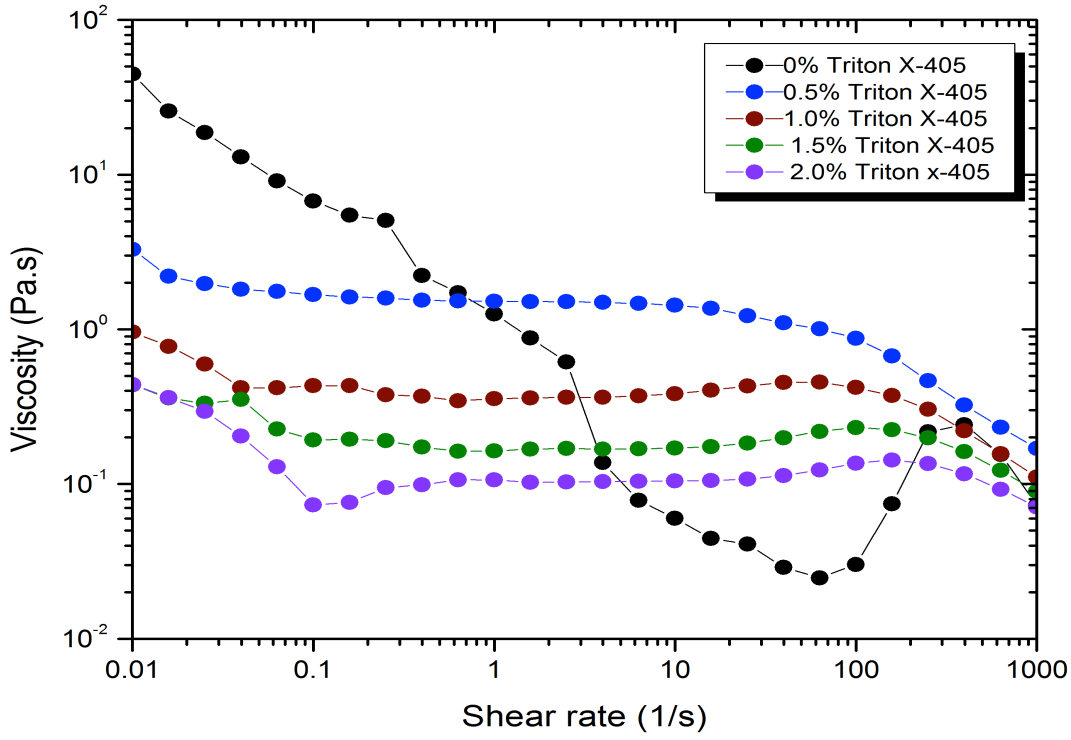

Rhoplex VSR-1050 + 0.3% HEUR RM-825 + Triton X-405

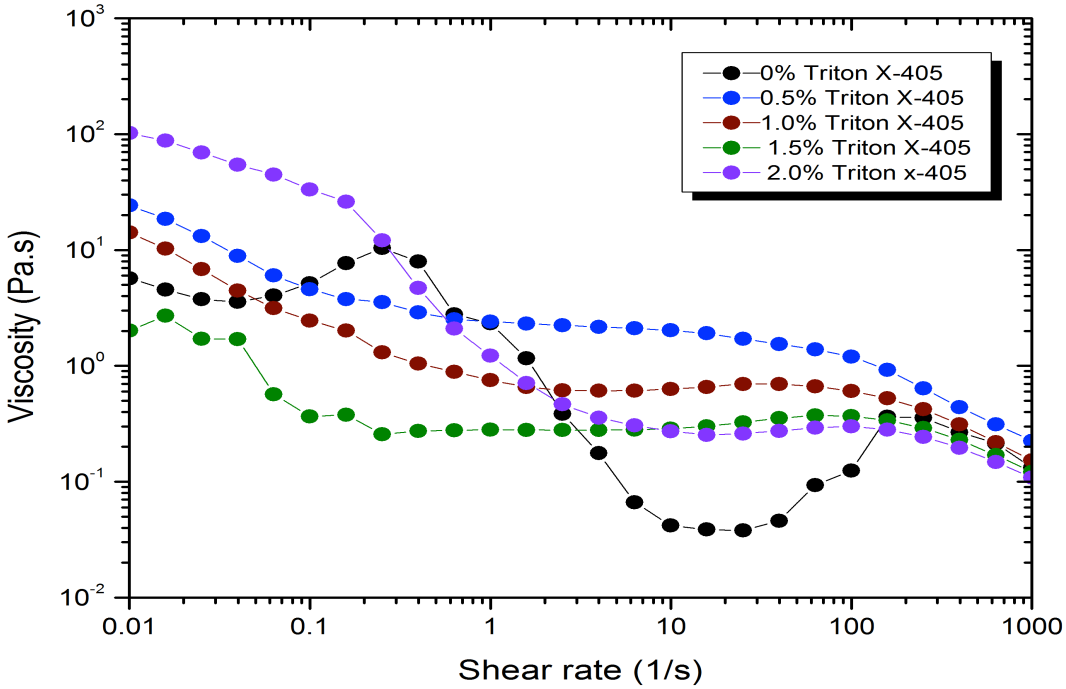

Rhoplex VSR-1050 + 0.4% HEUR RM-825 + Triton X-405

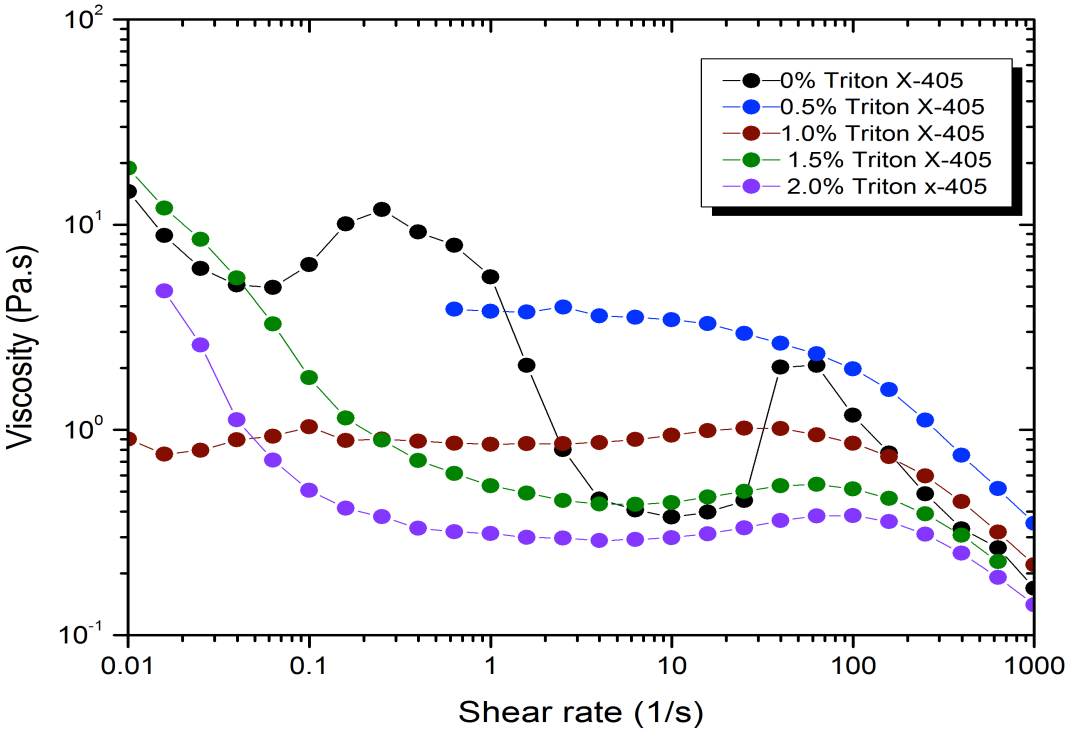

Rhoplex VSR-1050 + 0.5% HEUR RM-825 + Triton X-405

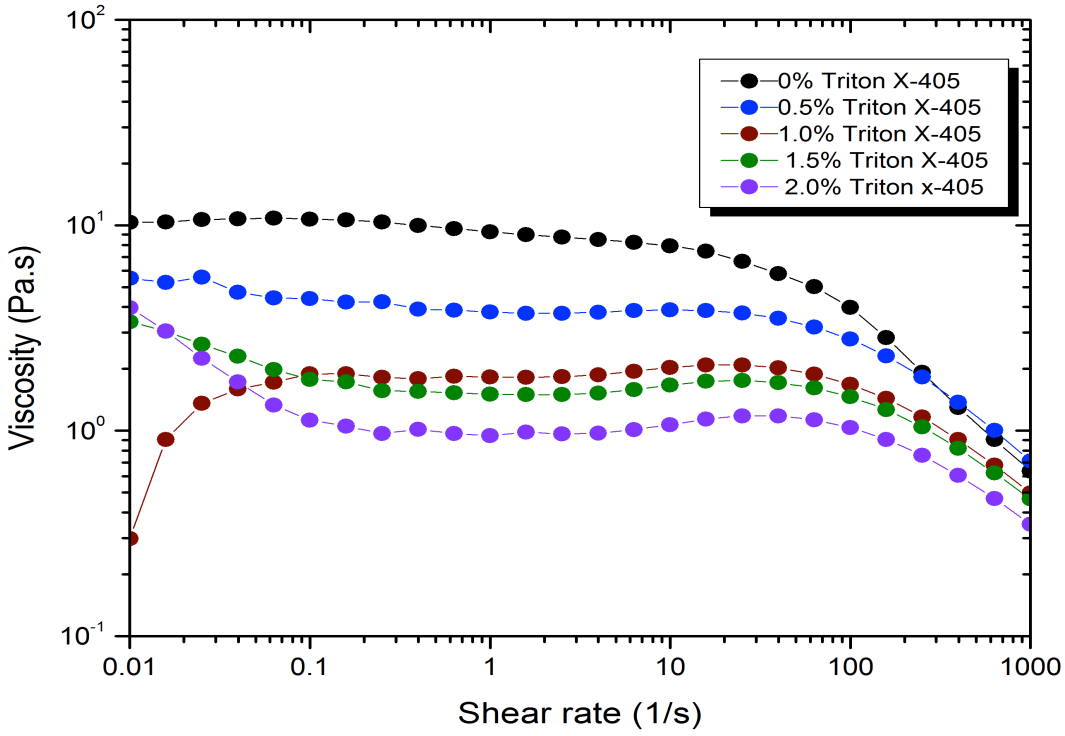

Rhoplex VSR-1050 + 1.0% HEUR RM-825 + Triton X-405

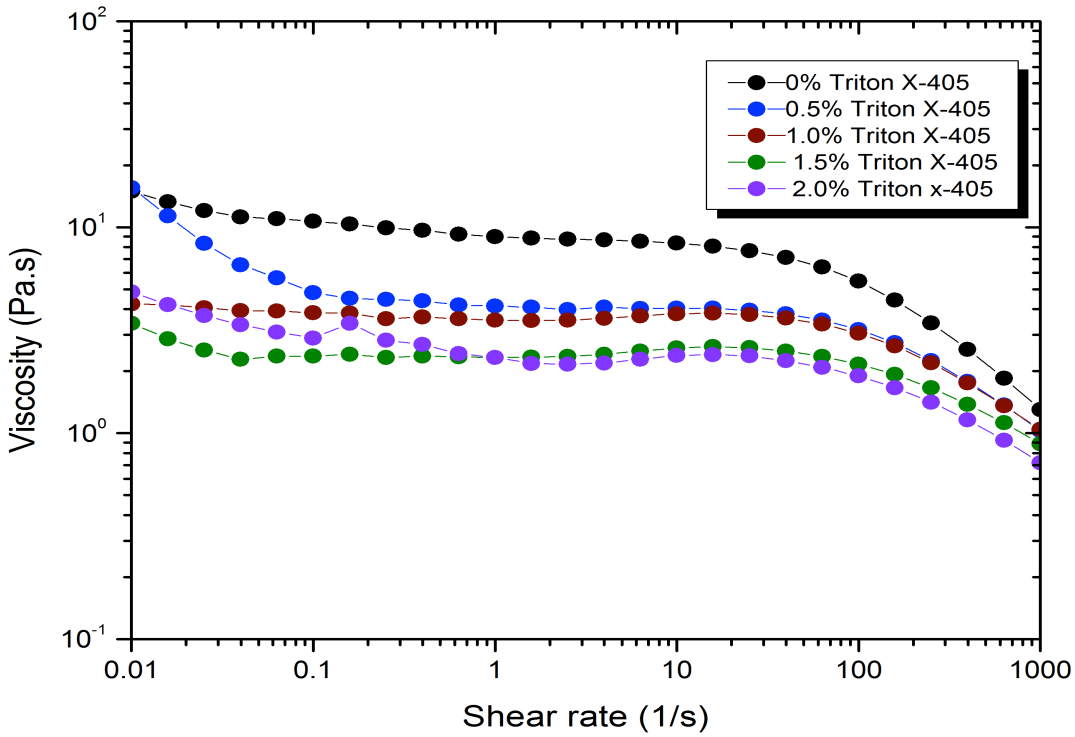

Rhoplex VSR-1050 + 1.5% HEUR RM-825 + Triton X-405

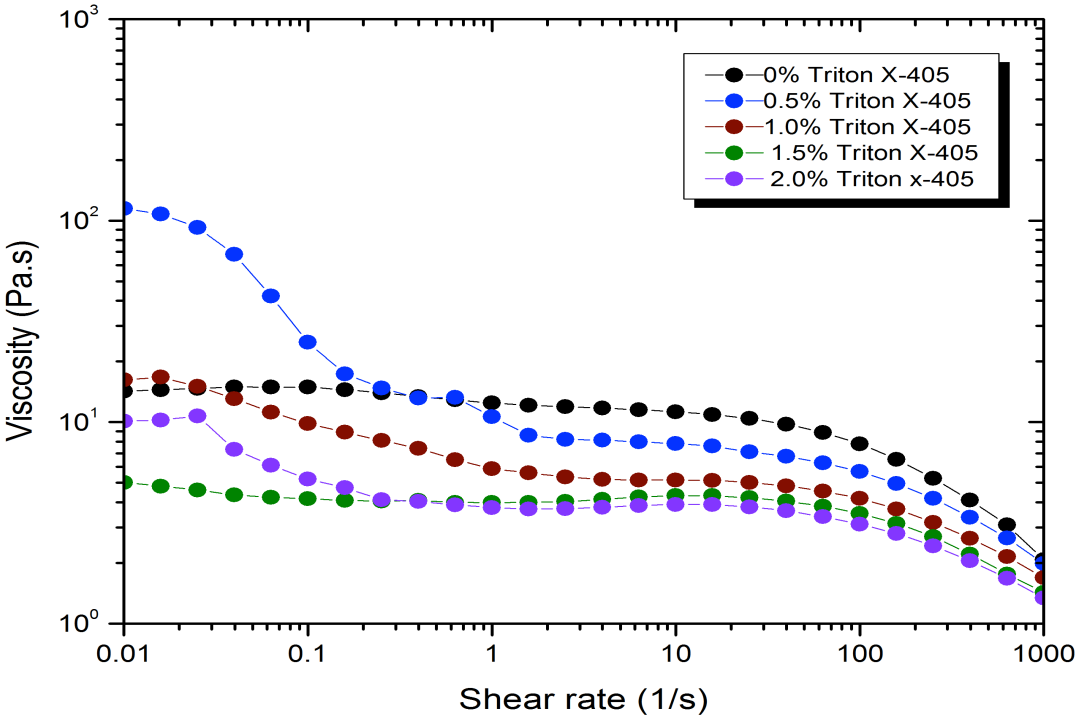

Rhoplex VSR-1050 + 2.0% HEUR RM-825 + Triton X-405

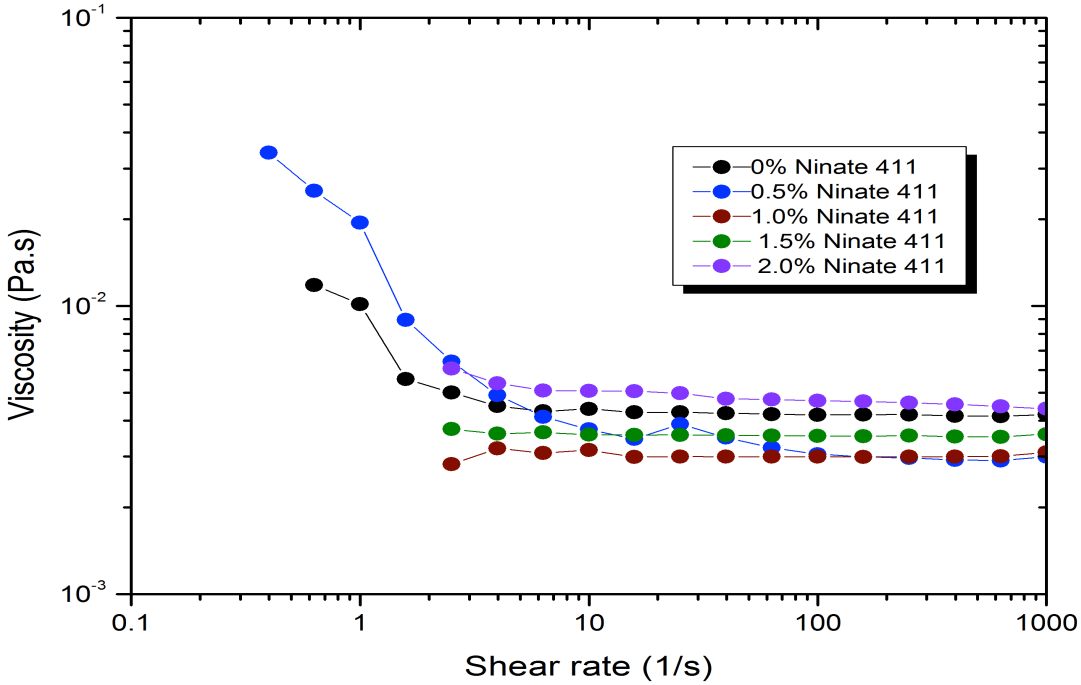

Rhoplex VSR-1050 + 0% HEUR RM-825 + Ninate 411

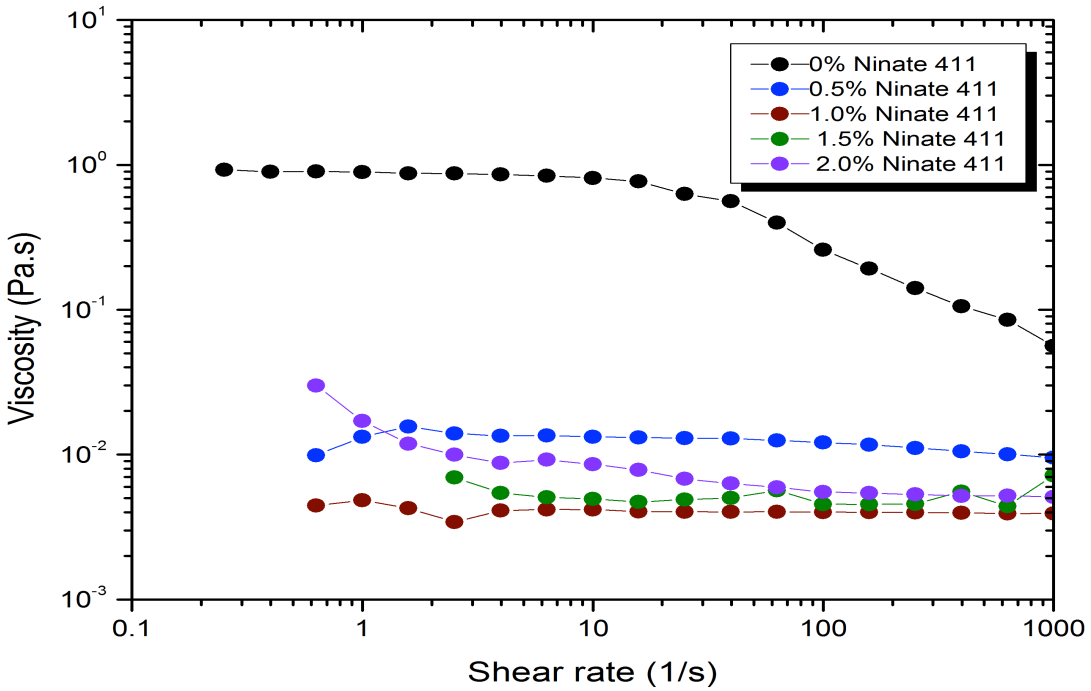

Rhoplex VSR-1050 + 0.1% HEUR RM-825 + Ninate 411

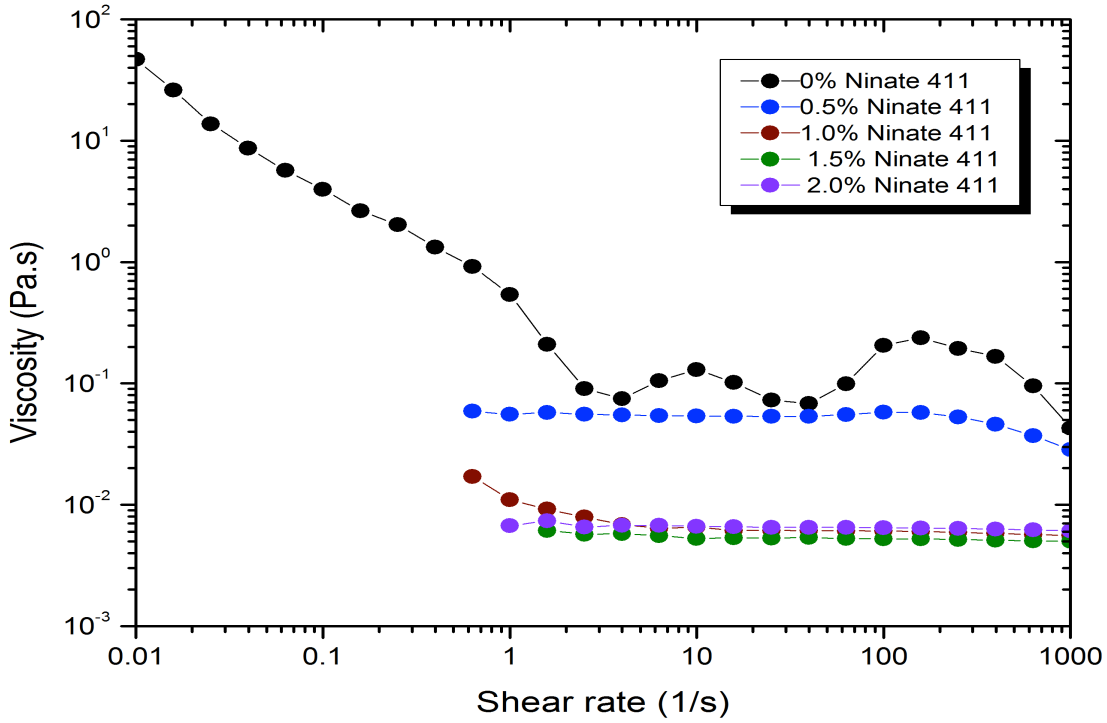

Rhoplex VSR-1050 + 0.2% HEUR RM-825 + Ninate 411

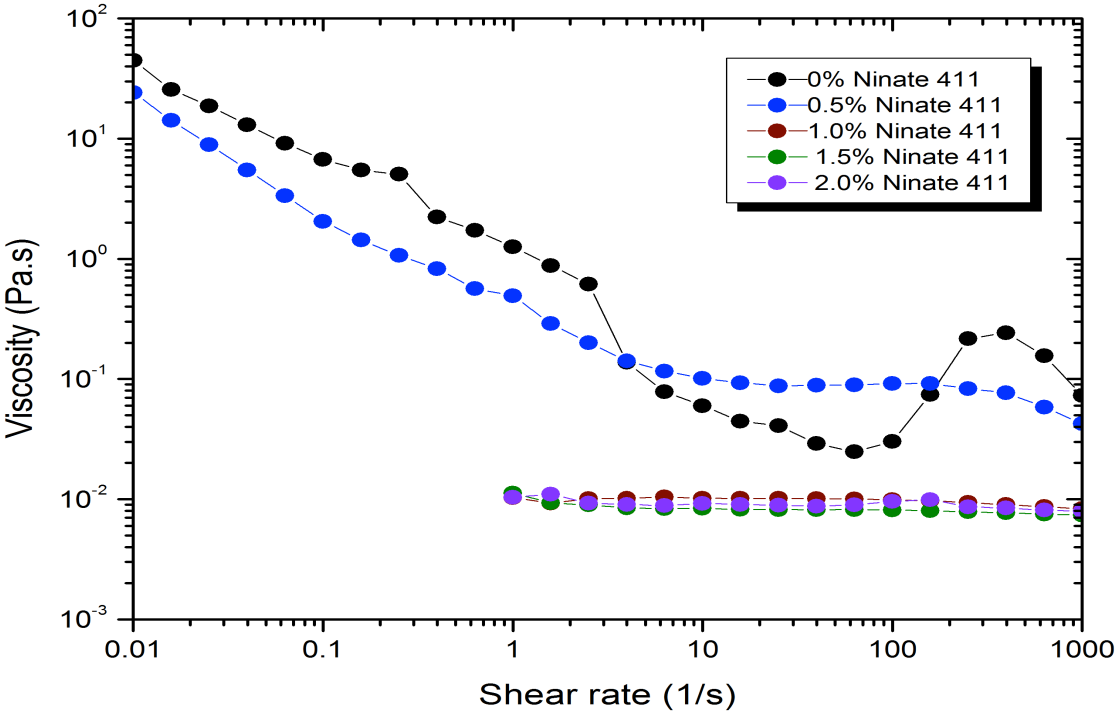

Rhoplex VSR-1050 + 0.3% HEUR RM-825 + Ninate 411

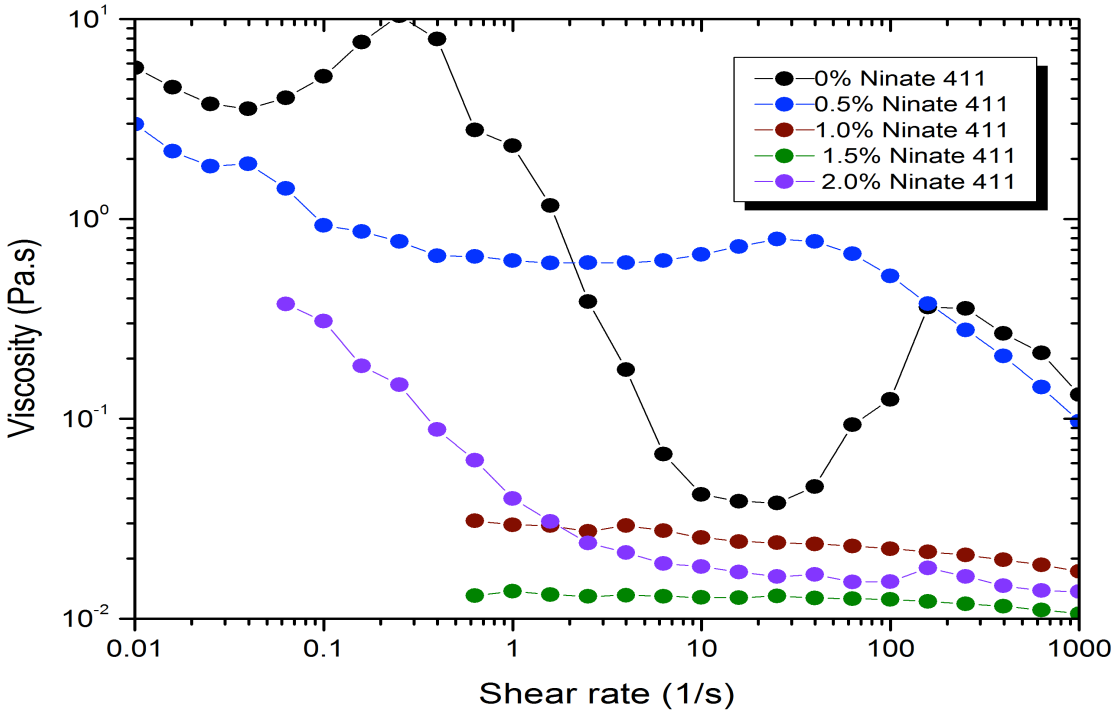

Rhoplex VSR-1050 + 0.4% HEUR RM-825 + Ninate 411

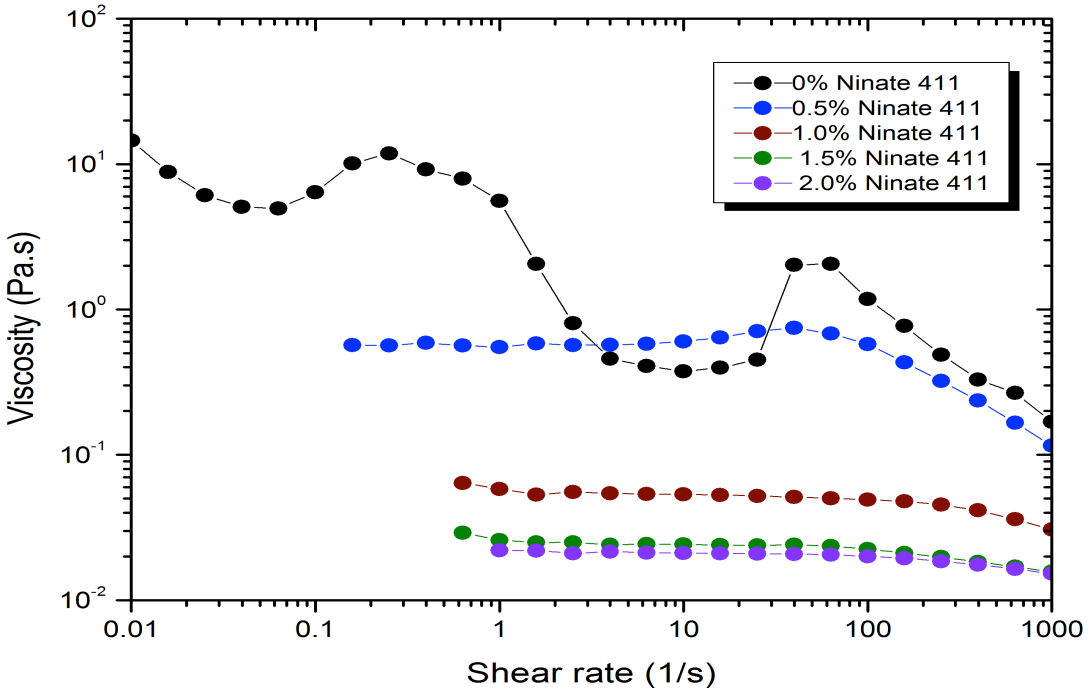

Rhoplex VSR-1050 + 0.5% HEUR RM-825 + Ninate 411

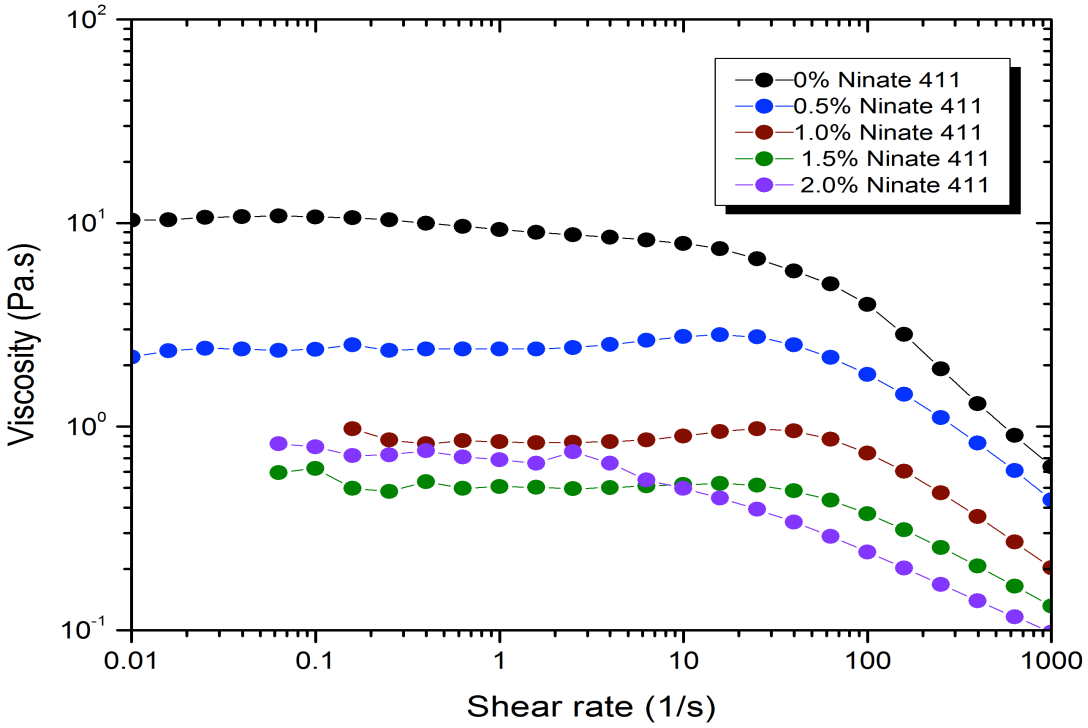

Rhoplex VSR-1050 + 1.0% HEUR RM-825 + Ninate 411

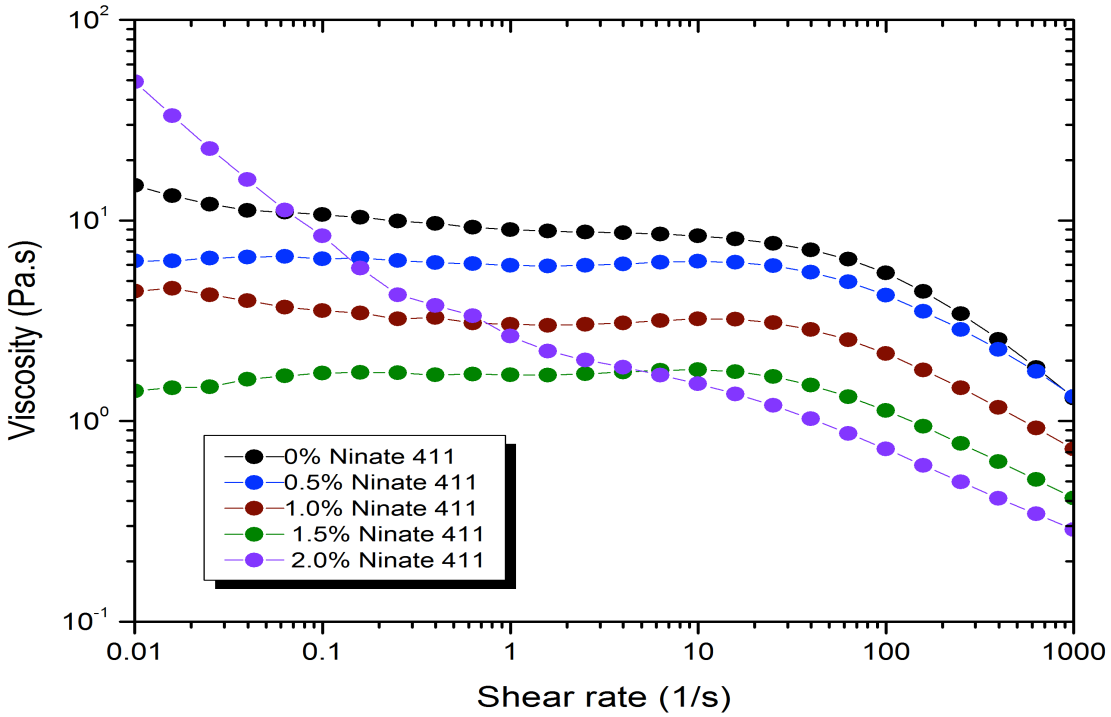

Rhoplex VSR-1050 + 1.5% HEUR RM-825 + Ninate 411

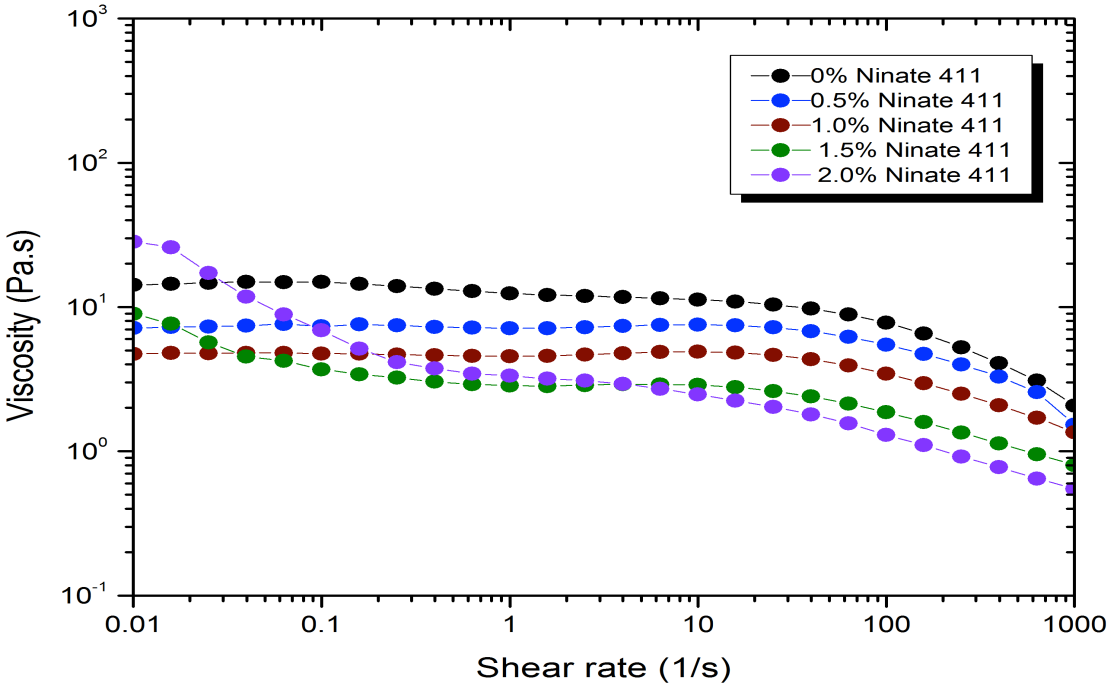

Rhoplex VSR-1050 + 2.0% HEUR RM-825 + Ninate 411

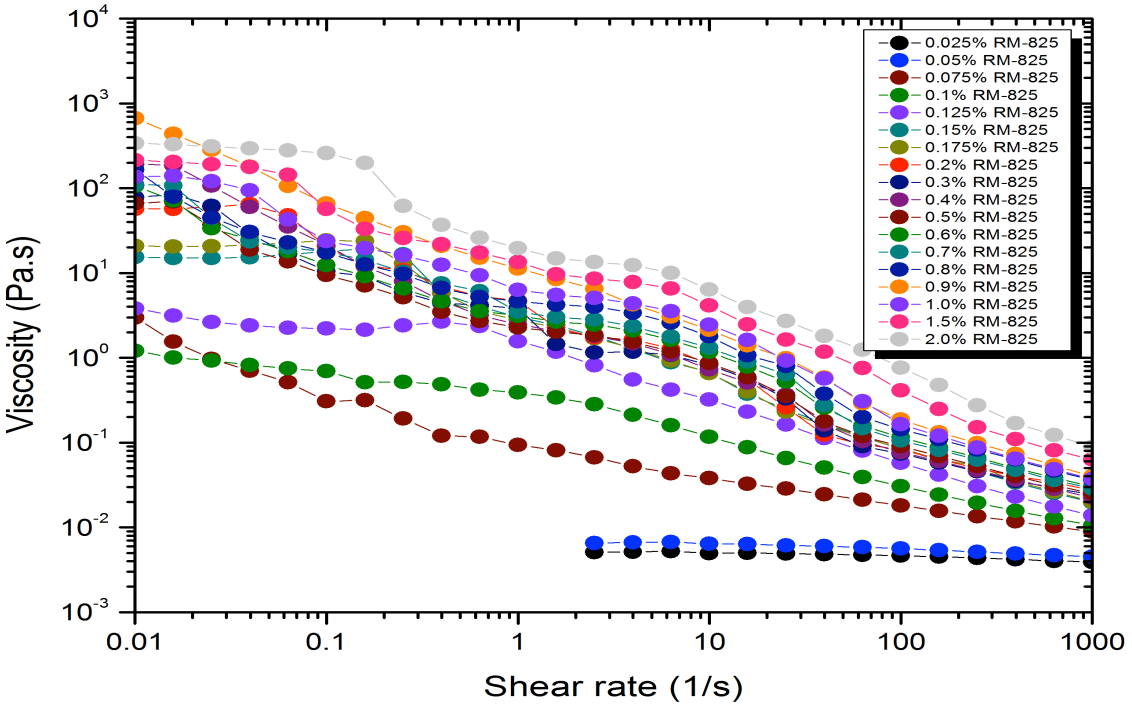

Rhoplex VSR-1050 + HEUR RM-995

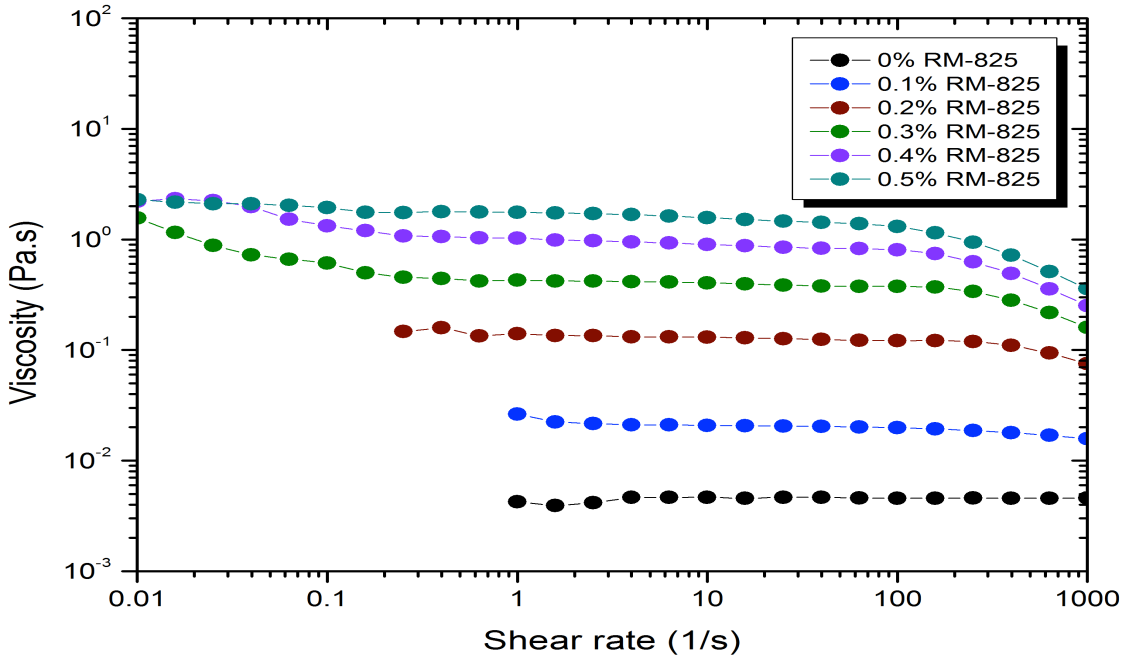

Hybridur 570 + HEUR RM-825

PART B

1 Introduction

Organic-inorganic hybrid photovoltaics have received plenty of research interest in the past decade. They are promising candidates for future low-cost photovoltaics. This is mainly due to the solution processability of hybrid nanomaterials, allowing it to be used in printing/coating techniques. The advantages of both organic and inorganic semiconductors are utilized in hybrid photovoltaics. In organic-inorganic photovoltaics, the organic component consists of organic materials such as conjugated polymers that absorb light as the donor, as shown in Figure 27.

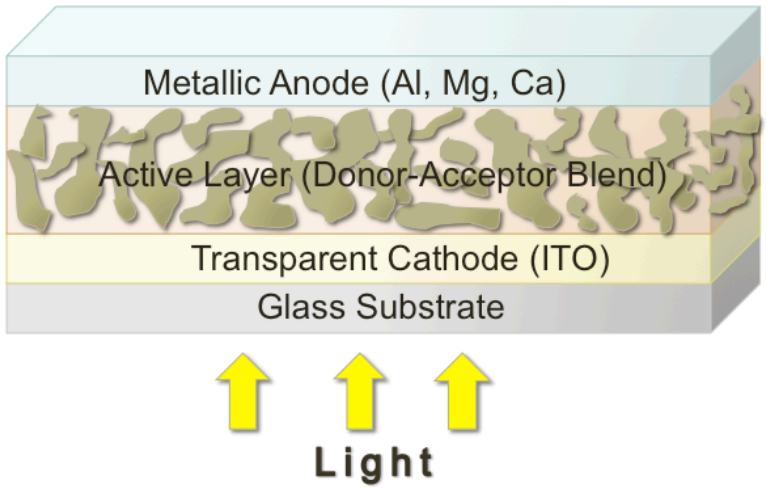

Figure 27. Schematic diagram of a hybrid organic-inorganic solar cell.

The inorganic components in hybrid photovoltaics such as CdSe, TiO_2, ZnO, PbS, and silicon nanoparticles act as the acceptor and the electron transporter in the structure. Organic solar cells generate electrical power by the generation of electrons and holes at the interface between the electron-donating and electron-accepting semiconductors.[1] The use of hybrid organic-inorganic nancomposites combines both the advantages of organic and inorganic particles. In addition, inorganic particles are more environmentally stable than organic

particles. Inorganic particles are efficient light absorbers at spectral regions covered by sunlight, making them better than just their organic counterpart.

New interest in the field is focused on the development of organic-inorganic core-shell hybrid nancomposites, here the conjugated polymer is attached onto 1-D inorganic nanoparticles.[2-6] The outcome of this organic-inorganic core-shell hybrid nanocomposite gives a controllable morphology of the electron donor and acceptor at the nanolevel. Additionally, this hybrid composite can form lyotropic liquid crystalline (LLC) phases in solution above a critical concentrations.[6] Under external forces, the LLC phases are aligned parallel or perpendicular to the substrate conditional on the processing condition. Printing and coating involves various shear forces and extensional forces in order to apply the ink or coating well to the substrate. Due to this fact, the printing of LLC materials can result in well aligned ordered structures.[7-9] In this part of the project, a model nanocomposite was made using poly(3-hexylthiophene) (P3HT) (Figure 28) as the conjugated polymer serving as the electron donor and modified zinc oxide with dodecanethiol (ZnO-DDT) (Figure 29) as the inorganic material serving as the electron acceptor.

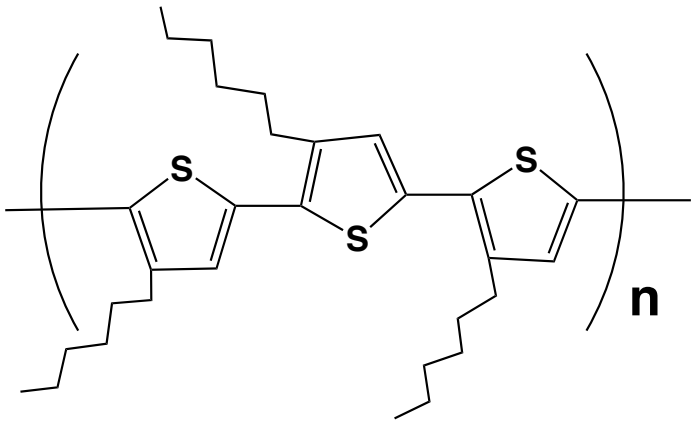

Figure 28. Structure of poly(3-hexylthiophene) (P3HT).

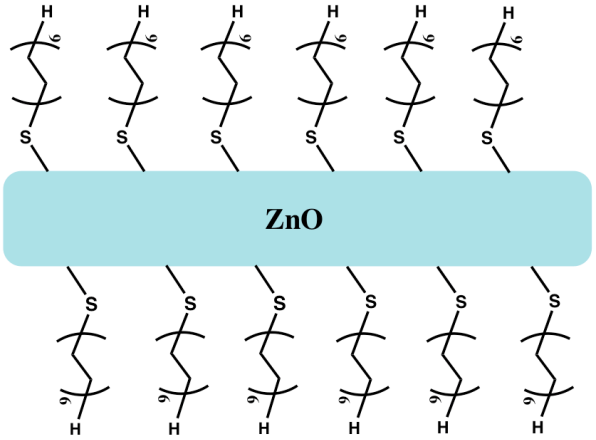

Figure 29. Structure of dodecanethiol (DDT) modified zinc oxide (ZnO-DDT).

1.1 Poly(3-hexylthiophene) (P3HT)

Poly(3-hexylthiophene) (P3HT) is from a group of polythiophenes, which are electrically conductive. P3HT has an outstanding electronic and optical properties with good solubility in common organic solvents.[10] This is due to the structure of P3HT which includes intermolecular π-π stacking of its conjugated backbones.[11] P3HT is one of the most studied conducting polymers because of its high solubility in organic solvents, relatively high charge mobility, thermal properties, and environmental stability.[11] The regioregularity of P3HT plays role in the conductivity of P3HT. The head-to-tail regioregularity of the chain gives a higher conductivity than other regioregularities.[12] Furthermore, P3HT are semicrytalline in nature, possessing a complex conduction mechanism. The crystalline portion of the polymer can conduct current via intrachain and interchain transport, while the amorphous portion of the polymer conducts current through hopping and tunneling process.[13] The self-assembled 1D nanostructures of P3HT enhances the crystallinity, mechanical flexibility, and the speed of charge transport relative to 2D thin films.[14]

1.2 Zinc Oxide (ZnO)

Inorganic particles such as ZnO nanoparticles are used as an alternative to fullerene derivative to make hybrid organic-inorganic photovoltaics. ZnO has a high electron mobility and relative environmental stability and when combined with conjugated polymers, such as P3HT, shows promising result in producing high-efficient,low-cost photovoltaics.[15] ZnO nanowires has the ability to assemble into macroscopically aligned structures. This alignment of nanowires has significantly improved the device performance in thin film transistors and solar cells.[16]

1.3 Active Layer Architecture

The active layer of the hybrid organic-inorganic solar cells is the main focus of this project. The active layer of a device largely determines the efficiency of a device. In order to have a better device efficiency the morphology of the active layer must be controlled. Figure 30 illustrates three different active layer architectures.

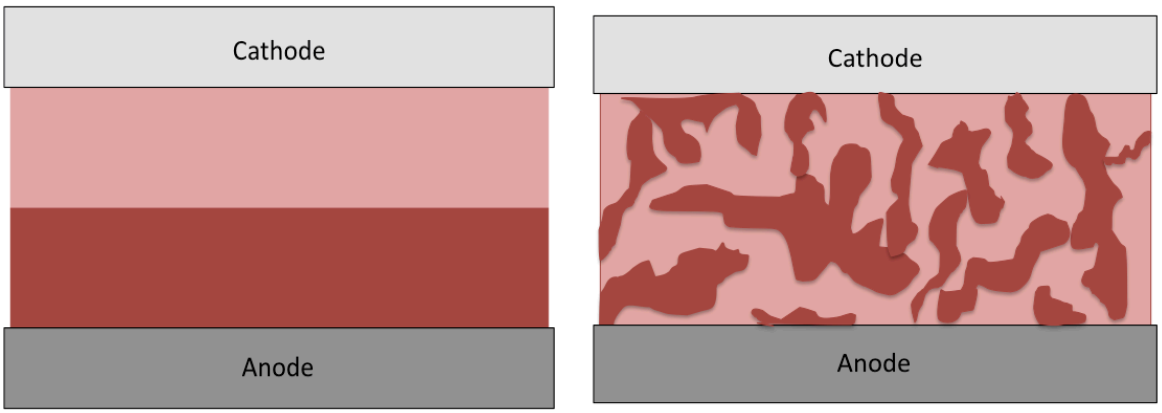

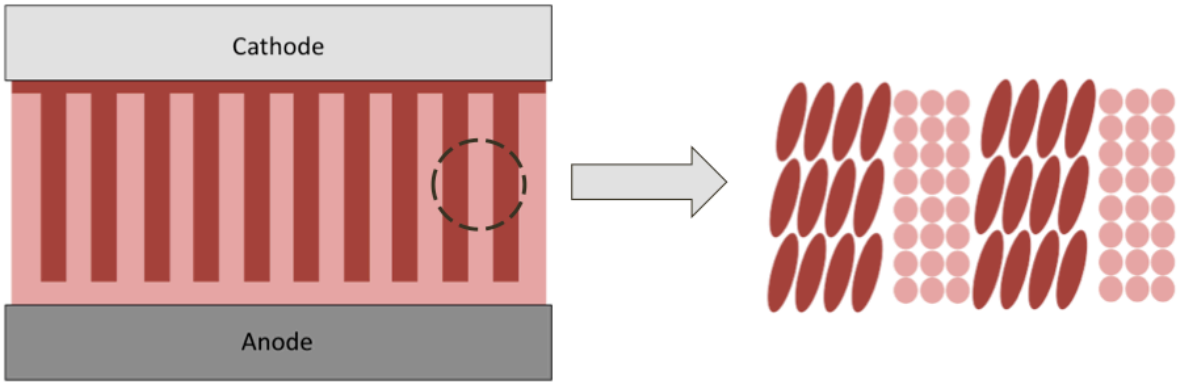

Figure 30. (a) bilayer heterojunction (b) bulk heterojunction (c) ordered heterojuntion

Based on many studies, the bilayer and bulk heterojunction have an active layer architecture that does not produce high efficiency devices. In a bilayer heterojunction, the interfacial layer between the organic and inorganic components is small therefore it is difficult to separate and transport the charge. In bulk heterojunctions, although better than the bilayer architecture, also have a poor charge transport mainly due to the random domain resulting to a less efficient charge transport. In order to address these dilemmas and to potentially improve device performance, ordered heterojunctions are used. Ordered heterojunctions are capable of alignment due to the nanowires which can be aligned with the use of mechanical shear.

1.4 Lyotropic Liquid Crystal

Liquid crystals are of big research interest due to its utilization of flexible electronics. Liquid crystals are matter that has properties between that of conventional liquid and those of solid crystals. A liquid crystal has the ability to flow like a liquid but its molecules may be oriented in a crystal-like configuration. Liquid crystals are divided intro different phases: thermotropic, lyotropic, and metallotropic. For the purpose of this project, I am focusing mainly on lyotropic liquid crystals (LLC). LLC exhibit phase transitions due to both temperature and concentration of the liquid crystal molecules in solvent. LLC phases are

present and abundant in living systems, for instance, many proteins and cell membranes are liquid crystals. When combined with water, soaps and detergents form LLC.

Semiconductor nanowires such as ZnO have rigid or rodlike macromolecule geometry. According to Onsager's theory of the phase transition from the isotropic fluid to nematic liquid crystal phase, LLC orders occurs spontaneously in solutions with rod-shaped or anistropic objects from isotropic phase to nematic phase above a critical volume fraction.[17] With increasing concentration LLC, can form nematic phases: isotropic, biphasic, and nematic. In their LLC solution, alignment of the liquid crystal molecules can be a result of shear. The LLC can self-assembly to highly ordered domain for better device efficiency. In this project, the effect of the shear flow on the alignment of 1-D hybrid nanocomposites in their LLC phases was studied.

1.5 Screen Printing

Screen printing is a widely used technique to produce films with a thickness in the range of 10-100 μm. Screen printing involves various shear forces that can influence the alignment of the nanowires. The quality of the screen-printed layer is highly dependent on factors including printer settings, screen options, substrate preparation, and the rheology of the ink. The study of the viscoelastic properties of the ink is crucial in order to properly print on a substrate.

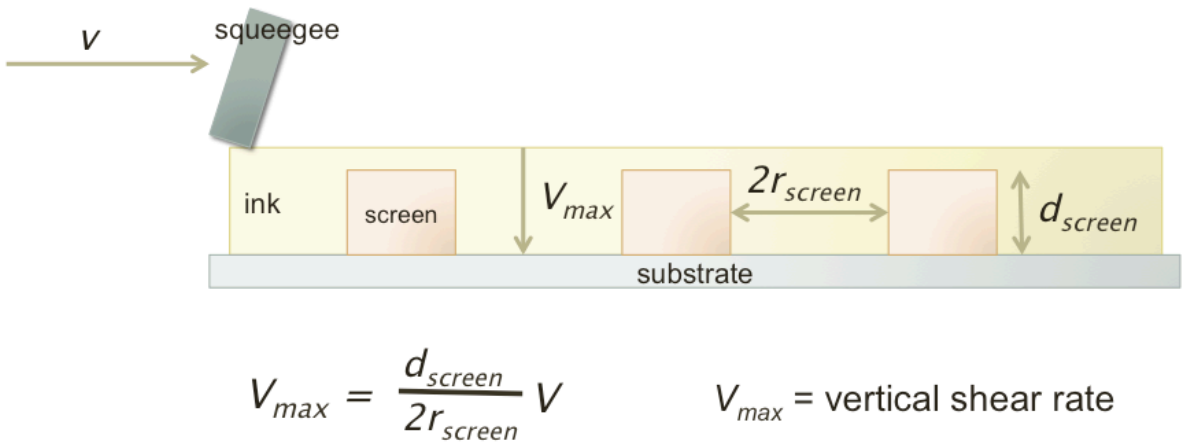

Figure 31. Schematic of a typical screen printing process.

In a typical screen printing process, a squeegee, a screen, a substrate, and the ink are used. When the squeegee is moved allowing the ink to be casted on the substrate, a vertical force is produced when the ink goes through the diameter of the screen as seen in Figure 31. This vertical force corresponds to a vertical shear which enables us to calculate the vertical shear rate using the height of the screen (d_{screen}), the size of the screen ($2r_{screen}$), and the shear rate of which the squeegee was moved. This vertical shear rate can induce a vertical alignment thus giving us an ordered heterojunction that can potentially give us a better device performance.

1.6 Rheology

Printing quality is highly dependent on the rheological properties of the ink. Some of these rheological properties are the viscosity, thixotropy, and the viscoelasticity of the ink.[18] In general, the viscosity of LLC solution increased with increasing concentration until it reaches a maximum viscosity and then the viscosity falls to a minimum value in a single LC phase.[18] However, with increasing shear rate, the viscosity of the solution decreased, this is known as shear-thinning, as previously described in Part A of this project. The low viscosity

and the shear-thinning effect is ideal for printing, this is accomplished by squeegeeing ink over the small opening in the screen when screen-printing. The application of ink through screen-printing involves a relatively high shear rate, therefore a detailed study of the viscosity profiles of hybrid nanocomposites of P3HT and ZnO-DDT is crucial for this project.

Similar to shear-thinning, it is important that the ink possesses the ability to be thixotropic. Thixotropy is also known as time dependent shear-thinning or the time dependent change in viscosity. This is related to the temporary breakup and recovery of interactions with the paste-like ink. After the application of shear stress, which causes the breakdown of interactions, the internal network of the material is reformed, along with the increase in viscosity. During screen-printing, after the application of the ink to the substrate by squeegee, the interaction is broken down, allowing the ink to pass through the screen. As soon as the ink is applied, the viscosity of the ink will increase, allowing networks to reform.

The viscoelastic properties of the ink are also an integral part of this study. Dynamic viscoelastic tests as function of shear strain and frequency can be studied under sinusoidal oscillation mode, as shown in Figure 32.

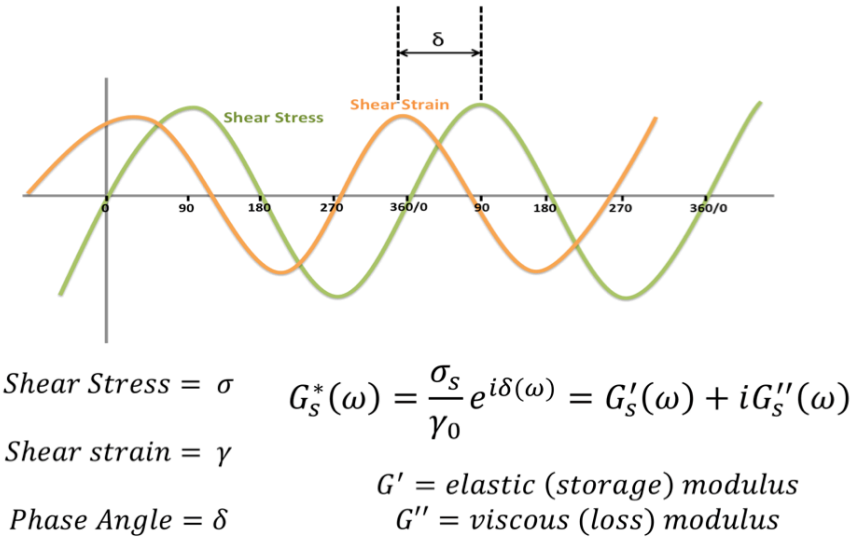

Figure 32. Dynamic Oscillatory Rheology.

Under the sinusoidal oscillation mode, the resultant stress response is measured along with frequency of oscillation of the shear deformation. By subjecting samples to an oscillatory stress and determining the response, both the elastic and viscous or damping characteristics can be obtained. The elastic property of the sample is described as G' or the shear storage modulus. G' measures how elastic or solid-like the sample is; elastic materials deform instantly as shear is applied. The viscous property of the sample is described as G" or the shear loss modulus. G" measures how viscous or liquid-like a material is; viscous materials however have a lag in deformation as shear is applied. During testing, the sample is continuously excited but never exceeds a strain large enough to destroy the structure. A test called amplitude sweep over a stress or strain range is performed in order to determine the linear viscoelastic region. Once the linear viscoelastic region is determined, a frequency sweep at a stress in this area can be used to determine the nature of the material. This will determine the viscoelastic properties of material. It gives a clear indication of the behavior of the sample, whether viscous or elastically dominated over a given frequency range.

1.7 Gelation of Hybrid Nanocomposites

Many conjugated polymers form gels at moderate concentrations in organic solvents. The self-assembly of P3HT can be ideal as a platform to generate stable and structurally optimized network structures.[19] They can self-assemble into interconnected network structures. Based on recent research, the gel phase of P3HT has been shown to have a much higher conductivity relative to films generated using traditional coating processes. Despite many advances in research involving the increased conductivity of P3HT gels, the structure about how the conjugated polymers evolves during gelation is unknown. Initially in this project, we found that the addition of ZnO-DDT to P3HT in dicholorbenzene (DCB), promotes gelation, providing a shorter gelation time with an increase loading of ZnO-DDT. It is also important to take note that the gelation process occurred with the use of a "good solvent", dichlorobenzene. Based on past literature studies, it is known that the solvent has a significant effect on the crystallization of nanocomposites with P3HT.[19-23] Here we present the kinetics of this gelation process and a possible mechanism.

2 Methods and Materials

Regioregular (> 96%) poly(3-hexylthiophene) (P3HT, average M_w = 60,000-75,000 g/mol, Rieke Metlas Inc.) was used as received without any further purification. The dodecanthiol (DDT) modified zinc oxide (ZnO-DDT) was synthesized in lab having an average length of 1 μm and an average diameter of 50 nm with an aspect ratio of about 20 based on atomic force microscopy (AFM) images. P3HT and ZnO-DDT were mixed together in dichlorbenzene (DCB) forming a nanocomposite. The concentrations of P3HT and ZnO-DDT in the nanocomposites were varied according to their percent weight. P3HT and ZnO-DDT nanocomposites were prepared with DCB and sonicated for 1 hr at 60° C or until a homogenous mixture is achieved.

2.1 Instrumental Methods and Analysis

Samples were characterized using TA Instruments HR-2 Rheometer equipped with a 40 mm, 2° cone, and 55 μm gap. Different rheological test parameters were used to characterize the prepared nanocomposite:

Steady-State Shear:

During the steady shear test, the change in viscosity was observed over a range of shear rate (0.01-1000 s^{-1}). Tests were conducted at a constant temperature with a total test time of approximately 26 minutes.

Dynamic Oscillatory:

Dynamic oscillatory testing was conducted. First a strain sweep was performed to visualize the linear viscoelastic region. Once this was determined, the strain % was chosen (1%) and a frequency sweep was performed (0.01 Hz to 100 Hz) to analyze the viscoelastic properties of the gels.

Gelation Kinetics:

Gelation kinetics measurement were performed at various temperature for the 10% P3HT + 10% ZnO-DDT by weight nanocomposite. Temperatures of 15°, 17°, and 20° were tested for 3600 sec to 5400 sec depending on the gelation time at a given temperature. The G' and G" were observed at 1% strain and 1 Hz. Samples were first sonicated at 60° to liquefy the nanocomposites, it was then loaded on the rheomoter giving a 5-minute euqilibration time before data was collected.

3 Results and Discussion

3.1 Rheological Profiles of ZnO-DDT

ZnO can form LLC phase above a critical concentration. In the first part of this part of the project, various concentration of modified ZnO-DDT was examined through rheology. Figure 33 shows the steady-state shear test of different concentrations of ZnO-DDT in dichlorobenzene.

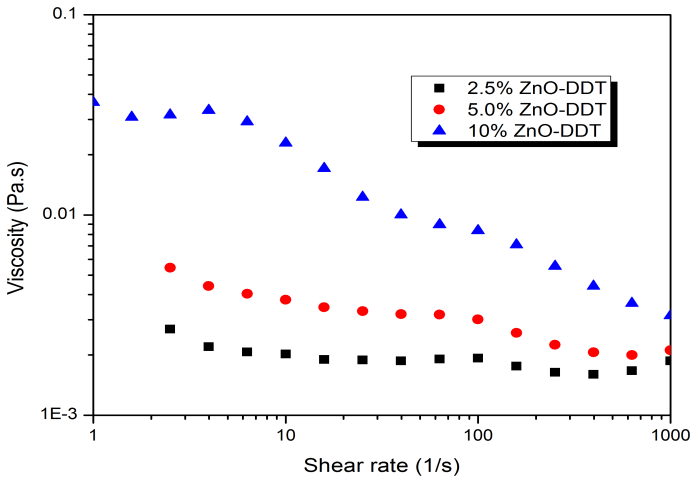

Figure 33. Steady-state shear test of ZnO-DDT to determime the lyotropic liquid crystal phase.

Due to the samples' low viscosity, the rheological profiles of 2.5% (wt) ZnO-DDT and 5% (wt) ZnO-DDT were almost Newtonian, a slight shear-thinning and shear-thickening was observed. This is comparable to previous literature studies were at concentrations where lyotropic polymer liquid crystals phase exists exhibits rheological profiles with a Newtonian plateau at low shear rates followed by shear-thickening at intermediate shear rates and another plateau at high shear rates. At 10% (wt) ZnO-DDT, the rheological profile observed is different from 2.5% and 5% (wt) presumably because they exist in two different phases, 2.5% and 5% at isotropic phase while 10% ZnO-DDT is in nematic ordered phase. The distinct regions were not observed in 10% ZnO-DDT, instead a shear-thinning behavior was

observed, which can be attributed to the higher viscosity at this concentration, inhibiting the formation of nematic ordered phase as the shear rate is increased. To further support this finding, Figure 34 shows steady-state shear viscosity plot compared with the complex viscosity determined in dynamic oscillatory testing.

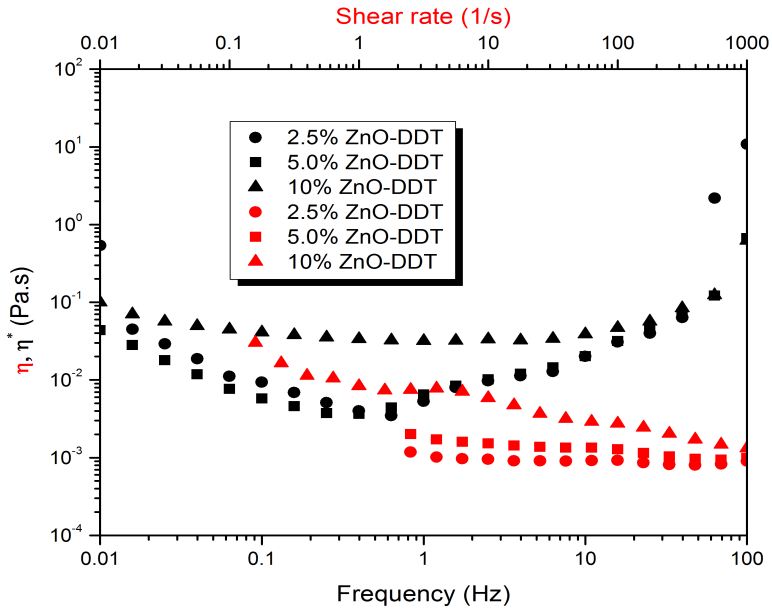

Figure 34. Comparison of steady-state viscosity (red) and complex viscosity (black) to determine if the Cox-Merz rule is followed at a given concentration.

Comparison of the steady-state viscosity (red) and complex viscosity (black) was performed to determine if the profiles follow the Cox-Merz Rule.[18] In general, the rheological profiles of lyotropic liquid crystals and gels does not follow the Cox-Merz rule, which states that the steady-state viscosity, η, and complex viscosity, η*, are equal when compared at the same shear rate and frequency.

3.2 Rheological Profiles of P3HT-ZnO-DDT Nanocomposites

The preparation of the nanocomposites at a high concentration was crucial for printing purposes. Figure 31 shows a comparison of the steady-state shear and complex viscosity.

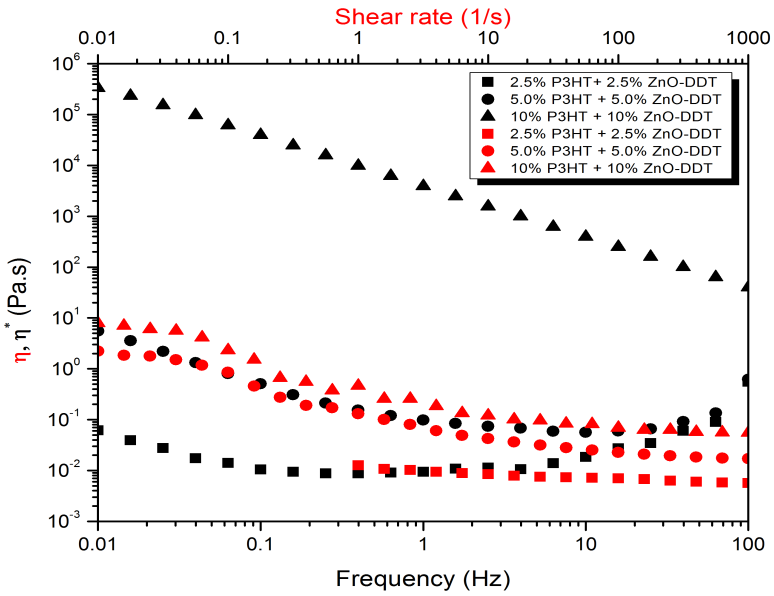

Figure 35. Comparison of steady-state viscosity and complex viscosity of various 1:1 concentration of P3HT and ZnO-DDT nanocomposites in dichlorobenzene.

Relative to the plot with just ZnO-DDT in Figure 35, the steady-state viscosity and complex viscosity for 2.5% P3HT + 2.5% ZnO-DDT and 5% P3HT + 5% ZnO-DDT were similar signifying that at these concentrations, the nanocomposites are not in lyotropic liquid crystal phase. The addition of P3HT caused minimal structural conformation therefore at these concentrations, the solutions are not in lyotropic liquid crystal phase. At 10% P3HT + 10% ZnO, the nanocomposite was a gel, inhibiting the formation of nematic ordered phase.

3.2.1 Gelation

Upon the preparation of a 10% by weight of P3HT, a gelation was observed over time at room temperature. Over time, gelation in 5% P3HT + 5% ZnO-DDT was observed. Based

on this, the gelation of the nanocomposites is time, temperature, and concentration dependent. Figure 36 shows a steady-shear state comparison of three different concentrations at 1:1 addition of P3HT and ZnO-DDT at 25°C, 24 hrs after synthesis; the 1:1 ratio of P3HT and ZnO-DDT is the typical ratio used in device fabrication.

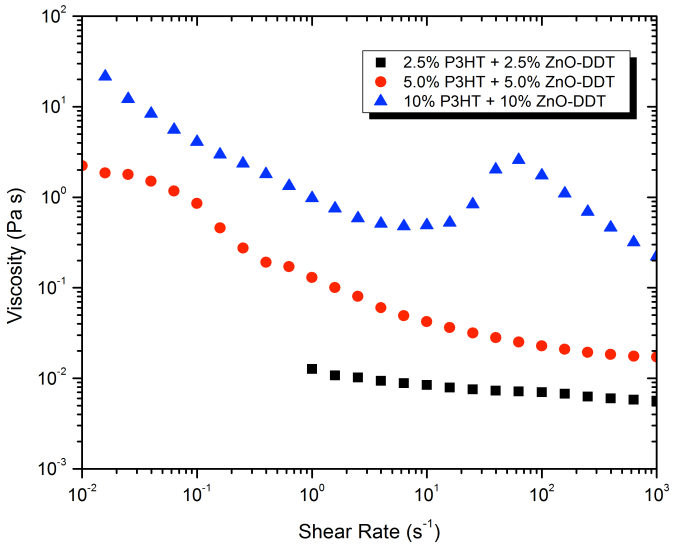

Figure 36. Steady-state shear comparison of different loadings of 1:1 ratio of P3HT + ZnO-DDT.

At 25°C after equilibration over night, the 10% P3HT + 10% ZnO-DDT nanocomposites formed a gel. In addition, it was observed that upon varying the concentration of the added ZnO-DDT to a constant concentration of P3HT, the gelation time also varied: the higher level loading of ZnO-DDT, the faster the gelation. Figure 37 shows s steady-state shear viscosity graph of 10% P3HT with various loading of ZnO-DDT (1%, 5% and 10%) at 25°C.

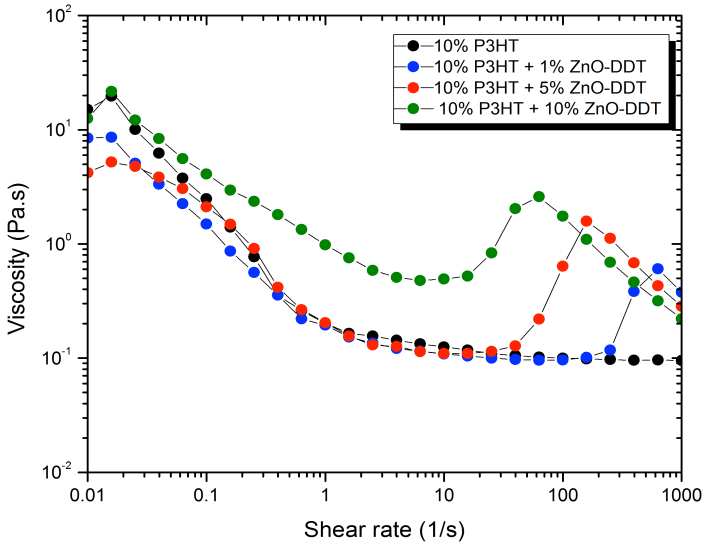

Figure 37. Steady-state shear viscosity profiles to study the effects of the concentration of ZnO added to 10% P3HT.

At this given concentration of P3HT, 10% (wt) gel was observed indicated by the high viscosity at a very low shear rate. As the shear rate was increased, a shear-thinning profile was observed, at intermediate shear rate or mid-shear rate for samples with ZnO-DDT shear-thickening was observed, followed by shear-thinning at high shear rate. Pristine P3HT did not show any shear-thickening, only shear-thinning and a Newtonian plateau. The shear-thickening observed was indicative that with the addition of ZnO-DDT, networks were formed and a conformational change occurred induced by the increase in shear rate, at a higher shear rate shear-thickening disappeared, replaced by shear-thinning, when the molecules are aligned again.

The rheological profile at different temperatures was also examined. Figure 38 shows steady-state shear graph comparing the rheological profiles at 25°C and 75°C of 10% P3HT + 10% ZnO.

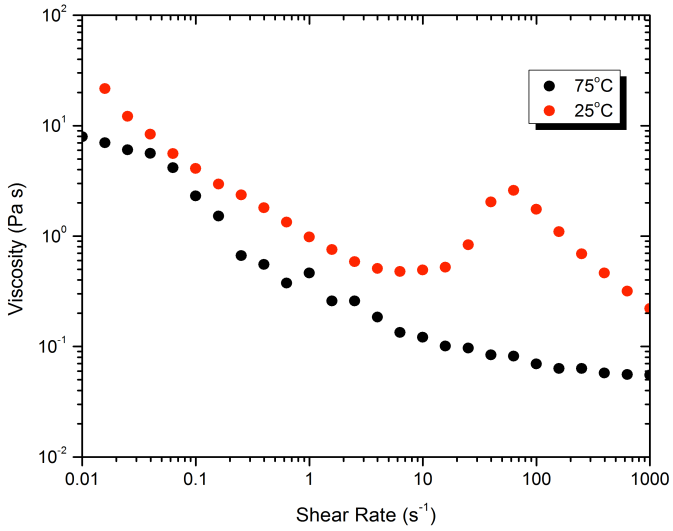

Figure 38. Steady-state viscosity of 10% P3HT + 10% ZnO-DDT at 25°C and 75°C.

Previous literature studies have stated that P3HT exhibits thermochromism. This means that there is a conformation change in the molecular level with the change in temperature. At high temperature, P3HT stays solvated and is in coil formation, when temperatures are decreased, a coil-to-rod transition occurs. This phenomenon is also characterized by the change in color of the nanocomposites: an orange color signifies a coil state while a purple color signifies the rod state. At 75°C the nanocomposite is in a coil state and is characterized by the shear-thinning rheological profile. However, at 25°C the nanocomposite is in a rod state conformation and is characterized by the shear-thickening profile at mid-shear rate. The critical gelation temperature was also determined, as shown in Figure 39-41 for 10% P3HT + 1% ZnO-DDT, 10% P3HT + 5% ZnO-DDT, and 10% P3HT +1% ZnO-DDT, respectively.

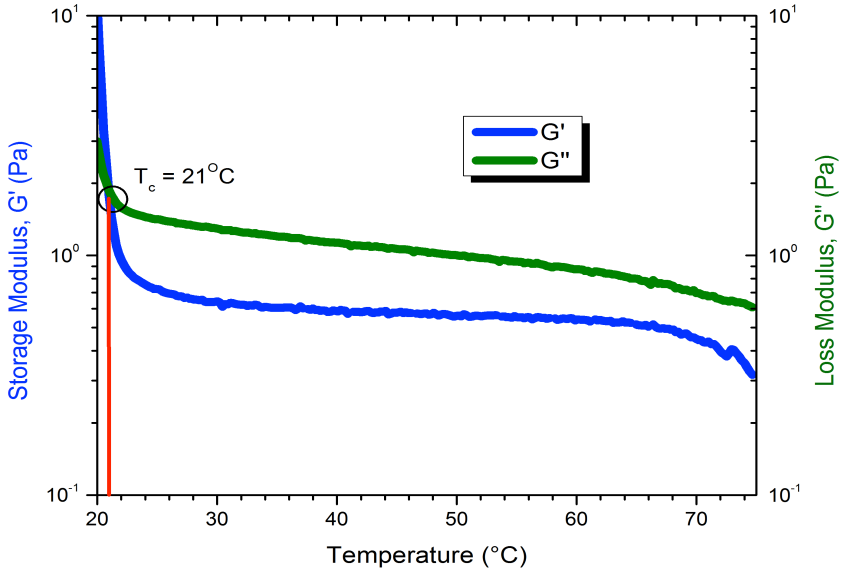

Figure 39. Critical gelation temperature (Tc) of 10% P3HT + 1% ZnO-DDT.

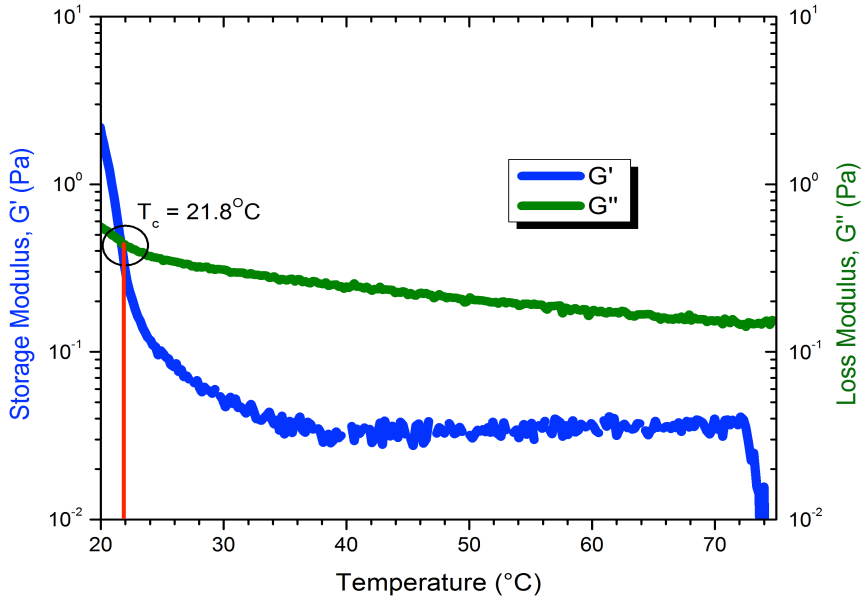

Figure 40. Critical gelation temperature (Tc) of 10% P3HT + 5% ZnO-DDT.

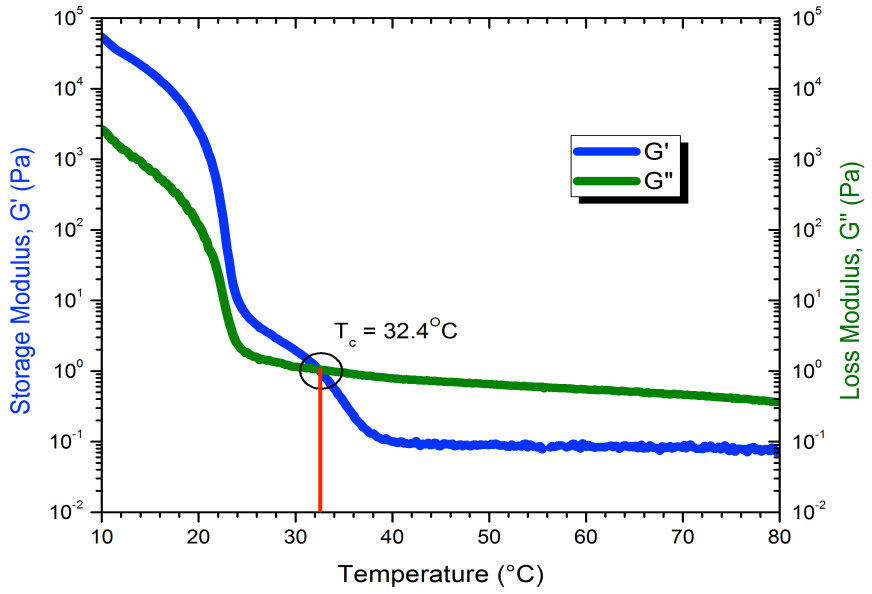

Figure 41. Critical gelation temperature (Tc) of 10% P3HT + 10% ZnO-DDT.

Shown here are cooling curves; to obtain these plots, the G' and G" were observed at 1% strain and 1 Hz at a temperature range of 75°C to 25°C. The critical gelation temperature is described as the point where the G" and G' intersect, signifying a sol-gel transition.[24] At high temperatures, the nanocomposite is dominated by the viscous modulus and with the decrease in temperature, the elastic modulus will start to dominate. This occurs due to the ongoing gelation and the slow development of a network. Table 5 summarizes the critical gelation temperatures of nanocomposites with constant 10% P3HT and various ZnO-DDT concentrations.

Table 5. The critical gelation temperature (T_c) of P3HT + ZnO-DDT nanocomposites at various loading of ZnO-DDT.

	10% P3HT + 1% ZnO-DDT	**10% P3HT + 5% ZnO-DDDT**	**10% P3HT +10% ZnO-DDT**
T_c (°C)	21	21.8	32.4

For cooling temperature ramps, the addition of ZnO-DDT increased the critical gelation temperature; this further verifies that the addition of ZnO-DDT in P3HT promotes gelation.

3.2.2 Kinetic Process of Gelation

According to the percolation theory, the elastic part of the system G' can be expressed as G'~ ω^2 below the gel point and G' ~ constant above the gel point. This means that the storage modulus, G' is more changeable than the loss modulus, G" before and after the gel point. A gel system storage modulus is independent of the frequency and more dependent on the time, which is associated with the number of cross-links in the network of the structure.[24] As a result, a reaction conversion equation can be used to correlate the change of storage modulus, G' in the system:

$$X(t) = \frac{G'(t) - G'(0)}{G'(\max) - G'(0)} \qquad (2)$$

where G'(t) is the value of the storage modules at time t, G'(0) is the value of the storage modulus at the start of the experiment, and G'(max) is the value of the storage modulus at the maximum gelation time. The conversion of G' to X(t) is plotted in Figure 42.

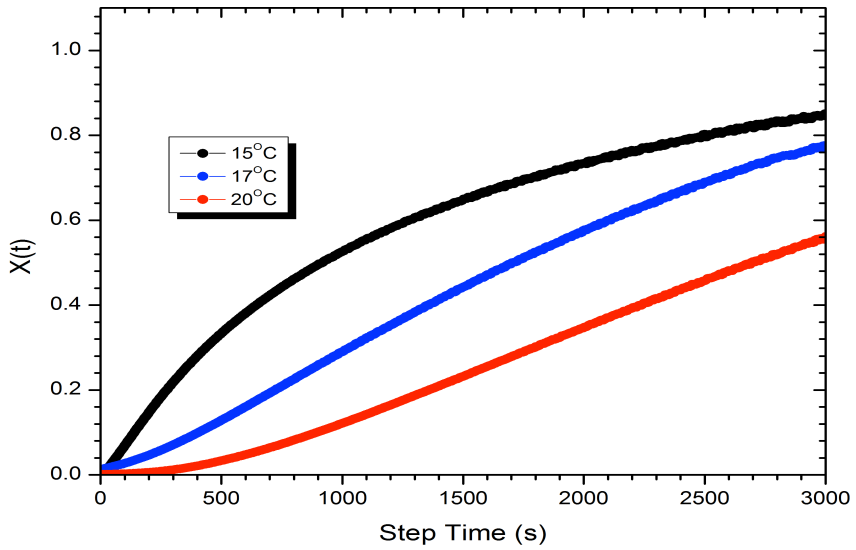

Figure 42. Conversion of G' to X(t), correlating the change in G' that occurs during gelation.

With the increase of temperature, gelation happens slower. Within the temperature range that was chosen for the purpose of this experiment, 15°C showed the fastest gelation while 20°C showed a relatively slower gelation process.

Using the data obtained, two simple reaction rate equations for first-order kinetics and second-order kinetics can be applied[24]:

for the first-order reaction kinetics

$$-\ln[1 - X(t)] = k_1 t \qquad (3)$$

for the second-order reaction kinetics

$$\frac{1}{[1 - X(t)]} = k_2 C_o t + 1 \qquad (4)$$

Here, k_1 and k_2 are the reaction constants and C_o is the initial concentration of the reactive functional group. Figure 43-45 plots the conversion versus the reaction time based on first-order reaction kinetics given by equation 3 and the second-order reaction kinetics given by equation 4 for at different temperatures.

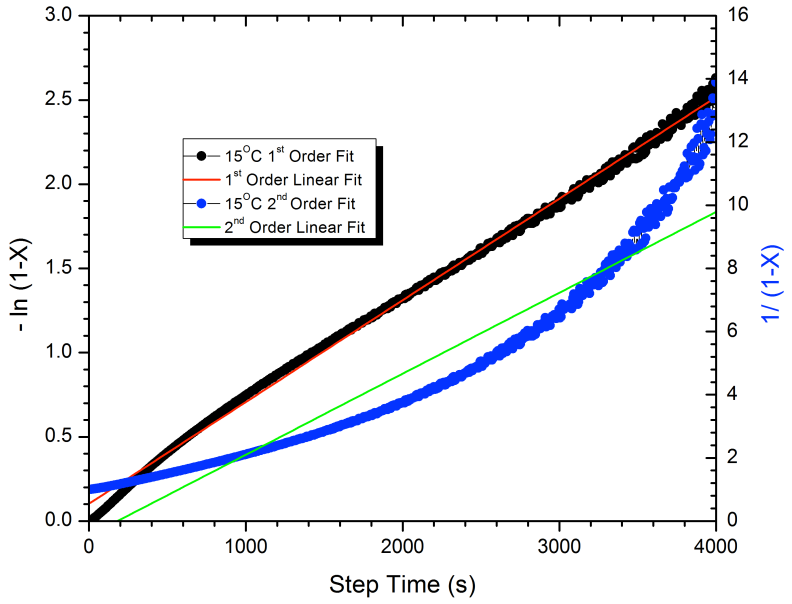

Figure 43. Plots of conversion versus reaction time based on first-order and second-order reaction kinetics for 10% P3HT + 10% ZnO-DDT at 15°C.

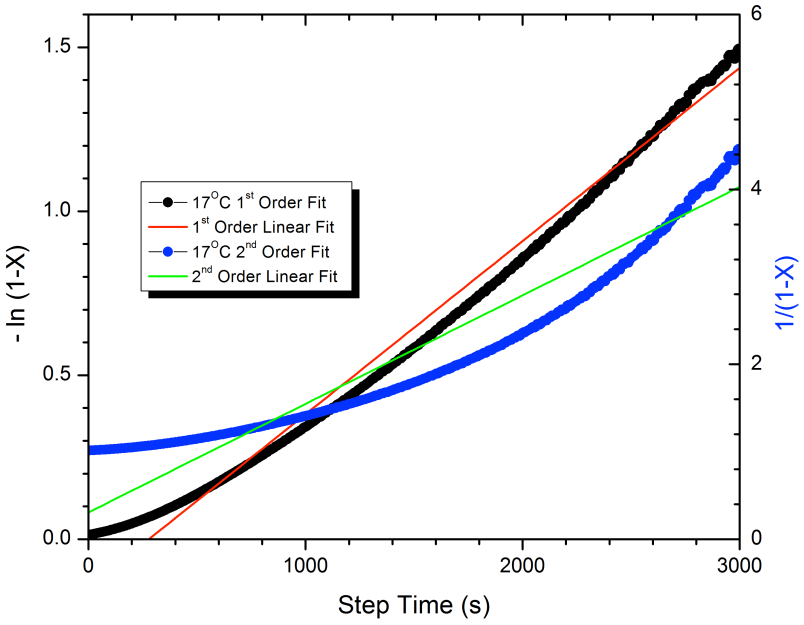

Figure 44. Plots of conversion versus reaction time based on first-order and second-order reaction kinetics for 10% P3HT + 10% ZnO-DDT at 17°

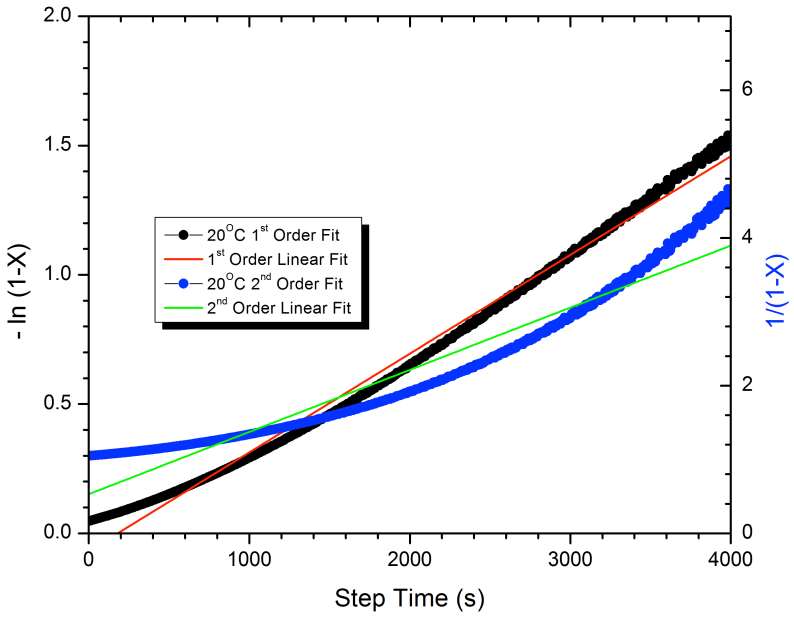

Figure 45. Plots of conversion versus reaction time based on first-order and second-order reaction kinetics for 10% P3HT + 10% ZnO-DDT at 20°C.

It is evident that the reaction kinetics for the gelation of 10% P3HT + 10% ZnO-DDT is a first-order reaction kinetics. This indicates that the incorporation of ZnO-DDT with P3HT has an effect on the gelation of the system.

3.2.3 Mechanism of Gelation

The effect of the addition of ZnO-DDT can be analyzed further with UV-Vis spectrophotometry. Figure 46 shows a UV-Vis spectra of 10% P3HT with various loading of ZnO-DDT.

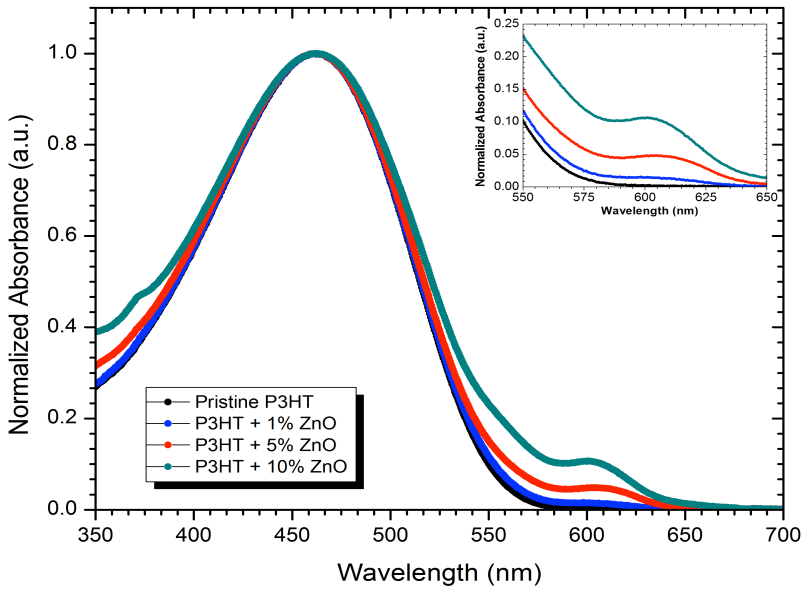

Figure 46. UV-Vis spectra of 10% P3HT with various loading of ZnO-DDT.

With the addition of ZnO-DDT, we can see the formation of nanowires at 600 nm. The peak at 600 nm increases as the ZnO-DDT loading was increased.

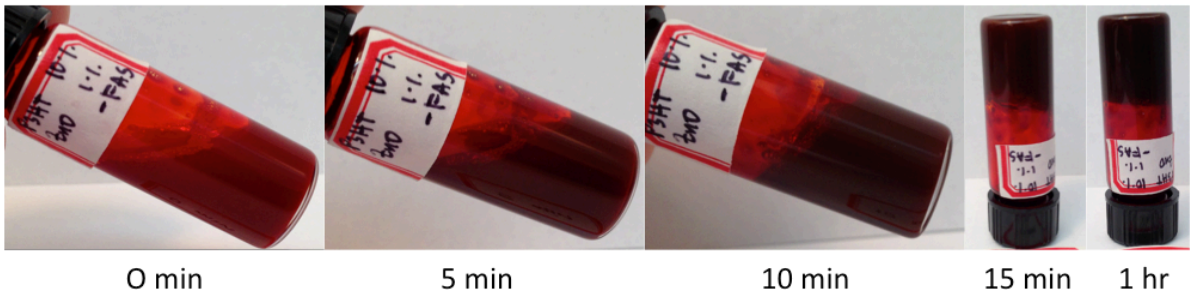

Figure 47. Color change and gelation process of 10% P3HT + 1% ZnO-DDT.

Figure 47 shows photographs depicting the color change and the gelation of 10% P3HT + 1% ZnO-DDT at room temperature. At 0 min, it is evident that the nanocomposite is still in its liquid form. At around 10 minutes at room temperature, a color change was observed due to thermochromism and at 15 minutes, the nanocomposite is a clear gel. The mechanism of this gelation can be described in the schematic in Figure 48.

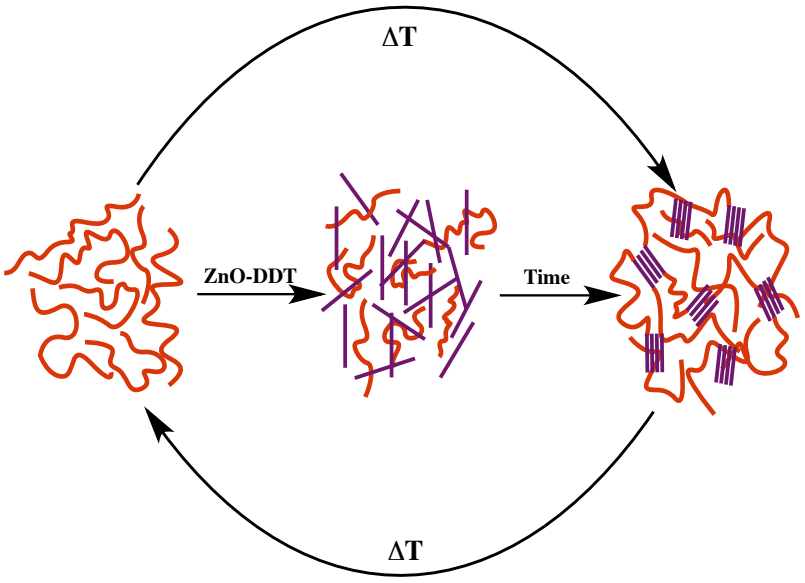

Figure 48. Schematic describing the formation of gel upon the addition of ZnO-DDT to P3HT.

The gelation of the nanocomposite of P3HT and ZnO-DDT starts out in the coil state. Upon the addition of ZnO-DDT, we observed a transition where some P3HT molecules, with the aid of ZnO-DDT, are in the rod state while some are still in a coil state. Over time, depending on the concentration of ZnO added, some molecules are still left at the coil state and the rods that are formed serves as a cross-linker, similar to the fringe micelle model. In this state, networks are formed, leading to gelation. This is evident from the UV-Vis spectra were the peaks at 600 nm did not dominate the system. For a complete coil-to-rod transition, the peak at 600 nm should dominate. Furthermore, due to the nature of P3HT, this transition is also dependent on temperature. The gelation is thermoreversible, at a high temperature it is in a coil state and at low temperatures it transitions to a rod causing the formation of gel networks.

4 Conclusion

In this study, it was evident that the addition of ZnO-DDT nanowires to P3HT induced gelation in a good solvent. Furthermore, we are able to deduce that the gelation process is first-order reaction kinetics. The gelation process is also helpful in the printing of this hybrid organic-inorganic nanocomposites towards the use for photovoltaics or flexible electronics. The study of the rheology of these nanocomposites is not only important for printing/coating process but also in determining the properties of these hybrid nanocomposites.

References

(1) Carrasco-Orozco, M.; Tsoi, W. C.; O'Neill, M.; Aldred, M. P.; Vlachos, P.; Kelly, S. M. New Photovoltaic Concept: Liquid-Crystal Solar Cells Using a Nematic Gel Template. *Adv. Mater.* 2006, *18*, 1754–1758.

(2) Briseno, A. L.; Holcombe, T. W.; Boukai, A. I.; Garnett, E. C.; Shelton, S. W.; Frechet, J. J.; Yang, P.: Oligo- and polythiophene/ZnO hybrid nanowire solar cells. Nano Lett 2010, 10, 334-40.

(3) Rodd, C. M.; Agarwal, R.: Enhancement of interfacial polymer crystallinity using chromism in single inorganic nanowire-polymer nanohybrids for photovoltaic applications. Nano Lett 2011, 11, 3460-7.

(4) Lin, Z.: Organic-inorganic nanohybrids through the direct tailoring of semiconductor nanocrystals with conjugated polymers. Chemistry 2008, 14, 6294-301.

(5) Mawyin, J.; Shupyk, I.; Wang, M.; Poize, G.; Atienzar, P.; Ishwara, T.; Durrant, J. R.; Nelson, J.; Kanehira, D.; Yoshimoto, N.; Martini, C.; Shilova, E.; Secondo, P.; Brisset, H.; Fages, F.; Ackermann, J. r.: Hybrid Heterojunction Nanorods for Nanoscale Controlled Morphology in Bulk Heterojunction Solar Cells. The Journal of Physical Chemistry C 2011, 115, 10881-10888.

(6) Zhang, S.; Pelligra, C. I.; Keskar, G.; Jiang, J.; Majewski, P. W.; Taylor, A. D.; Ismail-Beigi, S.; Pfefferle, L. D.; Osuji, C. O.: Directed Self-Assembly of Hybrid Oxide/Polymer Core/Shell Nanowires with Transport Optimized Morphology for Photovoltaics. Advanced Materials 2012, 24, 82-87.

(7) Byun, S.-U.; Park, H.-G.; Lee, K.-I.; Lim, B.-J.; Lee, H.-J.; Seo, D.-S.: Application of Electrohydrodynamic Printing for Liquid Crystal Alignment. Electrochemical and Solid-State Letters 2012, 15, J28.

(8) Hwang, J.-Y.; Chien, L.-C.: Liquid crystal alignment on inkjet printed and air-buffed polyimide with nano-grove surface. Journal of Physics D: Applied Physics 2009, 42, 055305.

(9) Kushida, T.; Nagase, T.; Naito, H.: Mobility enhancement in solution-processable organic transistors through polymer chain alignment by roll-transfer printing. Organic Electronics 2011, 12, 2140-2143.

(10) Boon, F.; Desbief, S.; Cutaia, L.; Douhéret, O.; Minoia, A.; Ruelle, B.; Clément, S.; Coulembier, O.; Cornil, J.; Dubois, P. Synthesis and Characterization of Nanocomposites Based on Functional Regioregular Poly (3‑hexylthiophene) and Multiwall Carbon Nanotubes. Macromol. Rapid Commun. 2010, 31, 1427–1434.

(11) Adhikari, A.; Huang, M.; Bakhru, H.; Chipara, M.; Ryu, C.; Ajayan, P. Thermal

property of regioregular poly (3-hexylthiophene)/nanotube composites using modified single-walled carbon nanotubes via ion irradiation. Nanotechnology 2006, 17, 5947.

(12) Saini, V.; Li, Z.; Bourdo, S.; Dervishi, E.; Xu, Y.; Ma, X.; Kunets, V. P.; Salamo, G. J.; Viswanathan, T.; Biris, A. R. Electrical, optical, and morphological properties of P3HT-MWNT nanocomposites prepared by in situ polymerization. The Journal of Physical Chemistry C 2009, 113, 8023–8029.

(13) Malik, S.; Nandi, A. K. Crystallization mechanism of regioregular poly(3-alkyl thiophene)s. *J. Polym. Sci. B Polym. Phys.* 2002, *40*, 2073–2085.

(14) Oh, J. Y.; Shin, M.; Lee, T. I.; Jang, W. S.; Min, Y.; Myoung, J.-M.; Baik, H. K.; Jeong, U. Self-Seeded Growth of Poly(3-hexylthiophene) (P3HT) Nanofibrils by a Cycle of Cooling and Heating in Solutions. *Macromolecules* 2012, *45*, 7504–7513.

(15) Said, A. J.; Poize, G.; Martini, C.; Ferry, D.; Marine, W.; Giorgio, S.; Fages, F.; Hocq, J.; Bouclé, J.; Nelson, J.; Durrant, J. R.; Ackermann, J. Hybrid Bulk Heterojunction Solar Cells Based on P3HT and Porphyrin-Modified ZnO Nanorods. *J. Phys. Chem. C* 2010, *114*, 11273–11278.

(16) Zhang, S.; Majewski, P. W.; Keskar, G.; Pfefferle, L. D.; Osuji, C. O. Lyotropic Self-Assembly of High-Aspect-Ratio Semiconductor Nanowires of Single-Crystal ZnO. *Langmuir* 2011, *27*, 11616–11621.

(17) Onsager, L.: THE EFFECTS OF SHAPE ON THE INTERACTION OF COLLOIDAL PARTICLES. Annals of the New York Academy of Sciences 1949, 51, 627-659.

(18) Shafiei-Sabet, S.; Hamad, W. Y.; Hatzikiriakos, S. G. Rheology of Nanocrystalline Cellulose Aqueous Suspensions. *Langmuir* 2012, *28*, 17124–17133.

(19) Ureña-Benavides, E. E.; Ao, G.; Davis, V. A.; Kitchens, C. L. Rheology and Phase Behavior of Lyotropic Cellulose Nanocrystal Suspensions. *Macromolecules* 2011, *44*, 8990–8998.Gregory—structure and property development.

(20) Newbloom, G. M.; Weigandt, K. M.; Pozzo, D. C. Electrical, Mechanical, and Structural Characterization of Self-Assembly in Poly(3-hexylthiophene) Organogel Networks. *Macromolecules* 2012, *45*, 3452–3462.Gregory---electrical chemical structural.

(21) Koppe, M.; Brabec, C. J.; Heiml, S.; Schausberger, A.; Duffy, W.; Heeney, M.; McCulloch, I. Influence of Molecular Weight Distribution on the Gelation of P3HT and Its Impact on the Photovoltaic Performance. *Macromolecules* 2009, *42*, 4661–4666.

(22) Newbloom, G. M.; Weigandt, K. M.; Pozzo, D. C. Structure and property development

of poly(3-hexylthiophene) organogels probed with combined rheology, conductivity and small angle neutron scattering. *Soft Matter* 2012, *8*, 8854.

(23) Xu, W.; Tang, H.; Lv, H.; Li, J.; Zhao, X.; Li, H.; Wang, N.; Yang, X. Sol–gel transition of poly(3-hexylthiophene) revealed by capillary measurements: phase behaviors, gelation kinetics and the formation mechanism. *Soft Matter* 2011, *8*, 726.

(24) Xie, F.; Weiss, P.; Chauvet, O.; Bideau, J.; Tassin, J. F. Kinetic studies of a composite carbon nanotube-hydrogel for tissue engineering by rheological methods. *J Mater Sci: Mater Med* 2010, *21*, 1163–1168.

(25) Hobbie, E. K.; Fry, D. J. Rheology of concentrated carbon nanotube suspensions. *J. Chem. Phys.* 2007, *126*, 124907.

(26) Hobbie, E. K. Shear rheology of carbon nanotube suspensions. *Rheol Acta* 2010, *49*, 323–334.

(27) Zhou, H.; Heyer, P.; Kim, H.-J.; Song, J.-H.; Piao, L.; Kim, S.-H. Reversible Macroscopic Alignment of Ag Nanowires. *Chem. Mater.* 2011, *23*, 3622–3627.

(28) Cassagnau, P.; Zhang, W.; Charleux, B. Viscosity and dynamics of nanorod (carbon nanotubes, cellulose whiskers, stiff polymers and polymer fibers) suspensions. *Rheol Acta* 2013, *52*, 815–822.

(29) Zhang, S.; Pelligra, C. I.; Keskar, G.; Majewski, P. W.; Ren, F.; Pfefferle, L. D.; Osuji, C. O. Liquid Crystalline Order and Magnetocrystalline Anisotropy in Magnetically Doped Semiconducting ZnO Nanowires. *ACS Nano* 2011, *5*, 8357–8364.

(30) Teyssandier, F.; Cassagnau, P.; Gérard, J. F.; Mignard, N. Solâ€“gel transition and gelatinization kinetics of wheat starch. *Carbohydrate Polymers* 2011, *83*, 400–406.

(31) Zaidel, D. N. A.; Chronakis, I. S.; Meyer, A. S. Enzyme catalyzed oxidative gelation of sugar beet pectin: Kinetics and rheology. *Food hydrocolloids* 2012, *28*, 130–140.

(32) Yoshimura, M.; Nishinari, K. Dynamic viscoelastic study on the gelation of konjac glucomannan with different molecular weights. *Food hydrocolloids* 1999, *13*, 227–233.

Appendix D: Rheological Profiles of P3HT+ZnO-DDT

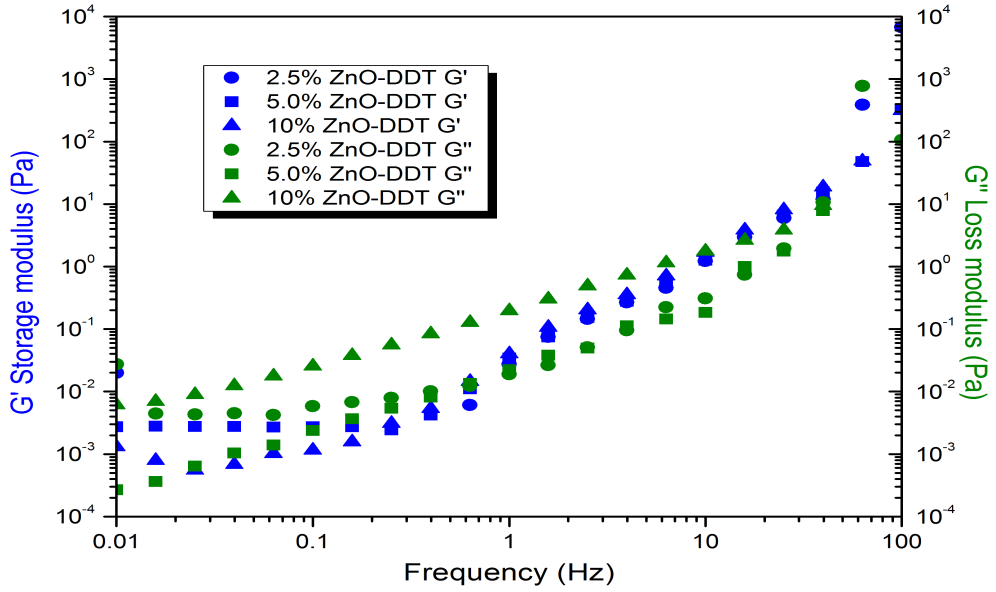

Frequency sweep of various concentration of ZnO-DDT

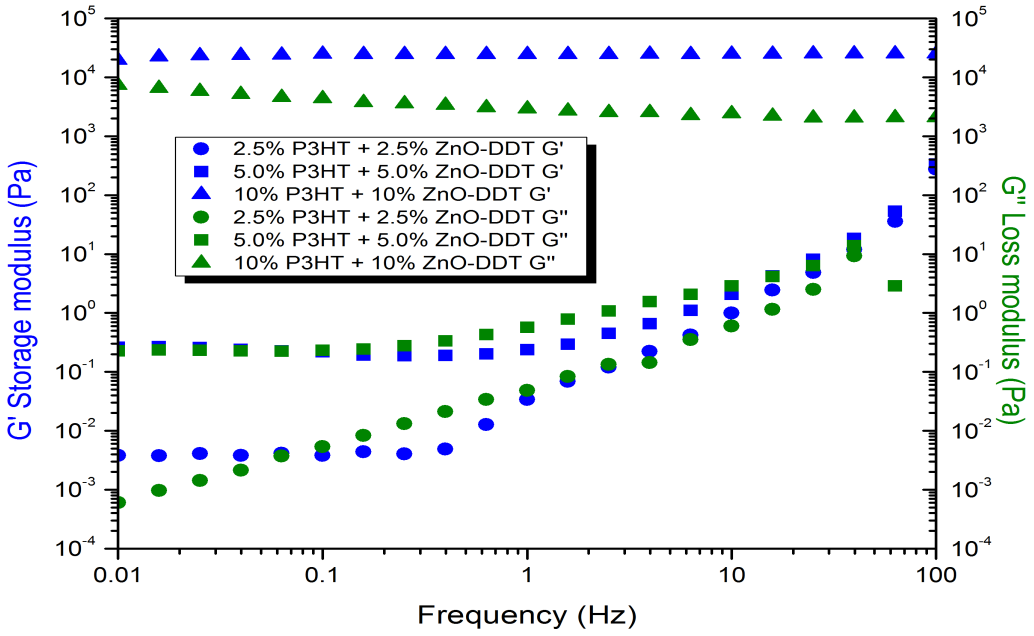

Frequency sweep of various concentration of P3HT + ZnO-DDT